University of Alberta

Development of Flexible-Based Electrode Array for Spinal Cord Interface

by

Imad Mohamad Khaled

A thesis submitted to the Faculty of Graduate Studies and Research
in partial fulfillment of the requirements for the degree of

Master of Science

Mechanical Engineering

Spring 2012
Edmonton, Alberta

Abstract

Multi-electrode arrays are essential tools to interface with the nervous system. The development of a flexible-based electrode array used to interface with the spinal cord is reported. A 2D finite element model (FEM) was developed to characterize the design parameters of such an array. A customizable, feasible and repeatable fabrication process is presented. The mechanical properties of the developed prototypes were characterized using the dynamic mechanical analysis. The arrays were implanted into surrogate cords that mimic the human spinal cord. The comparison between the strains measured across the cords implanted with flexible-based arrays and the ones implanted with other types of arrays (solid-based and individual wires) showed that the former arrays are mechanically more compliant with the cord than the rigid-based arrays. The experimental results validated the FEM, which was used to analyze the stresses induced by the electrodes of the different types of arrays on the cord. The obtained results confirmed the mechanical compliance of the flexible-based arrays with the cords.

Acknowledgment

This manuscript does not only reflect the countless hours I spent in the lab and my cubicle, but it also reflects an amazing experience I had in the past two years. This work would have not happened without the continuous support I had from my family, friends, advisors and the various people I met during my MSc career.

I was always inspired and pushed by the passion and enthusiasm of my supervisors. Their love and admiration for their work lit my way and pushed me to my extreme. The more I worked with you Dr. Mushahwar, the more I realized your uniqueness. There are very few people who have passion and dedication for their work. That was an inspiration by itself and I am really honoured for having the chance to work with you.

Dr. Moussa, I do not think I can count the lessons I learned from you. Your guidance, imagination, attitude, support and passion will always be an inspiration and a light to guide me. You simply sculptured the person I am now. For that, I sincerely thank you. It was more than a pleasure and honour to have you as my supervisor.

Special thanks go to my uncle Ahmad and to all my friends. They made my experience worth it. You gave me the support when I was down and always put a smile on my face. Thank you all.

Finally, words are not fair to show my gratitude to my Mom, Dad, Khaled and Rawad. I know that I am blessed for having you as my family. Dedicating this work to you will not be even express 0.01% of what I have in my mind and heart for you. Thank you all very much for always being there for me. I LOVE YOU. God bless you all.

Table of contents

List of Tables

List of Figures

Chapter 1

Introduction

In this introductory chapter, the objective of the current work and the motivation which initiated this research are presented. Then, the methodology used to study and achieve our goal is discussed. Finally, the outline of the thesis and the chapters is presented.

1.1 Objective

The objective of this work is to develop a customizable, feasible and repeatable fabrication process to rapidly design, prototype and assemble passive flexible-based electrode array (FBEA) to interface with the spinal cord (SC). The target is to set the ground for a standardized assembly process that would allow further developments in the design. The fabricated array has to meet different criteria to be used in such an application. The array has to be mechanically compatible with the SC; i.e. the array should deform with the SC as it deforms. The stiffness of the array is influenced by the base thickness; thus, the latter has to be customizable. The bottom surface of the array should be in full contact with the SC to prevent tissue growth. To ensure full contact, the curvature of the base of the array should match that of the SC. The electrode layout and density should be customizable due to anatomical and application differences between patients. Finally, the fabrication process should allow the alteration of all these parameters to enhance the design of the array.

1.2 Motivation

Spinal cord injury (SCI) has a major impact on the Canadian society and government. SCI is referred to injuries caused by a trauma. 85,556 persons suffer from SCI in Canada and almost 4,300 new SCIs are reported annually [1]. It is expected to have 121,000 Canadians suffering from SCI by 2030 [1]. The estimated annual cost of these spinal cord injuries is approximately 3.6 billion Canadian dollars [2]. The health care covers approximately fifty percent of this amount [2]. Thus, the number of spinal cord injuries in Canada is increasing tremendously, which means higher cost on the government through the health care system.

Spinal cord injuries are location specific. For example, the injuries affecting the lumbar and sacral regions of the spine cause reduction to full loss in the function of the lower extremities (legs, hips, urinary system, etc.). This function loss is caused by a disruption in the neural communication between the brain and the lower extremities at the point of injury [3, 4].

Intraspinal microstimulation is a technique that is being developed to help in lower extremities function restoration. It involves the implantation of hair like electrodes that stimulate motor neurons in the spinal cord. Current studies show that this methodology proves to be very promising in restoring lower extremities function and control [3,5–8]. However, the current technique uses individual wires which impose a very tedious implantation process. The implantation usually takes several hours which inflict many challenges (for example stress and fatigue) for the surgeon and increases the probability of human error. Thus, it is essential to fabricate a multi-electrode array that would facilitate and decrease the time of implantation. To develop such an array, the mechanical (stiffness) and geometrical (curvature) properties of the developed array should be compliant with the SC. Also, the array design should be customizable as the anatomy of the spinal cord varies from one patient to the other.

1.3 Methodology

First, a thorough literature review was done on the technology used to interface the nervous system. Both epi-neural and intra-neural arrays were studied for both the central and peripheral nervous systems. This study is used to conclude the required design for an array that would be used to interface with the SC.

The next step was to determine the specifications of the array that is compatible with the spinal cord. This was done through a 2D finite element model that was developed on ANSYS. The model was used to study the influence of the geometrical and mechanical properties of the different components of the array on

the mechanical interface between the latter and the cord. The geometry and material properties of these components were optimized to get the maximum mechanical compliance between the array and the cord.

Keeping the characteristics of the optimal design in mind, a repeatable and feasible fabrication process for FBEA was developed. Different materials for the various parts of the array were tested. Polydimethyl siloxane (PDMS) was selected as the base material. Different types of PDMS were examined to see which one meets the design requirements. Bent Pt/Ir and stainless steel (SS) microelectrode wires were examined. The geometry and layout of the arrays were determined via rapid prototype molds. Different fabrication protocols were defined to assemble the different parts of the array and peel it from the mold. These protocols include mold cleaning, PDMS casting and array peeling. Next, the fabricated arrays were adhered to a temporary rigid layer that facilitated its handling and implantation.

The fabricated prototypes were used to characterize the array; the repeatability of the fabrication process and the mechanical properties of the array were assessed. The former was examined by optically comparing the measured base thickness and the electrode separation distance, both longitudinally and transversely, to the targeted measurements. Once the repeatability of the fabrication processes was validated, the influence of the different parts of the array on its mechanical properties was studied. The influences of the polymerization temperature of PDMS, the base thickness and the lead wire diameter on the stiffness of the array were examined by measuring the axial stiffness of the device. The latter was measured using the dynamic mechanical analysis (DMA).

The fabrication protocol was used to develop additional prototypes that were implanted into surrogate cords that mimic the mechanical behaviour of the spinal cord. The cords with implanted arrays were subjected to 12% axial strain, which resembles the maximum deformation measured for human spinal cord during

daily activities [9]. The strains across the surrogate cord implanted with the flexible arrays were measured and compared to that with solid-based arrays, no-base arrays and control surrogate cords with no implanted arrays. This comparison gave us an understanding of the implanted flexible arrays influence on the mechanical properties of the surrogate cord.

The obtained results were used to validate the numerical model. The validated model was used to study the stresses induced by the electrodes of the different type of arrays on the SC when elongated and bent.

1.4 Thesis outline

The thesis is divided into five chapters.

The second chapter studies the different types of arrays used to interface with the nervous system. The arrays are divided into two categories based on the structure and type of interface: epi-neural (2D arrays) and intra-neural (3D arrays) interface arrays. Under each category the arrays are categorized based on their targeted neural system: Central nervous system or peripheral nervous system. The arrays are ordered chronologically according to the date of development. This study presents the different types of developed arrays; their structures, designs and how they functioned according to their target application. The study concludes with the required design for an array that would be used to interface with the SC.

The third chapter introduces a 2D finite element model that is used to analyze the influence of the geometrical and the mechanical properties of the different components of the array on the interface with the cord. This chapter is divided into two parts: The first part studies the influence of the array-base thickness, number and diameter of the electrodes on the mechanical behaviour of the spinal cord when implanted with an intra-neural array. The second part examines the influence of the modulus of elasticity of the base and the electrodes on the mechanical behaviour of the spinal cord. The obtained trends are used to conclude

the optimal design specifications for an array that would be used for our target application.

The fourth chapter is presents the work done to fabricate, characterize and bench test the FBEAs. In this chapter, we present the material selection, the different parts of the array and the methods used to assemble and peel off the array and bond it to a temporary stiff layer. The details about the defined protocols (mold fabrication and PDMS casting and peeling) are presented in Appendix A. The characterization results are then presented. The optical measurements of the different geometrical specifications of the array are presented and compared to the targeted measurements to examine the repeatability of the fabrication process. Also, the influence of base thickness, polymerization temperatures and lead-wire diameter on the stiffness of the array is studied. This section introduces the obtained experimental limitations. Then, a comparison between the influence of the FBEAs and the other types of arrays (no-base and rigid-base) on the mechanical behaviour of an elongated surrogate cord is presented. Finally, the experimental results are used to validate the results of the finite element model. The validated model is used to study the stresses caused by the electrodes of the different types of arrays (flexible-, rigid- and no-base) on the surrogate cord when elongated and flexed.

Finally, the conclusion and future work chapter is presented. In this chapter, a summary of the work and recommendations for the next steps that should be done to proceed with the work are reported.

1.5 Bibliography

[1] A. Farry and D. Baxter, “The Incidence and Prevalence of Spinal Cord Injury in Canada Overview and estimated based on current evidence,” Rick Hensen Institute, Project publication, Dec. 2010.

[2] “First of its kind research shows that as many as 86,000 Canadians are living with spinal cord injury | CPA Ontario.” [Online]. Available: http://www.cpaont.org/news/all-regions/first-its-kind-research-shows-many-86000-canadians-living-spinal-cord-injury. [Accessed: 28-Oct-2011].

[3] V. K. Mushahwar and K. W. Horch, “Proposed specifications for a lumbar spinal cord electrode array for control of lower extremities in paraplegia,” *IEEE Transactions on Rehabilitation Engineering: A Publication of the IEEE Engineering in Medicine and Biology Society*, vol. 5, no. 3, pp. 237-243, Sep. 1997.

[4] J. Hunter and P. Ashby, “Secondary changes in segmental neurons below a spinal cord lesion in man,” *Archives of Physical Medicine and Rehabilitation*, vol. 65, no. 11, pp. 702-705, Nov. 1984.

[5] V. K. Mushahwar, P. L. Jacobs, R. A. Normann, R. J. Triolo, and N. Kleitman, “New functional electrical stimulation approaches to standing and walking,” *Journal of Neural Engineering*, vol. 4, no. 3, p. S181-S197, Sep. 2007.

[6] D. McCreery, V. Pikov, A. Lossinsky, L. Bullara, and W. Agnew, “Arrays for chronic functional microstimulation of the lumbosacral spinal cord,” *IEEE Transactions on Neural Systems and Rehabilitation Engineering: A Publication of the IEEE Engineering in Medicine and Biology Society*, vol. 12, no. 2, pp. 195-207, Jun. 2004.

[7] R. Saigal, C. Renzi, and V. K. Mushahwar, “Intraspinal microstimulation generates functional movements after spinal-cord injury,” *IEEE Transactions on Neural Systems and Rehabilitation Engineering: A Publication of the IEEE Engineering in Medicine and Biology Society*, vol. 12, no. 4, pp. 430-440, Dec. 2004.

[8] R. B. North, “Neural Interface Devices: Spinal Cord Stimulation Technology,” *Proceedings of the IEEE*, vol. 96, no. 7, pp. 1108-1119, 2008.

[9] S. S. Margulies, D. F. Meaney, L. B. Bilston, L. E. Thibault, N. G. Campeau, and S. J. Riederer, “In Vivo Motion of the Human Cervical Spinal Cord in Extension and Flexion,” in *Proceedings of the 1992 International IRCOBI Conference on the Biomechanics of impacts*, VERONA, ITALY, 1992.

Chapter 2[1]

Literature Review

[1] A version of this chapter has been submitted for publication. I. Khaled, W. Moussa 2011. The Open Biomedical Engineering Journal. BSP-TOBEJ-2011-48

2.1. Introduction

Electrodes act as neural interfaces that either stimulate or record the activity of different neural structures. Metal electrodes have been extensively used since the late 1800s to investigate the somatic and autonomic nervous systems, and have played a substantial role in revealing the various functions of the nervous system. Since the early 1950s, electrodes have become important interfaces in clinical applications; focused on restoring and modulating lost and aberrant neural function following injury or disease. Since then, substantial effort has been invested in designing single and multi-electrode arrays capable of distributed and selective stimulation of and recording from target structures throughout the nervous system.

Multi-electrode array fabrication poses various challenges: 1) the tissue has to accept the implanted array; 2) the electrodes should have appropriate impedances for measuring voltage (recording) or passing current (stimulating) to the neural structures; and 3) for most applications, the implanted array should seamlessly communicate with the external world without causing any physical damage to the tissue.

Various factors play an important role in meeting the above challenges, three of which are of primary importance. These are: the *chemical and biological biocompatibility* of the materials used in the different components of the array (base, shanks, contact pads or electrodes, and lead wires); the *mechanical biocompatibility* of the array and its interaction with the host tissue during natural movement; and the *geometry* of the various components of the array and its influence on tissue reaction and stability of the implant.

Chemical biocompatibility of an array refers to the inertness and cytotoxicity of the materials used in its construction. These materials also influence the electrical properties of the electrodes, in particular their impedance. Over the years, guidelines for safe materials used for implantation in the nervous system have been established [1, 2]. Chemical inertness reduces tissue reactively and the extent of array encapsulation, thus allowing the electrode active sites to lie in close proximity to the target neuronal somata or axons. The initial arrays had

ceramic substrates [3] but most of the current arrays are based on silicon or polymeric substrates. The electrode active sites are also made of different inert metals, the choice of which is important for determining the impedance of the sites and their functionality. For example, recording requires high impedance while stimulation requires low impedance [4]. Commonly used metals are gold, platinum (Pt), and iridium (Ir). To enhance the biological compatibility of the array different sterilization methods are utilized. These include UV radiation, autoclaving, dry heat, chemical sterilizers and ethylene oxide [5–9], and all are targeted at eliminating the presence of bioactive organisms on the array surface that can cause infection following implantation.

Mechanical biocompatibility refers to the compliance of the materials used for the various array components and the similarity of their mechanical properties to those of the tissue in the nervous system. Mechanical biocompatibility determines how the array and the host tissue interact with each other, and is influenced by two major factors: the stiffness of the array (or its modulus of elasticity), and the external forces that the array can apply on the tissue [10] The latter factor depends on the former but is also dependent on the method by which the array interfaces with an external control unit (i.e., lead wires and their anchoring in the body). To ensure acceptable mechanical biocompatibility and prevent physical damage to the host tissue, the stiffness of the array has to match that of the deformable neural tissue. Otherwise, the array has to float with the tissue, for example brain, without applying external mechanical forces on the tissue. In both cases, the base of the array should remain in full contact with the tissue; thus reducing the growth of connective tissue between the array's base and the surface of the neural structure in which it is implanted. This will in turn decrease the probability of array dislodgement over time. Lead wires connecting the array to an external control unit should take into consideration the physiological movement and deformation of the tissue in which the array is implanted. Care should be taken that the lead wires do not transfer mechanical forces to the array, a factor that is common with connectors fixed to external bony

surfaces. Moreover, the geometry of the lead wires has an impact on the mechanical properties of the array [11].

The geometry of an array plays a substantial role in its acceptance by the host tissue and in the selectivity of its stimulation and recording capabilities. Geometrical features of importance are the thickness of the base and the layout and size of the array shafts and active sites. The base should ideally be very thin and confined to the biological space between the target neural structure and the closest barrier (bone, dura matter, muscle, etc.). Moreover, the size of the shaft(s) in an array plays a critical role in the extent of astrocyte recruitment and shaft encapsulation [12]. For planer silicon arrays, it has been suggested that wider shafts result in thicker encapsulation; this in turn produces a larger separation between the active sites and the target neurons. The shape of the shaft also appears to have an effect on the extent of encapsulation [12]. Shafts with sharper edges tend to have thicker layers of connective tissue than ones with smoother edges [12]. The layout of the active sites (separation distance between sites) and their geometry (cross-sectional area and height of sites) determine the specificity of the recording or stimulation capacity of the array. As the size of the active site becomes smaller, the recorded potentials become more specific and limited to local field potentials (LFPs) of a small number of neurons (typically 1 – 3 neurons). Stimulation specificity also increases as the size of the active site decreases; however, the charge density increases thus running the risk of causing tissue damage [13, 14].

The chemical and mechanical biocompatibility of an array and its geometry are directly impacted by the available fabrication techniques. Early arrays utilized drilling to create the active sites [3]. As time progressed, microfabrication became the major cornerstone for array fabrication. Advances in microfabrication technologies, especially the big boost in lithography and packaging techniques over the last four decades have helped researchers to establish more sophisticated arrays with smaller features. The minimal feature size in fabrication processes decreased from 10μm to almost 10nm. Similarly, the

minimal size of electrode active sites has decreased from 200µm to 0.15µm (Figure 2.1).

The specifications for an array critically depend on the target neural structure in which the array is to be implanted and the purpose of the array. The array could be used for recording to characterize the neural activity of a target region, for example, in the brain [15], or stimulate neuronal networks to restore function, e.g., neuroprostheses [16], or a combination of both [17]. In the following sections we assess various designs suggested for epi-neural and intra-neural interfaces. For each family of arrays, we evaluate the chemical and mechanical biocompatibility features as well as the suitability of the array geometry. We then analyze the array's success/failure in achieving its intended goal. We conclude by proposing an array design that integrates different aspects of the arrays highlighted in this review, and discuss its suitability for various neural structures, especially the spinal cord.

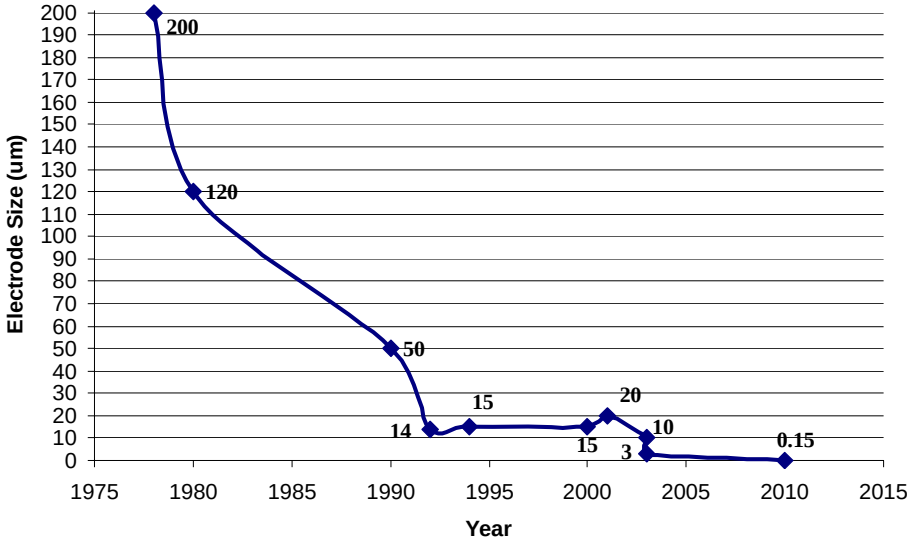

Figure 2.1 Electrode size progress in the past three decades**.**

2.2. Epi-neural interface

In 1965 Frishkoff proposed one of the first designs for a multi-contact epi-neural interface [3]. The concept was very novel at the time and involved the fabrication of arrays with metal contacts that can simultaneously record multiple LFPs from the surface of damaged nerves with the goal of understanding the

firing patterns of degenerating axons. This approach allowed, for the first time, distributed contact with the nerve, via the contact pads, which single electrodes could not provide.

The initial arrays demonstrated the powerful potential of using multi-contact recordings; however, a major challenge was encountered with respect to the fabrication reproducibility. This was due to the unavailability of repeatable micro-fabrication processes and technologies. As micro-fabrication techniques advanced, diverse and more sophisticated designs became available. Moreover, the reproducibility problems ceased but other challenges surfaced. The new challenges revolved around the design features of the array and electrode active sites as well as the chemical and mechanical biocompatibility of the arrays.

Nonetheless, the past five decades have witnessed many array architectures that addressed the above mentioned challenges. Current electrode designs and materials have improved tremendously resulting in substantial increases in the longevity of in vivo implants. While the initial arrays in the 1960s were stiff, thick (a constraint imposed by the materials and machinery used to fabricate the array) and relied on axonal regeneration through holes in their base for acceptable recording. Current arrays are thinner, more flexible and conformable to the nerve. Moreover, electrode sites come in very close contact with the surface of the nerve, thus allowing for acceptable neural recordings.

In the proceeding subsections we describe epi-neural arrays aimed at interfacing with the peripheral and central nervous systems (PNS and CNS respectively). We highlight design features that addressed the above mentioned challenges.

2.2.1. Interfaces with the peripheral nervous system

Many designs have been proposed for epi-neural interfaces with the peripheral nervous system. These designs fall into two primary categories, sieve electrode arrays and cuff electrode arrays. The two categories have evolved in parallel: the sieve arrays were placed in series with the nerve while the cuff arrays surrounded (wrapped around) the nerve.

2.2.1.1 Sieve arrays.

The goal of sieve arrays is to align and record from regenerating axons in peripheral nerves that had been completely severed [3]. The arrays contain through holes for aligning the regenerating axons and the holes are plated with metal for recording the neural signals. To enhance the quality of recordings, full contact between the active sites and the axons is necessary as it affects the signal-to-noise ratio. This contact can be affected by the size of the holes and the length of the array. The size of the holes is ideally chosen to match that of the regenerating axons, with smaller holes allowing for better alignment. The length of the array is usually chosen to optimize axonal alignment while decreasing the chance of connective tissue encapsulation [18]. Very short arrays are ineffective in aligning regenerating axons while very long arrays are invaded by connective tissue faster than the rate of axonal growth which in turn prevents axonal progression through the holes [18]. In addition to array dimensions, the material of the array also affects axonal regeneration

Frishkoff et al., 1965 reported the first sieve array [19]. Using lasers for drilling, they placed 25 μm holes in ceramic buttons with 1 cm diameter and 0.25 mm thickness. These feature sizes were remarkable at that time. Each substrate included four active sites which were connected to the external world via platinum wires [19]. The arrays were implanted between the severed sciatic nerves of cats. However, no neural activity was recorded due to poor contact between the array and the severed nerve [19].

The first neural recordings using a sieve array were obtained in 1974 by *Mannard et al.* [3] who used a polyethylene cuff around the array to improve the contact between the nerve and the active sites. The cuff also acted as an insulator that focused the neural signals within the array. The array consisted of 100 μm diameter holes drilled in a 700 μm thick epoxy substrate containing Teflon-coated silver wires.

A new design of sieve arrays which used photolithography techniques was proposed by *Loeb et al.* in 1977 [20]. Photolithography allowed for more sputtering precision and smaller feature (active site) size. The design was based

on several (15µm thick) Parylene-C layers stacked above each other. The layers were adhered to each other using epoxy resin. The surface of each layer was sputtered with Gold Titanium, and then plated with platinum, to form the contact pads, lead wires and active sites. Photolithography and etching were used to form 12 parallel lead wires which connected the 80mm apart contact pads and active sites. This entire electrical setup, except for the active sites, was insulated with a layer of photoresist. The active sites formed parts of the bottom surface of several plastic tubes that were placed perpendicular to the lead wires (Figure 2.2a). These plastic tubes were 25µm apart and created a pathway for axonal regeneration. For that time, this was a very distinguished flexible design; however, the array was unable to record local field potentials due to problems with the nerve anchoring and connections to the control module.

2.2.1.1.1. Silicon based sieve arrays.

The use of micro-fabrication techniques continued with *Matsuo et al. 1978* who was the first to use silicon substrates as the base for sieve arrays [3]. Silicon gave Matsuo a bigger material design margin as silicon lithography was well established in the microfabrication domain. The proposed array was 0.2mm thick with 200µm x 200µm via holes which included buffer metal-oxide-semiconductor field-effect transistors (MOSFET). However, the large size of the holes caused poor contact and thus low signal-to-noise ratios which made these arrays another unsuccessful attempt to record action potentials.

Edell et al. (1980) continued with *Matsuo et al.* work and decreased the thickness and the holes size which allowed for better contact thus making his array the first signal recording silicon-substrate sieve microelectrode array [3]. The 0.14 mm thick array contained 0.12mm x 0.15mm holes with 10 microelectrodes and Teflon-coated silver lead wires. All of his experiments were done on the sciatic nerve of rabbits.

To further enhance the recorded signals, *Rosen et al.* 1990, proposed a new design of the holes. The conical shaped holes had an entrance diameter of 50µm and exit diameter of 8µm. The holes were laser drilled on the silicon

substrate. The recorded signal from the sciatic nerves of rats showed a small improvement [3] which was due to the better alignment of the axons because the bigger entrance holes allowed more space for the axons and the smaller exit diameter allowed for a better contact with the nerves.

Further work on silicon-substrate sieve arrays was done by *Kovacs et al.*, 1992 (Figure 2.2b) who extended the previous designs' capabilities. The new design aimed to record from and stimulate the nerves [3]. They enhanced the fabrication process by using micro-fabrication processes that are compatible with complementary metal-oxide-semiconductor (CMOS) processes for on-chip signal process. The design was based on a 79 µm thick silicon substrate that included sixty four 100µm x 100µm probe pads covered with thin film of iridium to decrease the impedance of the electrodes. They were able to successfully stimulate and record from the peroneal nerves of rats indicating full contact with the active sites. The only problem with this array was its rigidity, more stiff than the nerve, which caused mechanical damage to the tissue, specifically near the electrodes, while implanting the array.

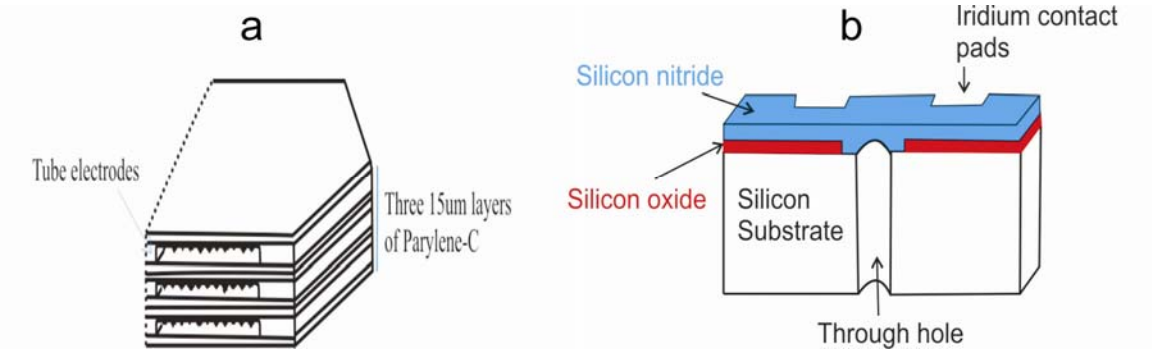

Figure 2.2 *Example of sieve and silicone base arrays*. (a) Tip of Loeb et al array showing the three layers of Parlyene-C with the plastic tubes creating pathways for axonal regeneration [20]. *(b)* Silicon based array developed by Kovacs et al. consisting of through vias for the axons to regenerate with Iridium active sites to record signals [3]. IEEE copyrights.

2.2.1.2 Cuff electrode arrays.

In 1975, *Stein et al.* was the first group to record long-term signal from peripheral nerves using cuff electrode arrays (CEA) [21]. These regeneration type arrays were based on the same concept as the sieve arrays. Stein and his colleagues believed that the new design will enhance the performance of the sieve

arrays due to the better contact and anchoring between the array and the targeted peripheral nerves. The concept of CEA was to wrap the nerve with a cylindrical shaped array containing electrodes on its inner surface that are able to pick up the signals carried by the nerve. Since then, different designs of these arrays have been proposed to interface with different peripheral nerves. These arrays are currently well established and commercially available. They can perform three major functions [10]: Stimulate nerves, record nerve activity, or modulate the nerve activity by delivering certain drugs.

Various design specifications should be met by the CEA to ensure good interface with the targeted nerves. Each type of interface has its own various requirements; however, both stimulation and recording CEAs share four [10]: 1.Electrode-nerve contact: the electrode pads should be in full contact with the nerve. 2. Chemical compatibility: the materials used should not introduce any toxins. 3.Mechanical compatibility: the array should interface with the nerve without causing any mechanical forces that can cause physical damage to the nerve- i.e. the array's edges should not be sharp and its stiffness should be compliant with the targeted nerve. 4. Array structure: to facilitate implantation and avoid external forces, the array should be easy to manipulate and the lead wires connecting it to the external world should be very flexible. In addition to these requirements each interface pathway imposes its own requirements.

For recording, the CEAs should meet the following specifications: A. To record high local field potentials, the arrays should have non-conductive walls with a length three times bigger than the space constant of the axons- the distance the action potential will travel along an axon [22] B. To eliminate any external signal, the array should have a uniform cross sectional area with no breaks in the walls and the electrode pads are spread equidistantly from each other across the array's length [23] C. To have a high signal-to-noise ratio the electrode pads should have low and uniform electrical impedances [24]. D. The cylindrical cross sectional area should allow for some space for tissue growth and any potential edema [25].

On the other hand, stimulation requires a different set of specifications: A. To avoid the disintegration (flaking off) of the electrode pads, they should have sufficient surface area and be made of the appropriate materials [26]. B. To stimulate the fibers homogeneously, electrodes should be separated longitudinally at a distance similar to the nerve fibers' space constant [10]. C. To increase selectivity it is suggested to use multi-polar electrodes [27].

Many researchers proposed different designs and fabrication processes to meet the above mentioned requirements [28]: Loeb et al. 1980 suggested stitching wires into the inner surface of silicon rubber tubes. This was a very reasonable and technologically feasible solution at that time [29]. Julien et al. 1982 proposed using a dental impression compound to mold wires wrapped around the nerve [30]. Naples et al. 1988 used a simple mechanical engineering concept to suggest the spiral cuff array: the pre-stress affect. They used foil between 2 pre-stressed silicon rubber sheets [31]. The stress difference between the two layers caused the array to curve into its cuff shape. Sahin et al. 1992 elaborated Naples' concept and suggested sandwiching foil bands between two Silastic sheets with different stresses [32] (Figure 2.3). Van der Puije et al. 1993 used thin flexible polymer substrate and photolithography to pattern the active sites [33]. Haugland et al. 1996 used rubber bands to fix Platinum foil electrodes on a dip-coated silicon array [34]. Crampon et al. 1998 proposed a new method to install the silicon rubber cylindrical cuff array in which shape memory alloy wires were used to close the array around the nerves [37]. Tyler et al. 2002 proposed the Flat Interface Nerve Electrode (FINE). This cuff array has a rectangular cross-sectional area and is fabricated by molding silicon where it is intended to reorganize the shape of the nerve and its fascicles into ovals by applying a low circumferential force on them [36]. However, the array was unable to control the nerve reshaping time. Caparso et al. 2009 enhanced the FINE design to solve its quick nerve reshaping problem. The reshaping time was controlled by coating the stretched FINE array with a layer of Poly Lactic-co-glycolic Acid (PLGA) [37]. Lee et al. 2010 used bioMEMS techniques to develop the polyimide-based cuff array with platinum (Pt), iridium (Ir) and iridium oxide electrodes [38].

The above mentioned designs have made CEA one of the most developed and established epi-neural interface arrays. As noted above, every design used the up-to-date technology to enhance the recorded signal and to increase the biocompatibility of the array. It is obvious that the concept of these arrays is working perfectly and that the different designs were intended to improve their capabilities. This allowed for commercializing most of these arrays. Today, these arrays are being used with different nerves to monitor different signals or to stimulate certain muscles.

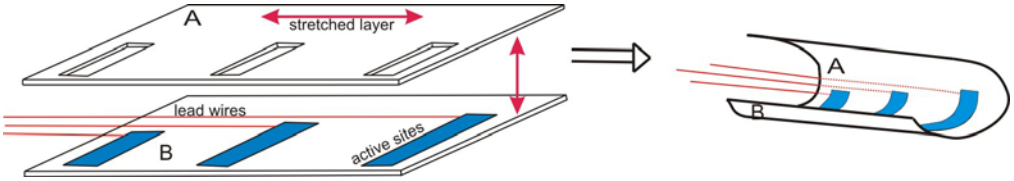

Figure 2.3 *Schematic of Spiral cuff array*. Layer A was stretched before adhering it to layer B. The stress difference between both layers shaped the array into a cuff shape [32]. IEEE copyrights

2.2.1.3 Other designs.

Different array designs for epi-neural interface with the PNS have been proposed by other researchers. Most of these arrays have been designed for scientific research. In this section we present an example of such arrays, i.e. designs that do not belong to either of the above two array types.

The glass base array was proposed by *Grumet et al.* in *2000* with an intention to record and stimulate from an isolated retina [39]. The proposed array was 0.81mm thick and consisted of two electrode-site-clusters that were several hundred microns apart. The first cluster consisted of 70µm center-to-center recording sites arranged in a hexagonal manner. The second cluster was made of 25µm center-to-center stimulating sites fabricated in a rectangular arrangement. The 10µm thick electrode sites were made of gold coated with Pt black. They were connected to the contact pads via chrome/gold wires that were insulated with a combination of silicon nitride and polyimide. A connector was used to connect the contact pads to a PCB which communicated with the external world.

This array was tested on isolated retinas of rabbits and was successful in simultaneously recording and stimulating their nerves [39]. Thus, the theory of having two distant clusters of electrode sites, one for recording and the other one

for stimulation, proved to be successful. The success in recording/stimulating was due to the fact that each cluster contained the required site design specifications for the intended interface pathway. However, the major drawback of this array is the material of the base. Glass is very stiff and has sharp edges which can introduce external mechanical forces that may damage the nerve.

In conclusion, two major concepts, besides other scientific investigations, have been proposed to interface with the PNS. The initial attempts included various designs of the sieve arrays. The target of the initial sieve array was to record LFPs; it was based on laser drilling which primarily did not allow for small holes leading to poor contact, thus causing the design to fail. As technologies advanced, microfabrication became a cornerstone in fabricating the new designs allowing smaller holes, down to 8µm [3], with more moderate array thickness, down to 79µm [3], and even changed hole shapes to become conical [3]. These modifications enhanced the contact between the electrode pads and the nerves. Thus it increased, with the change in material, the signal-to-noise ratios allowing for more successful attempts in recording LFPs. The change of the material used in the contact pads [3] lowered the impedance allowing these arrays to stimulate and record at the same time.

In parallel to the advancements that were done on the sieve arrays, another concept of arrays, with similar goals, was being studied: the cuff electrode array. Currently, the cuff array designs have met most of the challenges and requirements mentioned above; thus, allowing for well established and commercially available designs that have enhanced and saved the lives of many people.

2.2.2. Interface with the CNS

Interfacing with the central nervous system allows a better understanding and control of various nerves and muscles. For example, stimulating the CNS for lower limb movement restoration has many advantages over stimulating the lower limbs through the PNS [40]; muscle fatigue is much lower when stimulating the

CNS. Also, to get the same limb movement, it is sufficient to use one array on the SC to replace the arrays that would be used on the different leg muscles [40].

However, the central nervous system is a totally different environment than that of the peripheral nervous system. Unlike the tissues of the peripheral nervous system, CNS tissues do not regenerate after being damaged [41]. Also, the CNS tissues have a modulus of elasticity smaller than that of the PNS tissue [42, 43]. In addition, there are architectural (geometrical) differences between both systems' tissues: the CNS tissues are non-uniform, especially the brain. All of these differences make the interface with the CNS more specific and delicate.

The above mentioned challenges impose the following design requirements on the arrays interfacing with the CNS: 1. Conformity: the array's base should fully conform to the targeted tissue to ensure full contact between the active sites and the geometrically non-uniform tissue, especially the brain. 2. Anchoring: the array should anchor completely to the neural target, to insure stability and full contact between the substrate surface and the tissue. 3. Mechanical compliance: the array should not apply any mechanical forces that might damage the tissue. The same thing applies to the wires connecting the array to the external world. 4. Connection to the external world: the optimal case is to have a wireless system to ensure that no forces are transformed from the connecting wires to the array. 5. Material selection: the materials used should not introduce any kind of toxins after implantation. At the same time, the substrate should allow gas and fluid diffusion between the surrounding environment and the tissue. 6. Array's geometry: the substrate should not have any sharp edges that might damage the tissue. Also, the electrodes' position and layout should be controlled with high resolution to ensure high specificity and selectivity of the arrays.

In the following sections we study and analyze the design specifications of various arrays proposed to interface with the CNS. We study how each design addressed the above mentioned design requirements and how successful they were in accomplishing their goals.

2.2.2.1. Interface with the brain.

Interfacing with the brain is very critical and important for neural prostheses. Several attempts were done to interface with the brain for various reasons: to restore functionality (vision for example) [44], to ameliorate the symptoms of certain diseases (Parkinson's disease for example) [45] and many other reasons. *Brindley et al.* at Cambridge University in England reported one of the first arrays to interface with the brain in the 1960s. The array, which consisted of 180 Pt disk electrodes, was developed to interface with the visual cortex of a blind patient [46]. Further work on visual restoration arrays was done by *William Dobelle et al.* in the 1970s at the University of Utah.

In this section we focus our study on the arrays reported during and after the photolithography-techniques' big boom in early 1990s. This big boom has allowed researchers to fabricate very sophisticated designs and meet many of the challenges proposed by the nature of the interface and neural target- brain in this case.

One of the first reported conformable epi-neural arrays to interface with the CNS was proposed by *Boppart et al.* in 1992. Their target was to design a flexible conformal array that measures evoked potentials from hippocampal slices of rats [47]. The proposed design used photolithography and reactive ion etching (RIE) to pattern the electrode sites. The usage of RIE allowed for a better control over the geometry and design of the active sites and contact pads. The 13µm thick array consisted of different size through-holes (perforations). The array consisted of thirty two (4x8) gold electrode sites (14µm diameter and 200µm apart), lead wires (20µm wide) and contact pads (0.75x5mm) sandwiched between two thin polyimide layers (10µm and 2µm thick). The contact pads were press fitted to an etched circuit board to connect with the data acquisition system. The array was tested in-vitro only and was successful in recording signals [47].

The perforations allowed for the diffusion of CSF and oxygen to the tissue. They, also, enhanced the array anchoring as the tissue grew through them. However, the way the array was connected to the control module (contact pads press fit into a printed circuit board, PCB) limited the subdural long term

implantation as it added a rigid thick surface to the side of the array. On the other hand, this array initiated the idea of surface-conformity, setting the basic design for future epi-neural arrays that will interface with the CNS in general and with the brain in particular.

In 2005, *Hollenberg et al.* reported an array that was used to record signal from the cerebral cortex of rats [15]. The 75µm thick array was fabricated on a Kapton substrate (polyamide) and consisted of sixty-four gold electrode sites (150µm diameter). The use of photolithography allowed flexibility in the design of electrode shapes and layouts. The electrodes were connected to the gold contact pads via gold lead wires insulated with SU-8. A zebra elastomeric connector was used to connect the array to a fabricated PCB which connected to the external world.

The polyamide was chosen to replace polyimide in *Boppart's* array due to its retention of mechanical and electrical properties over time. *Hollenberg's* array was, also, successful in recording signals. However, the array had the same problem with electrical connection and thickness (bulkiness) as the contacts were connected into a bulky PCB. The PCB and the Zebra connector limited the system from the long term implantation.

Molina-Luna et al. (2006) continued the work on thin-film-microelectrode-array technology. Their 14µm thick polyimide-foil-based array consisted of seventy two titanium nitrite electrode sites (100µm diameter) with central indentation to increase surface-contact with the nerve. Perforations, 100µm in diameter, were done to ensure fluid exchange with the tissue. The use of photolithography gave flexibility to the geometry and site-to-site spacing. The gold lead wires were patterned on a flat polyimide cable that connected the array to the connector. The array was implanted subdurally and anchored to rats' skulls using two screws, bone cement and plastic frame (figure 2.4a). The array was successful in stimulating and mapping the brains of the rats [49]. Also, the histological assessment, which was done after two weeks, showed no signs of edema, tissue tethering, or inflammatory response, thus indicating no injury [49].

The array was successful in interfacing with the brain for a short time (two weeks); however, they believed that the array should be able to function normally up to 12 months [50]. The major concern was the connection to the data acquisition system. Figure 2.3a shows that the array was press fit to a PCB which would prevent it from being used for long term chronic implantation.

In 2006 *Kitzmiller et al.* proposed a novel microelectrode design that was successful in recording signals from the surface of pigs' cerebral cortex [51]. The new design was based on 200 μm^2 platinum active electrode sites (with 400µm bi-directional pitch) suspended from the 1cm thick polydimethylsiloxane (PDMS) substrate. The electrode sites were wire bonded to 30µm aluminum lead wires connected to the contact pads. These pads connected to the data acquisition system via 150 µm silver coated aluminum wires. All the materials used in fabricating this array were approved for human use and the results of the qualitative and quantitative cytotoxicity tests showed that the array was suitable for human implantations. Also, the electrical characterization of the array showed a robust design. The array showed promising results for the interface with the brain and spinal cord [51]. The only concern is the base thickness (1cm) which is believed to be a technicality and can be decreased.

Yeager et al. 2008 proposed the electrocorticography (ECoG) electrode arrays for chronic recordings [52]. Their 60.3µm thick polyimide array was successful in recording signals from the cortical surfaces of three rats. They utilized the commonly used titanium-tungsten adhesion layer to enhance the bond between the photolithographically patterned gold electrode sites and the polyimide base. The use of micro-fabrication technique gave flexibility over the arrangement and geometry of the electrodes. Yeager and his colleagues reported reliable recording over 100 days from the rats' cortical surfaces.

The ECoG electrode arrays had contact with the cortical surface, thus recording higher frequency signals [52]. The fact that Yeager was able to record signal for 100 days suggest that there were no difficulties with the connection to the control module. Thus, the recorded signals and the biocompatibility of the

materials used show that these arrays have good capabilities in interfacing with the CNS.

In 2009 *Yu et al.* proposed the elastically deformable microelectrode array or stretchable microelectrode array (SMEA). This array was capable of undergoing up to 20% strain (when bi-axially stretched) while maintaining functionality [53]. This was a remarkable improvement over the previous arrays. The array consisted of twelve 100µm x 100µm electrode sites (3nm Cr/75nm Au/ 3nm Cr) which were sandwiched between two mechanically different layers of PDMS; the first one was 280µm thick with Young's modulus (E) of approximately 1MPa, and the second layer was 15µm thick ($E \approx 160 MPa$) and acted as an elastomeric electrical insulator. The electrode sites were electroplated with Platinum black to enhance the recordings. To allow for in vitro testing, the arrays were packaged between two PCBs with circular openings in the middle to function as culture wells. These PCBs interfaced with the data acquisition system. The arrays were able to record signals, from rats' hippocampal tissue, before and after controlled deformations were applied to the brain tissues.

Yu and his colleagues reported two major limitations of the SMEA [53]: the electrode size, which was limited to the smallest feature that can be patterned on PDMS, and the number of electrodes they had on the array (12 electrodes) which was limited to the size of the hippocampal slices they experimented on. The first limitation made the array incapable of allocating recordings to a specific anatomical structure. This limitation was a technological problem which has been solved [54]. The second limitation was an experimental one. Thus, with the two limitations being solvable, the array proves to be a very promising system.

One of the most recent reported arrays was done by *Kim et al. 2010* (Figure 2.4b). They suggested a new novel technique to be able to implant very thin arrays. This piece-of-art design was based on a polyimide-based-array with different thicknesses placed on a dissolvable supportive stiff-silk-film [55]. As the silk layer (thickness can range from 20 to 50µm) dissolved, the thin array would conform to the brain's surface. This stiff layer allowed Kim and his colleagues to experiment with polyimide-base-arrays that were as thin as 2.5µm. The array

consisted of thirty 500µm x 500µm gold electrode sites (150nm thick) that were spaced by 2 mm. The interconnection wires were insulated with a 1.2µm thick polyimide overcoat and located on the “neutral mechanical plane” to minimize any fracture that can be caused by bending [55]. An anisotropic conductive (ACF) film was used to connect the contact pads to the control module. The arrays were successful in mapping the cortex of feline animal models. Also, histological experiments post 4 weeks of implantation reported no immune response.

This technique allows the usage of ultimately thin arrays that would conform to the surface of the brain in particular. The major drawback is controlling the electrode position over the neural target. As the silk layer dissolves, the polyimide array will slowly start deforming with no control on where the electrode sites will contact the neural target. However, the affects of this drawback can be ameliorated with an increased number of active sites which allow for more contact with the brain tissue.

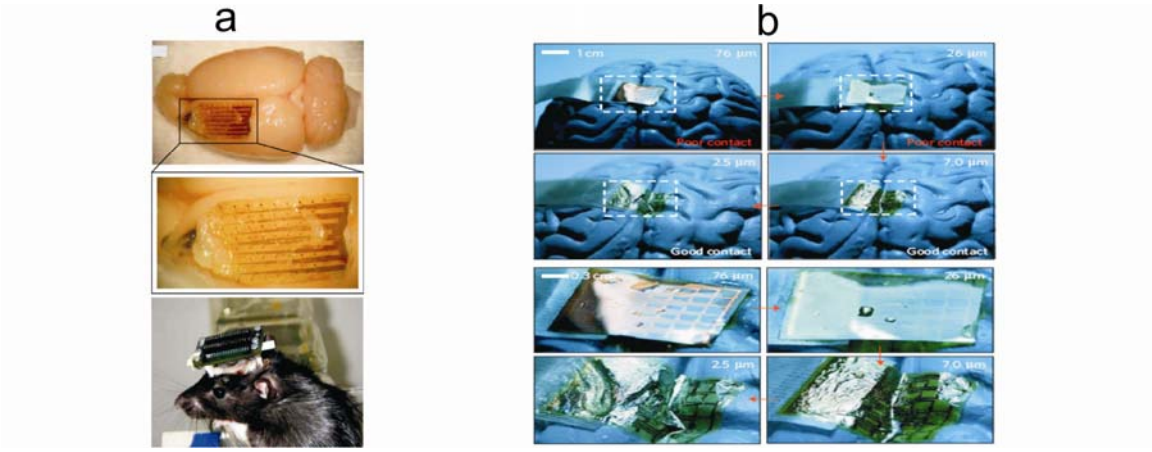

Figure 2.4 *Brain interfacing epi-neural arrays.* (a) Molina-Luna et al. thin-film-microelectrode-array implanted on the surface of a rat brain. The top two figures show the size of the array compared to the rat brain size while the third picture shows how the array was press fitted to the PCB to connect to the external world [49] Reprinted with Elsevier permission.(b) The 2.5 and 7 µm thick arrays (second picture in the left column) show the best contact compared to the other thickness (76µm, 26µm) which demonstrates the need of such silk dissolving technique to be able to implant very thin arrays[55]. Reprinted with Nature Publishing Group transaction permission

2.2.2.2. Interface with the spinal cord.

One of the initial attempts to interface with the spinal cord was done in 1967 through the Dorsal Column Stimulation, currently known as Spinal Cord Stimulation (SCS) [56]. This interface was a particular application of gate-control

theory that was reported in 1965 [57]. In 1967, *Wall et al.* showed that stimulating the SC via electrodes can relieve pain in humans [58]. In March of the same year, *Shealy et al.* stitched a vitallium alloy electrode (3x4mm) to the dura of dorsal columns of a dying cancer patient [59]. The electrode was covered with Dow Corning Medical Grade Adhesive and Silastic [59]. The stimulation gave very promising results.

However, the SCS was not widely accepted and recognized by the medical community until the early 1990s due to the lack of understanding of the pain relief mechanisms [60]. In 2002, almost 14000 SCS implantations were done worldwide [61]. This shows the huge development of the SCS electrode industry in that decade.

The first designs were based on Torresan's Cardiac Pacemaker [56]. In the 1970s flexible percutaneous electrodes with single active sites were designed to be chronically implanted via needles [56]. These designs were developed to carry four to eight sites in the 1980s [56]. Two-dimensional arrays of such electrodes can be created by implanting two of them next to each other.

Currently there are two types of electrodes that are commercially available: Percutaneous electrodes and laminectomy electrodes. Both of them are implanted into the epidural space. The first type is implanted via a needle; while the second requires a laminectomy. The type and design specifications of the electrodes are selected based on the patient's situation (pain intensity and dorsal roots of interest) [62].

The percutaneous electrode is a cylindrical flexible polymer-based tube with an outer diameter in the range of 1.3mm [61]. It holds four or eight platinum rings near the tip. Each ring's typical length is 3mm; however, longer contacts (such as 6mm) are commercially available [63]. This length would affect the impedance of the contact site [63]. The contact site spacing can range between 4 and 9mm depending on the targeted spaced [63]. The metallic lead wires are insulated and placed in the tube forming the shaft of the electrode.

The laminectomy electrode has a flat polymeric substrate (approximately 8mm wide and 40 mm long) with four or eight active sites [61]. The traditional

electrodes consisted of four round sites with a 4mm diameter and 6mm center-to-center spacing. However, the advancement in fabrication technologies has allowed the current electrodes to consist of one, two or three columns of electrode sites. These electrodes had smaller diameter and some of which had a rectangular shape [61].

During their attempts to relief pain, physicians noticed the electrodes' ability to improve certain body functions such as exercise tolerance and bladder control [56]. This caused them to think of using such arrays to interface with the spinal cord for neuroprostheses purposes.

One of the attempts for using epidural interface for neuroprostheses purposes was done by *Rodger et al., 2006.* Their flexible parylene-based array was primary designed to stimulate the retina and was extended to modulate the neurons responsible for reflex-arc in subjects with spinal cord injury [44]. The approximately 17µm thick array consisted of multiple 125µm diameter Titanium/Platinum electrode sites. Flexible cable and radiofrequency coils were used to connect the array with the external world. The array had a young's modulus of approximately 4GPa. It was implanted on the spinal cord (under the dura mater) of two mice. An electromyogram (EMG) was used to measure signals from the muscles (opposed to observing the reaction) after stimulating the spinal cord, thus proving the efficacy of the array. In 2008, Rodger and his colleagues enhanced the life time of their array by using a high temperature stabilized parylene and high surface-area platinum electroplating. They were, also, successful in creating arrays with Iridium electrodes which increased the charge capacity. All of these changes allowed the array to successfully stimulate and record from the spinal cord of rats [64].

The conformity of the thin parylene base has a big advantage. However, the modulus of elasticity of this layer was almost 45 times larger than that of the spinal cord; 4GPa for the base [64] opposed to 89kPa for the spinal cord [65]. This huge difference is enough, if chronically implanted, to cause physical damage to spinal cord as it moves.

Another spinal-cord-interference-attempt was done by *Meacham et al. 2007*. The 80µm-thick PDMS-array was made of patterned gold microelectrodes (less than 60µm diameter), gold contact pads and gold interconnection wires. The interconnection wires had an intersecting serpentine layout to increase the substrate maximum strain up to 8%. The layout of the electrodes was flexible as it depended on photolithography masks. Silver wires were pressed on the contact pads to connect the array to the control module. The array was tested on a plastic tube and showed perfect conformity. It was, also, tested on an isolated rat spinal cord and successfully activated the selected white matter tracts [11]. It also showed similar stimulus precision and activated the surface tracts with a lower charge density when compared to rigid electrodes placed on the surface of the isolated spinal cords.

The conformity of these arrays and their ability to activate white matter is very promising; however, in the in-vitro experiments the array was wrapped around the spinal cord. This is very challenging in chronic implantation as it requires the removal of the entire vertebra or pulling out the SC to get enough space to wrap the array around it. Thus, more analysis should be done on how to place the electrodes in the right location (from the dorsal side of the spinal cord) to activate the specific targeted axons.

Many different designs have been proposed to interface with the CNS. Most of these arrays were designed to interface with the brain. Spinal Cord Stimulation Arrays are well established and several thousand implantations are done yearly to relieve several types of pain in humans. However, there are very few proposed neuroprostheses arrays that interface with the spinal cord [11, 44, 64]. The complications imposed by the geometry, and the flexibility of the spinal cord are still being addressed by researchers. Thus, more sophisticated designs need to be proposed and tested to restore the function of the limbs. On the other hand, more designs and attempts have been done to interface with the brain and were successful in both recording [15, 51–53, 55] and stimulating [49]. However, none of these arrays, except the ones for SCS, were chronically implanted for a

long time as they were not able to meet the entire biological, chemical (material), mechanical, and geometrical challenges proposed by the CNS.

2.3. Intra-neural interface

As shown above, the epi-neural interface is not a very powerful and effective method to selectively record or stimulate the minimal number of neurons. Also, in the case of stimulation, epi-neural array electrodes can cause local burns, dermal irritation and pain [66]. Thus, the need for arrays that are able to interface with very small number of neurons without causing any damage or pain is clear. This can be achieved through intra-neural interfacing arrays.

Intra-neural silicon-based arrays were pioneered by Angell and Starr in May 1966 at Stanford University [67]. The two professors initiated the work on silicon technology with the goal of fabricating arrays that would record from the nervous system. Their work formed the base for neural interface with the CNS. Intra-neural interface allows researchers to record signals with high spatial resolution allowing further electrophysiological understanding of the studied nerves. In the case of neuroprostheses, intra-neural electrodes are able to activate neurons with a charge that is three orders of magnitude smaller than the one required with epi-neural electrodes [68]. This increases the interference life due to the reduction in the probability of any potential neural damage, due to fatigue. Also, it decreases the pain or the irritation that the epi-neural stimulations may cause.

The intra-neural-interface-arrays are highly dependent on micro-fabrication techniques. That caused the arrays to dramatically evolve from their initial design. The primary arrays faced design and reproducibility problems [69] due to the fabrication technology limitations at that time. Most of the technological problems have been solved with the micro-fabrication technology boost in the early 1990s making the fabrication of 3-D arrays a very well established domain. As a result, different sophisticated novel designs were proposed, most of which were based on silicon substrates, and some of which

have been commercialized. In the following section we study some of these different array designs based on the neural target.

2.3.1. Interface with the brain

Interfacing with the brain using intra-neural arrays is very critical and has proven to be an effective method of ameliorating the symptoms of certain disorders [45]. It also gives scientists more control on the interface as it interacts with a very small number of neurons. To ensure a good interface, various challenges have to be met: 1- The materials have to be chemically compatible and do not degrade or introduce any kind of toxins over time. 2- Full contact between the array's base and the tissue should be ensured to decrease tissue growth or encapsulation, which can lead to electrode dislodgment. 3- The array should not be fixed to the bone and should float with the brain to prevent any physical damage that can be caused by the electrodes dragging on the brain tissue. 4- Lead wires should be very flexible. The ideal case is to interact with the external world wirelessly. 5- In the case of wireless communication, heat dissipation should not be a problem. 6- The materials used for the electrodes should be appropriate for the goal of the interface (for example low/high impedance for stimulation/recording respectively). 7- The electrodes length and geometry should be controlled with high precision in order to hit the targeted neurons. In the following section, we study the different designs that have been proposed to interface with the brain and how they tackled the above mentioned challenges.

2.3.1.1. Rigid-based arrays.

In 1970 Kensall Wise, James Angell and Arnold Starr proposed one of the first designs of micro-machined sensors which became one of the first proposed 3-D arrays [67] (Figure 2.5). The array consisted of gold probes/electrodes extending 50µm from the silicon base [69]. The 10µm spaced electrodes had diameters (width) less than 80µm, tips as small as 2µm (recording area of $15\,\mu m^2$) and 0.4µm insulation layer of silicon dioxide (except for tip/recording area). The adhesion between gold and silicon dioxide was enhanced by a thin

layer of nickel deposited in between the two layers. The use of micro-fabrication allowed flexibility in the electrode layout. Wires (75µm in diameter), connecting the array to the control module, were thermo-compressed to the contact pads. The probes were mounted on the edge of a tapered glass tube which was insulated with an insulating lacquer, except for tips. The entire fabrication took 1 to 2 weeks of work.

The electrodes were subdurally implanted in the brains of cats. The electrodes had good mechanical stability; i.e. no buckling took place during implantation. However, out of 40 tested electrodes, only 7 succeeded in recording signals from single nerve units. The probes were designed for extracellular recording and could not be used in this shape for intracellular recording [69]. Another limitation was the size of the silicon base, which was large when compared to the electrodes. This limits the ability of such an array to be chronically implanted.

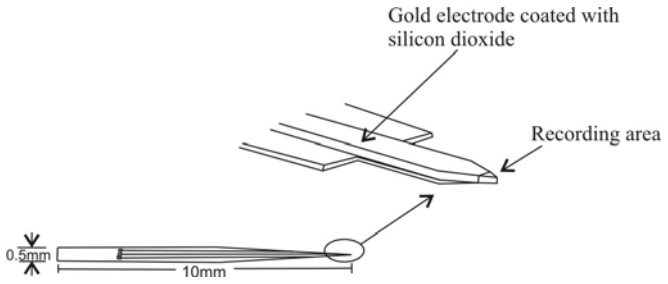

Figure 2.5 Wise et al. extracellular microelectrode. One of the primary 3-D electrode arrays [69]. IEEE copyrights.

In 1991 *Richard A. Normann's lab* in the University of Utah designed and fabricated what will become to be one of the most used intra-neural interference microelectrode arrays: the Utah Electrode Array (UEA) (figure 2.6a) [70]. This silicon-based array was fabricated using micro-fabrication techniques. This allowed for high flexibility over the electrodes' design and geometry. The 4.2mm x 4.2mm array consisted of 0.12mm (0.2mm in later experiments) thick silicon base and one hundred, 0.4mm bilaterally spaced, tapered microelectrodes (0.09mm wide at the base) that are 1.5 mm long. The $3.01\text{x}10^{-4} cm^2$ tips of the

electrodes were coated with platinum. Later, it was changed to iridium oxide to enhance the charge capacity [68]. Gold electrical contact pads for each electrode are patterned on the back of silicon base where lead wires are bonded. The entire array except for the electrode tips is flooded with polyimide for insulation [70].

Many researchers have studied UEAs and implanted them in the cerebral cortex of various animals and proved the arrays' success to selectively record and stimulate very small numbers of neurons for more than one year. In fact, these arrays have allowed for the longest successful chronic implants to date [67]. This has allowed for testing the array on the human cerebral cortex [71, 72]. In this chapter we report the work done by Patrick Rousche and Richard A. Normann on the Utah array. The arrays were implanted subdurally in the cerebral cortex of cats and were used to record and stimulate the neurons with small duty cycles for up to 13 months [68, 73]. After 6 months of implantation more than 60% of the electrodes were still successfully recording signals. However, the recorded signals varied because they did not originate from the same neurons. Also, the stimulation charge threshold showed instability. Both of these observations were due to fibrous tissue growth between the cortex and the array. This caused the array to move up as the tissue grew and thus changed the position of the tips (lifted them up). Also, electrodes' impedance reduction was reported after 6 months due to the permeation of water vapor through polyimide. On the other hand, histological studies showed no signs of tissue reaction or scars except in very few cases [73].

The stiffness mismatch between the array's base and brain tissue has enhanced the encapsulation problem. Another impediment of this array is its planar arrangement which prevents it from recording/stimulating large range of neurons [66].

The planar arrangement impediment was solved in 2001 with the fabrication of the Utah Slanted Electrode Array (USEA) (figure 2.6b). The same UEA base geometries and materials were used except for the electrode shaft design [66]. The USEA consisted of electrodes with a base width of 0.08mm and shaft length ranging between 0.5 and 1.5mm. These electrodes were fabricated in

a slanted manner with a tip area of $0.005\,mm^2$. Also, they were electrically isolated from each other by a glass moat that surrounded the base.

The new design was successful in recording/stimulating more neurons at different depth, thus stimulating more muscles [66]. It, also, showed higher precision and broader control of muscle reaction force which lead to reducing muscle fatigue [66]. Also, results showed that stimulation in one fascicle did not spread to other fascicles [66]. However, the tissue encapsulation problems reported for the UEA persisted with the USEA which validates our assumption about the source of the problem: the stiffness mismatch between the silicon base and the brain tissue which did not allow for full contact between the interfacing media.

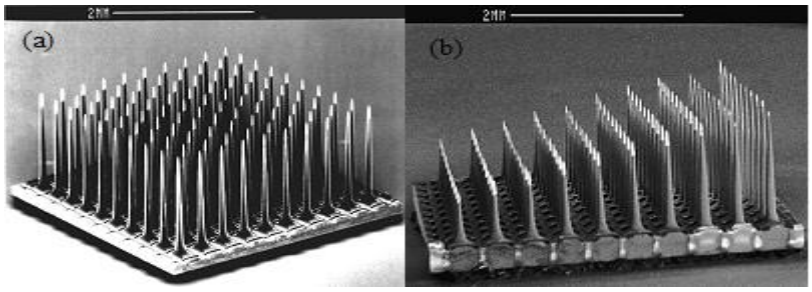

Figure 2. 6 *Utah array.* a) Utah Electrode Array. b) Utah Slanted Electrode Array. The two arrays have proved to be one of the best interfacing arrays to exist. [74]. Reprinted with Richard Normann permission

In 1994, *Hoogerwerf* and *Wise*, from the University of Michigan, micro-assembled planar silicon shanks to propose what became to be known as the Michigan Array. With a minimum separation of 100µm, shanks (15µm thick, 40µm wide and 3mm long) with gold bases were assembled (fixed with biocompatible silastic) into a micro-machined silicon platform with integrated ribbon cable [75]. The gold bases were connected to the lead wires using ultra sonic wire bonding. Then the platform was covered with a 1mm thick glass frit which allowed enough space for CMOS signal processing circuitry. Further experimentations on these arrays were done by *Bai* [76] with minor changes in the design due to experimental and performance reasons. The shank spacing (same as the electrodes) was changed to 200µm and the length became 2.5mm with electrode tips that were 2-3µm and active site areas (made of Pt/Ir) about

$100\,\mu m^2$. Also, Bai's arrays contained perforations in the platform to allow tissue growth and thus enhanced anchoring of the array.

The arrays were tested in vivo on cerebral cortex of guinea pig and were successful in recording signals. The arrays caused 1.5% tissue displacement after 3 weeks of implantation [76] and did not cause any major tissue reaction after 3 months [75]. Also, other studies showed that these arrays were able to successfully record signals for up to one year [77]. Glial cells formation near the tips was observed [75, 77] supporting the choice of having the recording site away from the tip. Also, the tissue damage caused by mechanical forces on lead wires was solved by using an integrated highly-flexible ribbon cable [76]. On the other hand, using CMOS technology caused heat dissipation problems [75] as the system heated up. Another problem that has to be considered is the rigidity of the silicon base which might, on the long run, lead to tissue encapsulation problems due to the gaps created between the rigid base and the tissue.

The ACREO microelectrode arrays (figures 2.7a and 2.7b) were another proposed design to record signals from the brain. Each array consisted of a shank with multiple electrodes extruding from a planar base. In this paper, we study the work that was done by *Jensen et al.*[78] and *Hofmann et al.* [79] on these arrays. Each array was patterned on silicon-on-insulator substrates. Each shank consisted of 1 to 8 parallel electrodes (spaced between 200µm and 600µm) with a 4 degrees tapered tip and a cross sectional area extending from 25µm x 38µm (at the electrode site) to 25µm x 200µm (at the base). Each electrode had multiple iridium recording sites (10µm x 10µm). The number and spacing of the latter sites varied and was flexible as it depended on the microfabrication process. The sites were connected to the contact pads found at the base of the shank through gold traces.

Hofmann wire-bonded the contact pads to flexible PCBs and was successful in recording signals from isolated guinea pig brain. Also, Jensen was able to record signals from the cerebral cortex of rats (2mm implant depth). These electrodes can be assembled using a polymer base to give a denser array. The

drawbacks of this design are the stiffness and sharp edges of planar silicon base (Figure 2.7a).

McCreery et al. 2006, proposed a new design for deep brain recording and stimulation as a potential solution for some movement disorders [45]. The array (16 mm in length and 2mm in diameter) consisted of sixteen 5-6mm long iridium electrodes (75µm diameter with 3µm layer of parylene-C insulation) extending from an epoxy cap. The electrodes were aligned –with a spacing of 350µm- in a 6mm long stainless steel cylinder. The electrodes had a blunt tip with a 5-6µm radius of curvature and an iridium oxide active site with an area of 500-2000 μm^2. Pt/Ir (90/10%) lead wires were micro-welded to the electrodes.

The arrays were implanted into the subthelamic nucleus in cats for 140-415 days and were able to record signals and stimulate neurons [45]. Histological studies showed tissue damage which was caused by the high charge capacity [45]. The base material makes the array rigid which might cause encapsulation problems.

Micro-fabrication was not the only method used to fabricate arrays. Other designs proposed assembling 33 micro-wires to form a recording array to interface with the brain [80]. Tungsten wires (8cm long, 35µm diameter plus 7µm polyimide insulation layer) were soldered to a 12-pin sub-miniature connector then sealed with epoxy. Poly-methyl-methacrylate (PMMA) was used to connect 3 different connectors containing the wires. The spacing (approximately 400µm) between each row (containing 11 electrodes) was controlled by a jig and was limited by the minimum gauge of the instrument wire.

The array was implanted in the cerebral cortex of guinea pigs with a final insertion depth between 700 and 900µm [80]. The first neural activity was recorded after 33 days of implantation which suggested that some kind of edema was initiated by the implantation. The unit activity recorded dropped within 9 weeks, yet recording was maintained for 3 months. The drop in the recording indicated that some kind of cell reaction/coating took place near the recording areas or tissue growth caused dislodgment of the array. The PMMA has a young's modulus between 1.8 and 3.1 GPa which is way higher than that of the brain

tissue. Thus, the space that existed between the base and the tissue might allowed for tissue growth and array dislodgment. Mechanically, the electrode stability was maintained with stainless-steel head screws.

Scherberger et al. reported another design that assembled micro wires was proposed to record signal from the brain [81]. The 4x8 array (fabricated by MicroProbe Inc., MD, USA) was a piece of art. It consisted of 75µm diameter tungsten wires (with different lengths) insulated with a 3µm diameter Parylene-C layer. Rigid epoxy glue was used to connect the electrodes to the connector (figure 2.7c). The array was implanted subdurally in the Macaque cortical sulci of 4 animals and was successful in recording single-unit activity. From the picture of the array (figure 2.7c), the base seems to be thick when compared to the electrodes length. Also, the array's base is rigid which might cause, if chronically implanted, tissue growth and encapsulation problems in the long run.

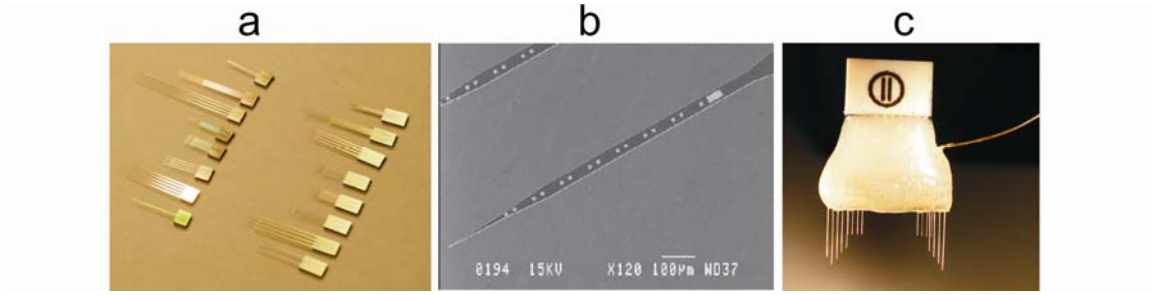

Figure 2.7 *Examples of rigid base 3-D arrays*. (a) The different shanks design for the ACREO microelectrode array [78]. IEEE copyrights. (b) An electrode in the ACREO microelectrode array shanks showing the different active sites [unpublished]. Reprinted with permission from Ulrich Hofmann. (c) Sherberger et al. microelectrode array showing the thick epoxy base with the different length electrodes [81]. Reprinted with permission from Martin Bak.

2.3.1.2. Flexible arrays/electrodes.

Rousche et al. proposed one of the first flexible base 3-D recording arrays/electrodes in 2001 (Figure 2.8). Photolithography techniques were used to fabricate the polyimide-based array (both base and electrodes) [82]. The patterned gold/chromium pads and traces, connecting the active sites to the connecting pads, were sandwiched between two electrical insulating flexible polyimide layers to give a base with a 2.793GPa modulus of elasticity. The arrays consisted of either one or three shafts: length of 1.5mm, width of 160µm and thickness less than 20µm. The recording sites were 20-40µm x 20-40µm. The electrodes

contained wells of bioactive material that were placed 40µm away from recording sites. Later, the design was improved to contain a polyimide cable to connect the array to the external world. The array successfully recorded neural activity from the cerebral cortex of rats [82].

The electrodes' position and design was customizable due to the use of microfabrication techniques. Also, the wells were designed to facilitate the integration between the electrodes and tissue after implantation. However, electrode buckling during implantation is a major impediment of this design as the electrodes' shafts are made of polyimide which makes the implantation procedure very delicate. Also, the modulus of elasticity mismatch between the array and the brain tissue will not allow for full contact, thus potentially causing tissue growth problems.

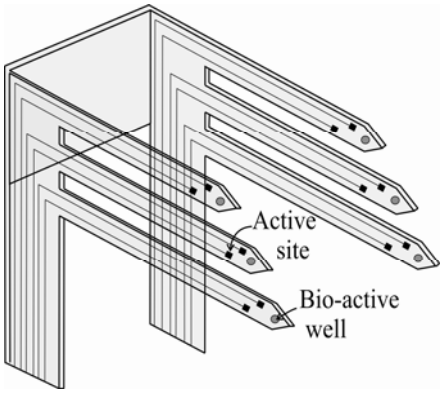

Figure 2.8 *Schematic of a flexible 3D multi-electrode array*. The schematic 3-D array developed by Rousche et al. shows the polyimide base and shafts carrying the active sites and the bio-active wells. [82]. IEEE copyrights.

Takeuchi et al. proposed another design for flexible recording arrays. The new design used magnetic field for batch assembly of the array. Polyimide was used as the material for the base and electrodes [83]. The polyimide electrodes contained a 5µm thick magnetic film, parylene-coated-nickel, on their backside and were vertically aligned from the 10µm thick polyimide base by an external magnetic field. These 25µm thick needle shaped electrodes (1.2mm long and 160µm wide) included three 20µm x 20µm recording titanium pads patterned at 0.65mm, 0.85mm and 1.05mm from the base. The lead wires were patterned in the base with the same micromachining techniques. The arrays were implanted subdurally in the rats' cortex and successfully recorded neural activity [83].

This design used a nickel layer to stiffen the electrodes and eliminate the buckling problems. However, the effective modulus of elasticity of the electrodes became 36.8GPa [83], which imposed potential tissue growth problems due to the huge mismatch with that of the brain tissue. Also, the magnetic film can cause problems for MRI imaging which limits the ability of using the MRI to image the array while chronically implanted.

Several arrays have been proposed to interface with the brain. The Utah array [17], Michigan array [75] and Huntington Medical Research Institute (HMRI) array [45] were the most tested and successful arrays. These 3 arrays are considered to be a piece-of-art from the engineering perspective and proved to work for a long time after they have been chronically implanted, especially the UEA. However, all of them still have the same problem which is the rigidity of their base. The fact that they float with the brain has decreased the affects of this problem; however, it still does not allow for full contact between the base and tissue which allows for tissue growth and encapsulation problems shifting the arrays from their initial position. Some attempts have been done to fix this issue; for example, perforations were created to enhance the anchoring but tissue growth and encapsulation still existed. The remarkable flexible arrays that were proposed to solve this stiffness mismatch problem [82, 83] had their own disadvantages, especially that the electrodes themselves were flexible. The attempt to stiffen up the electrodes had increased their stiffness to high values (approximately 40 GPa), thus the mechanical mismatch problem was unsolved [83]. As a result, more work is being done on these arrays and even new designs are being studied to address all the challenges and ensure the perfect interface between the arrays and the brain.

2.3.2. Interface with the spinal cord

Intra spinal micro stimulation has shown that it is possible to restore functionality in certain muscles (bladder, bowel and lower extremities for example) [16, 85-88]. However, interfacing with the spinal cord is more

challenging than that with the brain. The major challenge that surfaces, besides the various challenges that were mentioned for interfacing with the brain, is the spinal cord deformation and flexibility where it bends, elongates and twists (figure 2.9). Thus, the electrodes or arrays should take this deformation and flexibility into consideration and not cause/transform any external force, which will physically damage the tissue. In this section, we present the work of McCreery et al. This work was chosen because it resembles the generic design of a rigid-base array.

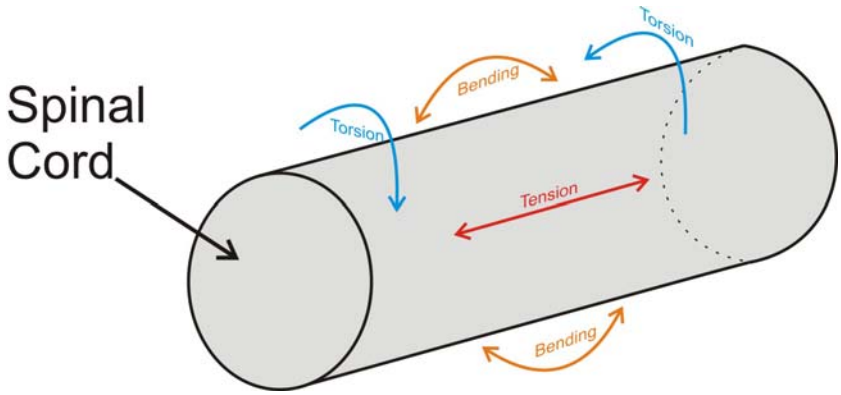

Figure 2.9 *Schematic of the spinal cord with the various deformations it undergoes*. The arrows represent the different directions at which the human spinal cord can move.

McCreery et al. proposed two arrays to interface with injured spinal cords to regain control of the bladder and bowel [16]. The first array consisted of 6 or 9 activated iridium electrodes and the second used ordered silicon-base-electrodes with multiple stimulation sites. The iridium electrodes were 75µm in diameter with a blunt tip (surface area between 1600 and 2400 μm^2) and 4-5µm radius of curvature. They were micro-welded to 25µm diameter Pt/Ir (90/10%) lead wires. The electrodes, except tip, and the lead wires were insulated with a 2.5µm thick Parylene-C layer. The first array consisted of three rows of electrodes; the two outer rows consisted of 6 electrodes ranging between 1.4-1.7 mm in length, to interface with bladder neurons, while the other 3 electrodes of the middle row ranged between 1.3-1.6mm. The second array consisted of two 1.4mm spaced silicon shanks: an interfacing shank with 3 multisite electrodes and a stabilizing shank with 3 dull (no sites) electrodes. Each shank was 2.25mm long and 15µm

thick. Each electrode contained 3 iridium oxide sites (surface area of 2000 μm^2) located at 1.2, 1.5 and 1.8 mm from the shank's base. In both arrays the lead wires were wound around a 1 mm diameter silicon rubber tubing with 0.5 mm lumen. Then they were coated with layers of silicon elastomer leading to a flexible cable.

The iridium electrodes and the silicon-probe arrays were implanted subdurally in 31 cats for 88 days and 3 cats for 58 days respectively [16]. For both arrays, the electrodes which hit the right targeted location were able to increase the pressure within the urinary bladder or the relaxation of the urethral sphincter [16]. The stimulation induced pressure increase or relaxation with small tissue damage when it was done with a 10% duty cycle while it caused severe tissue damage when done continuously [16]. Histological sections showed fibrous glial scars and traces of iridium indicating problems in the insertion method and degradation/erosion of the iridium tips. Also, the silicon base electrodes were very fragile and hard to implant. It should be noted that the studied arrays, from base to the tip of electrodes, were short (in the range of 5mm) which lowers the structure stiffness. It is important to study the behaviour of the cord when this array is used with longer electrodes. It is believed that the increase in the length of the electrodes will cause physical damage to the cord as it deforms due to the huge mismatch in the mechanical properties between the stiff array and the fragile flexible cord.

2.3.2.1. Arrays with no base.

Many attempts to interface with the spinal cord using individual electrodes have been done and some of them report back to the 1970s [84]. In this section, and as an example, we report four different individual electrode interfaces that have been studied by Mushahwar et al., Grill et al., Yoshida et al. and Snow et al.

Mushahwar et al. used an array of 6 tungsten rods, each100µm in diameter, insulated with epoxy except for the 50µm electrolytically sharpened tip to stimulate the spinal cord and selectively activate lower limb muscle groups.[40, 85]. Then, they used 6 to 12 Teflon insulated 30µm stainless steel wire electrodes to actuate hindlimb movement for 6 months [86, 87]. The only drawback of

implanting these electrode wires is the tedious surgery as each electrode is separately and manually implanted [88].

Grill et al. [89] used iridium electrodes with diameters of 50µm and 75µm and 1-3µm tip to successfully simulate the spinal cord of anesthetised cats to evoke the pressure in the bladder and urethra. The microelectrode wires were insulated with either Epoxylite or parylene except for the tips. Again, the wires were implanted separately which makes the surgery tedious.

Yoshida et al. implanted intrafascicular electrodes (with no base) in isolated spinal cord of mudpuppies [90]. The 60-75µm diameter electrodes were made of Platinum/Iridium (90% / 10%) with Teflon insulation. The active sites length was between 250 and 500µm. The electrodes were successful in stimulating and recording from the isolated spinal cord [90]. However, no chronic implantation was done. In case of chronic implantation the major issue would be the fixation of the lead wires. An external force caused on the lead wires should not transfer to the electrodes because of the potential drag affect which can physically damage the spinal cord. Also, the implantation time and precision would be another critical issue as each electrode has to be implanted separately.

Snow et al. 2006, tested individual electrodes on a setup, saran wrap over tofu, suggested by Mushahwar to resemble the spinal cord [91]. These standard optical fiber electrodes were 85µm in diameter, 4.4mm in length and had 40-80µm tapered polyimide tip. Gold stimulation sites, electroplated with iridium, and traces were patterned and insulated with polyimide. The contact pads were wire bonded to gold lead wires that connected with the control module.

Standard optical fiber was chosen due to its flexibility as it can withstand repeatable bending cycles without getting damaged. Also, various tip shapes were tested and the slant tip was chosen as it gave the minimum insertion force. These cylindrical electrode sites were able to pass current without getting damaged. All the used materials were biocompatible; however, the degradation of polyimide under a voltage bias in 37°C [48] remains a big concern.

Interfacing with the spinal cord is very challenging. Most studies that have been done are based on arrays of individual electrodes with no base, which complicates the implantation procedure and proposes extra challenges, such as very long (several hours) operation time since each electrode has to be implanted separately. The long operation time increases the probability of human error which may lead to damaging the electrode or accidently damaging the spinal cord while implanting. Therefore, the need for a base is clear. The rigid-based arrays have huge stiffness mismatch with the spinal cord. This mismatch can lead to damaging the cord as it deforms. Thus, none of the proposed rigid-based arrays mentioned in section 3.1 would work for such an interface. The arrays that were proposed and tested by McCreery [16] for spinal cord interface did not cause any major damage because of the small thickness of the entire array (from base to electrode tip); however, no tests were performed on the effect of the array on the mechanical behaviour of the cord. Also, the flexible arrays mentioned in section 3.1.2 have buckling problems due to the flexibility of the electrodes. As a result, the major challenge is to create an array that would consider the different deformation scenarios of the spinal cord and still meet all the biological and mechanical challenges that have been mentioned above.

2.4. Conclusion

Both interface methodologies have proven to be effective in mapping and stimulating nerves. However, the intra-neural interference showed to be superior over epi-neural interface as it can selectively interface with minimal number of neural units. Thus, using intra-neural interface will allow a higher resolution for the minimal unit signal recording and a lower charge threshold, up to 3 orders of magnitude [68], for specific unit stimulation. This increases the mapping capabilities and decreases the probability of any tissue damage due to fatigue. The specificity and resolution goals raise many mechanical and biological challenges for building 3-D arrays that will be used for long-term chronic implantations. Some of these challenges are: Full contact between the nerve and the array to prevent any tissue growth, biocompatibility and long-term implantation

capabilities of the used materials, variable electrode layout to interface with specific neural locations, the design and material of base and the lead wires to decrease any external forces and increase mechanical compliance between the array and the neural target to prevent tissue damage.

None of the reviewed intra-neural interface arrays meet all of the above mentioned challenges: Most of them have rigid bases that are several orders of magnitude stiffer than that of the neural tissue. The flexible arrays [82, 83] are made of flexible electrodes and had implantation problems due to buckling. While the individual electrodes with no base are tedious to implant. Also, forces are transferred from the lead wires to the electrodes causing them to move and potentially damage tissue.

To optimize the three different designs, we propose a new generic design which consists of a flexible base (silicone-based polymer) with stiff electrodes. These intraneural arrays will be custom fit to different neural targets based on their geometry and mechanical properties. With the spinal cord as an application, several challenging limitations will be addressed with such an array; A biocompatible base that is gas permeable to allow gas (oxygen) exchange with the tissue, curvature matching between the array's surface and the spinal cord to ensure full contact, mechanical compliance between the two media which will make the base deform with the spinal cord (check figure 2.9 for potential directions of deformation) without causing any physical damage to the latter, a lead wire design which will not transfer any external forces to the array (stress relieved lead wires), and a short turn around fabrication process that would allow for the design (electrode layout) flexibility as each array will be patient specific. The array should maintain its structure which can be achieved through a temporary stiff layer that would be removed post implantation. Such design parameters will solve the problems of several of the existing arrays and increase their interface capabilities.

2.5. Bibliography

[1] "ISO 10993 - Wikipedia, the free encyclopedia." [Online]. Available: http://en.wikipedia.org/wiki/ISO_10993. [Accessed: 11-Dec-2010].

[2] D. Ingles, “ISO 10993, Part 18: A structured approach to material characterisation,” *Medical Device Technology*, vol. 14, no. 5, pp. 18-19, Jun. 2003.

[3] G. T. A. Kovacs, C. W. Storment, and J. M. Rosen, “Regeneration microelectrode array for peripheral nerve recording and stimulation,” *Biomedical Engineering, IEEE Transactions on*, vol. 39, no. 9, pp. 893-902, 1992.

[4] K. D. Wise and J. B. Angell, “A Low-Capacitance Multielectrode Probe for Use in Extracellular Neurophysiology,” *Biomedical Engineering, IEEE Transactions on*, vol. 22, no. 3, pp. 212-219, 1975.

[5] “Microbial Inactivation by UV Light,” in *Ultraviolet Light in Food Technology*, CRC Press, 2010, pp. 69-101.

[6] K. Ayoub, L. Harris, and B. Thompson, “Determination of low-level residual ethylene oxide by using solid-phase microextraction and gas chromatography,” *Journal of AOAC International*, vol. 85, no. 6, pp. 1205-1209, Dec. 2002.

[7] T. Harper et al., “Round-robin evaluation of a solid-phase microextraction-gas chromatographic method for reliable determination of trace level ethylene oxide in sterilized medical devices,” *Biomedical Chromatography: BMC*, vol. 22, no. 2, pp. 136-148, Feb. 2008.

[8] E. L. Dewhurst and E. Hoxey, “Sterilzation Methods,” in *Guide to Microbiological Control in Pharmaceuticals and Medical Devices*, Second., CRC Press, 2006, pp. 229-272.

[9] E. Hoxey, N. Thomas, and D. J. G. Davies, “Principles of Sterilization,” in *Guide to Microbiological Control in Pharmaceuticals and Medical Devices*, Second edition., CRC Press, 2006, pp. 197-228.

[10] G. E. Loeb and R. A. Peck, “Cuff electrodes for chronic stimulation and recording of peripheral nerve activity,” *Journal of Neuroscience Methods*, vol. 64, no. 1, pp. 95-103, Jan. 1996.

[11] K. W. Meacham, R. J. Giuly, L. Guo, S. Hochman, and S. P. DeWeerth, “A lithographically-patterned, elastic multi-electrode array for surface stimulation of the spinal cord,” *Biomedical Microdevices*, vol. 10, no. 2, pp. 259-269, Oct. 2007.

[12] D. H. Szarowski et al., “Brain responses to micro-machined silicon devices,” *Brain Research*, vol. 983, no. 1-2, pp. 23-35, Sep. 2003.

[13] T. G. Yuen, W. F. Agnew, L. A. Bullara, S. Jacques, and D. B. McCreery, “Histological evaluation of neural damage from electrical stimulation:

considerations for the selection of parameters for clinical application," *Neurosurgery*, vol. 9, no. 3, pp. 292-299, Sep. 1981.

[14] D. B. McCreery, W. F. Agnew, T. G. H. Yuen, and L. Bullara, "Charge density and charge per phase as cofactors in neural injury induced by electrical stimulation," *Biomedical Engineering, IEEE Transactions on*, vol. 37, no. 10, pp. 996-1001, 1990.

[15] B. A. Hollenberg, C. D. Richards, R. Richards, D. F. Bahr, and D. M. Rector, "A MEMS fabricated flexible electrode array for recording surface field potentials," *Journal of Neuroscience Methods*, vol. 153, no. 1, pp. 147-153, May 2006.

[16] D. McCreery, V. Pikov, A. Lossinsky, L. Bullara, and W. Agnew, "Arrays for chronic functional microstimulation of the lumbosacral spinal cord," *IEEE Transactions on Neural Systems and Rehabilitation Engineering: A Publication of the IEEE Engineering in Medicine and Biology Society*, vol. 12, no. 2, pp. 195-207, Jun. 2004.

[17] R. A. Normann, "Technology Insight: Future Neuroprosthetic Therapies for Disorders: The Neural Interface: The Utah Electrode Arrays." [Online]. Available: http://www.medscape.com/viewarticle/560817_2. [Accessed: 03-Nov-2010].

[18] G. Lundborg et al., "Nerve regeneration in silicone chambers: Influence of gap length and of distal stump components," *Experimental Neurology*, vol. 76, no. 2, pp. 361-375, May 1982.

[19] G. T. A. Kovacs, "Regeneration microelectrode arrays for direct interface to nerves," in *Solid-State Sensors and Actuators. Digest of Technical Papers, International Conference on TRANSDUCERS ,*, 1991, pp. 116-119.

[20] G. E. Loeb, W. B. Marks, and P. G. Beatty, "Analysis and microelectronic design of tubular electrode arrays intended for chronic, multiple singleunit recording from captured nerve fibres," *Medical & Biological Engineering & Computing*, vol. 15, no. 2, pp. 195-201, Mar. 1977.

[21] D. G. Stuart, "The research career of Richard B. Stein (1940-)," *Canadian Journal of Physiology and Pharmacology*, vol. 82, no. 8-9, pp. 531-540, Sep. 2004.

[22] W. B. Marks and G. E. Loeb, "Action currents, intermodal potentials, and extracellular records of myelinated mammalian nerve fibers derived from node potentials," vol. 16, pp. 655-668, 1976.

[23] R. B. Stein, T. R. Nichols, J. Jhamandas, L. Davis, and D. Charles, "Stable long-term recordings from cat peripheral nerves," *Brain Research*, vol. 128, no. 1, pp. 21-38, Jun. 1977.

[24] R. B. Stein, D. Charles, T. Gordon, J.-A. Hoffer, and J. Jhamandas, "Impedance Properties of Metal Electrodes for Chronic Recording from Mammalian Nerves," *Biomedical Engineering, IEEE Transactions on*, vol. 25, no. 6, pp. 532-537, 1978.

[25] G. G. Naples, J. T. Mortimer, and T. G. H. Yuen, "Overview of peripheral nerve electrode design and implantation," in *Neural Prostheses*, Englewood Cliffs, NJ: Prentice-Hall, 1990, pp. 107-145.

[26] S. B. Brummer, L. S. Robblee, and F. T. Hambrecht, "Criteria for selecting electrodes for electrical stimulation: theoretical and practical considerations," *Annals of the New York Academy of Sciences*, vol. 405, pp. 159-171, 1983.

[27] C. Van Den Honert and J. T. Mortimer, "A Technique for Collision Block of Peripheral Nerve: Single Stimulus Analysis," *Biomedical Engineering, IEEE Transactions on*, vol. 28, no. 5, pp. 373-378, 1981.

[28] G. E. Loeb and R. A. Peck, "Cuff electrodes for chronic stimulation and recording of peripheral nerve activity," *Journal of Neuroscience Methods*, vol. 64, no. 1, pp. 95-103, Jan. 1996.

[29] G. E. Loeb, B. Walmsley, and J. Duysens, "Obtaining proprioceptiveinformation from natural limbs: implantable transducers vs. somatosensoryneuron recordings," in *M.R. Neuman (Ed.), Physical Sensors for Biomedical Applications. Proc. Workshop on Solid State Physical Sensors for Biomedical Application*, Boca Raton, FL: CRC Press, 1980.

[30] C. Julien and S. Rossignol, "Electroneurographic recordings with polymer cuff electrodes in paralyzed cats," *Journal of Neuroscience Methods*, vol. 5, no. 3, pp. 267-272, Mar. 1982.

[31] G. G. Naples, J. T. Mortimer, A. Scheiner, and J. D. Sweeney, "A spiral nerve cuff electrode for peripheral nerve stimulation," *Biomedical Engineering, IEEE Transactions on*, vol. 35, no. 11, pp. 905-916, 1988.

[32] M. Sahin, M. A. Haxhiu, D. M. Durand, and I. A. Dreshaj, "Spiral nerve cuff electrode for recordings of respiratory output," *J Appl Physiol*, vol. 83, no. 1, pp. 317-322, Jul. 1997.

[33] P. D. Van der Puije, R. Shelley, and G. E. Loeb, "A self-spiralling thin-film nerve cuff electrode," in *19th Canadian Medical and Biological Engineering Conference*, 1993, pp. 186-187.

[34] M. Haugland, "A flexible method for fabrication of nerve cuff electrodes," in *Engineering in Medicine and Biology Society, 1996. Bridging Disciplines for Biomedicine. Proceedings of the 18th Annual International Conference of the IEEE*, 1996, vol. 1, pp. 359-360 vol.1.

[35] M.-A. Crampon, M. Sawan, V. Brailovski, and F. Trochu, “New nerve cuff electrode based on a shape memory alloy armature,” in *Engineering in Medicine and Biology Society, 1998. Proceedings of the 20th Annual International Conference of the IEEE*, 1998, vol. 5, pp. 2556-2559 vol.5.

[36] D. J. Tyler and D. M. Durand, “Functionally selective peripheral nerve stimulation with a flat interface nerve electrode,” *Neural Systems and Rehabilitation Engineering, IEEE Transactions on*, vol. 10, no. 4, pp. 294-303, 2002.

[37] A. V. Caparso, D. M. Durand, and J. M. Mansour, “A Nerve Cuff Electrode for Controlled Reshaping of Nerve Geometry,” *Journal of Biomaterials Applications*, vol. 24, no. 3, pp. 247-273, Nov. 2008.

[38] S. H. Lee, J. H. Jung, Y. M. Chae, J.-K. F. Suh, and J. Y. Kang, “Fabrication and characterization of implantable and flexible nerve cuff electrodes with Pt, Ir and IrO films deposited by RF sputtering,” *Journal of Micromechanics and Microengineering*, vol. 20, no. 3, p. 035015, Mar. 2010.

[39] A. E. Grumet, Wyatt, and Rizzo, “Multi-electrode stimulation and recording in the isolated retina,” *Journal of Neuroscience Methods*, vol. 101, no. 1, pp. 31-42, Aug. 2000.

[40] V. K. Mushahwar and K. W. Horch, “Proposed specifications for a lumbar spinal cord electrode array for control of lower extremities in paraplegia,” *IEEE Transactions on Rehabilitation Engineering: A Publication of the IEEE Engineering in Medicine and Biology Society*, vol. 5, no. 3, pp. 237-243, Sep. 1997.

[41] D. R. Nisbet, K. E. Crompton, M. K. Horne, D. I. Finkelstein, and J. S. Forsythe, “Neural tissue engineering of the CNS using hydrogels,” *Journal of Biomedical Materials Research Part B: Applied Biomaterials*, vol. 87, no. 1, pp. 251-263, Oct. 2008.

[42] Z. Taylor and K. Miller, “Reassessment of brain elasticity for analysis of biomechanisms of hydrocephalus,” *Journal of Biomechanics*, vol. 37, no. 8, pp. 1263-1269, Aug. 2004.

[43] K. F. Doerner, “Nerve impulse propagation affected by sol-gel changes in axoplasm,” *Journal of Theoretical Biology*, vol. 32, no. 1, pp. 159-164, Jul. 1971.

[44] D. C. Rodger et al., “Flexible MicrofabricatedParylene Multielectrode Arraysfor Retinal Stimulation and Spinal Cord Field Modulation,” in *Technical Digest*, Okinawa, Japan, 2006.

[45] D. McCreery, A. Lossinsky, V. Pikov, and X. Liu, “Microelectrode array for chronic deep-brain microstimulation and recording,” *IEEE Transactions on Bio-Medical Engineering*, vol. 53, no. 4, pp. 726-737, Apr. 2006.

[46] R. A. Normann, E. M. Maynard, K. S. Guillory, and D. J. Warren, “Cortical implants for the blind,” *Spectrum, IEEE*, vol. 33, no. 5, pp. 54-59, 1996.

[47] S. A. Boppart, B. C. Wheeler, and C. S. Wallace, “A flexible perforated microelectrode array for extended neural recordings,” *IEEE Transactions on Bio-Medical Engineering*, vol. 39, no. 1, pp. 37-42, Jan. 1992.

[48] D. J. Edell, “Coatings for protection of integrated circuits,” Biomedical Microelectronics Lab, Quarterly Prog. Rep. NIH Ninth, Dec. 1989.

[49] K. Molina-Luna et al., “Cortical stimulation mapping using epidurally implanted thin-film microelectrode arrays,” *Journal of Neuroscience Methods*, vol. 161, no. 1, pp. 118-125, Mar. 2007.

[50] A. Stett, W. Barth, S. Weiss, H. Haemmerle, and E. Zrenner, “Electrical multisite stimulation of the isolated chicken retina,” *Vision Research*, vol. 40, no. 13, pp. 1785-1795, Jun. 2000.

[51] J. Kitzmiller, D. Beversdorf, and D. Hansford, “Fabrication and testing of microelectrodes for small-field cortical surface recordings,” *Biomedical Microdevices*, vol. 8, no. 1, pp. 81-85, Mar. 2006.

[52] J. D. Yeager, D. J. Phillips, D. M. Rector, and D. F. Bahr, “Characterization of flexible ECoG electrode arrays for chronic recording in awake rats,” *Journal of Neuroscience Methods*, vol. 173, no. 2, pp. 279-285, Aug. 2008.

[53] Z. Yu, O. Graudejus, C. Tsay, S. P. Lacour, S. Wagner, and B. Morrison, “Monitoring hippocampus electrical activity in vitro on an elastically deformable microelectrode array,” *Journal of Neurotrauma*, vol. 26, no. 7, pp. 1135-1145, Jul. 2009.

[54] G. Liang, K. K. Williams, R. J. Giuly, and S. P. DeWeerth, “A PDMS-based Elastic Multi-Electrode Array for Spinal Cord Surface Stimulation and Its Electrode Modification to Enhance Performance,” 2007.

[55] D.-H. Kim et al., “Dissolvable films of silk fibroin for ultrathin conformal bio-integrated electronics,” *Nat Mater*, vol. 9, no. 6, pp. 511-517, Jun. 2010.

[56] R. B. North, “Neural Interface Devices: Spinal Cord Stimulation Technology,” *Proceedings of the IEEE*, vol. 96, no. 7, pp. 1108-1119, 2008.

[57] R. Melzack and P. D. Wall, “Pain mechanisms: a new theory,” *Science (New York, N.Y.)*, vol. 150, no. 699, pp. 971-979, Nov. 1965.

[58] P. D. Wall and W. H. Sweet, “Temporary Abolition of Pain in Man,” *Science*, vol. 155, no. 3758, pp. 108-109, Jan. 1967.

[59] C. N. Shealy, J. T. Mortimer, and J. B. Reswick, “Electrical inhibition of pain by stimulation of the dorsal columns: preliminary clinical report,” *Anesthesia and Analgesia*, vol. 46, no. 4, pp. 489-491, Aug. 1967.

[60] G. Barolat and A. D. Sharan, “Future trends in spinal cord stimulation,” *Neurological Research*, vol. 22, no. 3, pp. 279-284, Apr. 2000.

[61] “Chronic, Intractable Pain.” [Online]. Available: http://www.ifess.org/Services/Consumer_Ed/Pain_Modulation.htm. [Accessed: 19-Nov-2010].

[62] A. Mailis-Gagnon, A. D. Furlan, MD PhD, J. A. Sandoval, and R. S. Taylor, “Spinal cord stimulation for chronic pain,” in *Cochrane Database of Systematic Reviews*, The Cochrane Collaboration and A. Mailis-Gagnon, Eds. Chichester, UK: John Wiley & Sons, Ltd, 2004.

[63] D. Zhou, *Implantable neural prostheses*. Dordrecht ;;New York: Springer Verlag, 2009.

[64] D. Rodger et al., “Flexible parylene-based multielectrode array technology for high-density neural stimulation and recording,” *Sensors and Actuators B: Chemical*, vol. 132, no. 2, pp. 449-460, Jun. 2008.

[65] E. L. Mazuchowski and L. E. Thibault, “Biomechanical Properties of the Human Spinal Cord and Pia Mater,” presented at the Summer Bioengineering Conference, Sonesta Beach Resort in Key Biscayne, Florida, 2003, pp. 1205,1206.

[66] A. Branner, R. B. Stein, and R. A. Normann, “Selective Stimulation of Cat Sciatic Nerve Using an Array of Varying-Length Microelectrodes,” *J Neurophysiol*, vol. 85, no. 4, pp. 1585-1594, Apr. 2001.

[67] K. D. Wise, “Silicon microsystems for neuroscience and neural prostheses,” *Engineering in Medicine and Biology Magazine, IEEE*, vol. 24, no. 5, pp. 22-29, 2005.

[68] P. J. Rousche and R. A. Normann, “Chronic intracortical microstimulation (ICMS) of cat sensory cortex using the Utah intracortical electrode array,” *Rehabilitation Engineering, IEEE Transactions on*, vol. 7, no. 1, pp. 56-68, 1999.

[69] K. D. Wise, J. B. Angell, and A. Starr, “An Integrated-Circuit Approach to Extracellular Microelectrodes,” *Biomedical Engineering, IEEE Transactions on*, vol. 17, no. 3, pp. 238-247, 1970.

[70] P. K. Campbell, K. E. Jones, R. J. Huber, K. W. Horch, and R. A. Normann, “A silicon-based, three-dimensional neural interface: manufacturing processes for an intracortical electrode array,” *Biomedical Engineering, IEEE Transactions on*, vol. 38, no. 8, pp. 758-768, 1991.

[71] “Implants and thought control.” [Online]. Available: http://www.wireheading.com/misc/implant.html. [Accessed: 11-Mar-2011].

[72] D. D. Zhou and E. Greenbaum, *Implantable Neural Prostheses 1: Devices and Applications*. Springer, 2009.

[73] P. J. Rousche and R. A. Normann, “Chronic recording capability of the Utah Intracortical Electrode Array in cat sensory cortex,” *Journal of Neuroscience Methods*, vol. 82, no. 1, pp. 1-15, Jul. 1998.

[74] “Imaging of Utah Electrode Array, Implanted in Cochlear Nerve.” [Online]. Available: http://www.sci.utah.edu/~gk/abstracts/bisti03/. [Accessed: 03-Dec-2010].

[75] A. C. Hoogerwerf and K. D. Wise, “A three-dimensional microelectrode array for chronic neural recording,” *IEEE Transactions on Bio-Medical Engineering*, vol. 41, no. 12, pp. 1136-1146, Dec. 1994.

[76] Qing Bai, K. D. Wise, and D. J. Anderson, “A high-yield microassembly structure for three-dimensional microelectrode arrays,” *Biomedical Engineering, IEEE Transactions on*, vol. 47, no. 3, pp. 281-289, 2000.

[77] D. R. Kipke, R. J. Vetter, J. C. Williams, and J. F. Hetke, “Silicon-substrate intracortical microelectrode arrays for long-term recording of neuronal spike activity in cerebral cortex,” *Neural Systems and Rehabilitation Engineering, IEEE Transactions on*, vol. 11, no. 2, pp. 151-155, 2003.

[78] W. Jensen, K. Yoshida, and U. G. Hofmann, “In-vivo implant mechanics of flexible, silicon-based ACREO microelectrode arrays in rat cerebral cortex,” *Biomedical Engineering, IEEE Transactions on*, vol. 53, no. 5, pp. 934-940, 2006.

[79] U. G. Hofmann et al., “TOWARDS A VERSATILE SYSTEM FOR ADVANCED NEURONAL RECORDINGS USING SILICON MULTISITE MICROELECTRODES.,” *Biomedizinische Technik/Biomedical Engineering*, vol. 45, no. 1, pp. 169-170, Jan. 2000.

[80] J. C. Williams, R. L. Rennaker, and D. R. Kipke, “Long-term neural recording characteristics of wire microelectrode arrays implanted in cerebral

cortex," *Brain Research. Brain Research Protocols*, vol. 4, no. 3, pp. 303-313, Dec. 1999.

[81] H. Scherberger et al., "Magnetic resonance image-guided implantation of chronic recording electrodes in the macaque intraparietal sulcus," *Journal of Neuroscience Methods*, vol. 130, no. 1, pp. 1-8, Nov. 2003.

[82] P. J. Rousche, D. S. Pellinen, D. P. Pivin, J. C. Williams, R. J. Vetter, and D. R. kirke, "Flexible polyimide-based intracortical electrode arrays with bioactive capability," *Biomedical Engineering, IEEE Transactions on*, vol. 48, no. 3, pp. 361-371, 2001.

[83] S. Takeuchi, T. Suzuki, K. Mabuchi, and H. Fujita, "3D flexible multichannel neural probe array," *Journal of Micromechanics and Microengineering*, vol. 14, no. 1, pp. 104-107, Jan. 2004.

[84] H. Friedman, B. S. Nashold Jr, and P. Senechal, "Spinal cord stimulation and bladder function in normal and paraplegic animals," *Journal of Neurosurgery*, vol. 36, no. 4, pp. 430-437, Apr. 1972.

[85] V. K. Mushahwar and K. W. Horch, "Selective activation of muscle groups in the feline hindlimb through electrical microstimulation of the ventral lumbo-sacral spinal cord," *IEEE Transactions on Rehabilitation Engineering: A Publication of the IEEE Engineering in Medicine and Biology Society*, vol. 8, no. 1, pp. 11-21, Mar. 2000.

[86] V. K. Mushahwar, D. F. Collins, and A. Prochazka, "Spinal Cord Microstimulation Generates Functional Limb Movements in Chronically Implanted Cats," *Experimental Neurology*, vol. 163, no. 2, pp. 422-429, Jun. 2000.

[87] J. A. Bamford, C. T. Putman, and V. K. Mushahwar, "Intraspinal microstimulation preferentially recruits fatigue-resistant muscle fibres and generates gradual force in rat," *The Journal of Physiology*, vol. 569, no. 3, pp. 873-884, Dec. 2005.

[88] V. K. Mushahwar, P. L. Jacobs, R. A. Normann, R. J. Triolo, and N. Kleitman, "New functional electrical stimulation approaches to standing and walking," *Journal of Neural Engineering*, vol. 4, no. 3, p. S181-S197, Sep. 2007.

[89] W. M. Grill, N. Bhadra, and B. Wang, "Bladder and urethral pressures evoked by microstimulation of the sacral spinal cord in cats," *Brain Research*, vol. 836, no. 1-2, pp. 19-30, Jul. 1999.

[90] K. Yoshida, K. Jovanovic, and R. B. Stein, "Intrafascicular electrodes for stimulation and recording from mudpuppy spinal roots," *Journal of Neuroscience Methods*, vol. 96, no. 1, pp. 47-55, Mar. 2000.

[91] S. Snow, S. C. Jacobsen, D. L. Wells, and K. W. Horch, “Microfabricated cylindrical multielectrodes for neural stimulation,” *Biomedical Engineering, IEEE Transactions on*, vol. 53, no. 2, pp. 320-326, 2006.

Chapter 3

Array Design

The goal of this work is to develop a multi-electrode array that does not cause physical damage to the spinal cord when implanted. The first step in the design process is to develop a finite element model that would examine the interaction between the different designs of the array and the spinal cord. Such a model would help to determine the optimal array specifications.

A 2D numerical model was developed using ANSYS 11.0 (Figure 3.1). The cord and the array base were assumed to be elastic. The electrodes were assumed to be 4mm in height and in full contact with the spinal cord. A cord diameter and length of 7.5mm 40mm respectively were assumed to resemble the experimental setup introduced later in this chapter. The modulus of elasticity of the cord was assumed to be 90kPa [1]. Finally, an eight node quadrilateral element with two degrees of freedom was used to mesh the model. The element used has large deflection and strain capabilities.

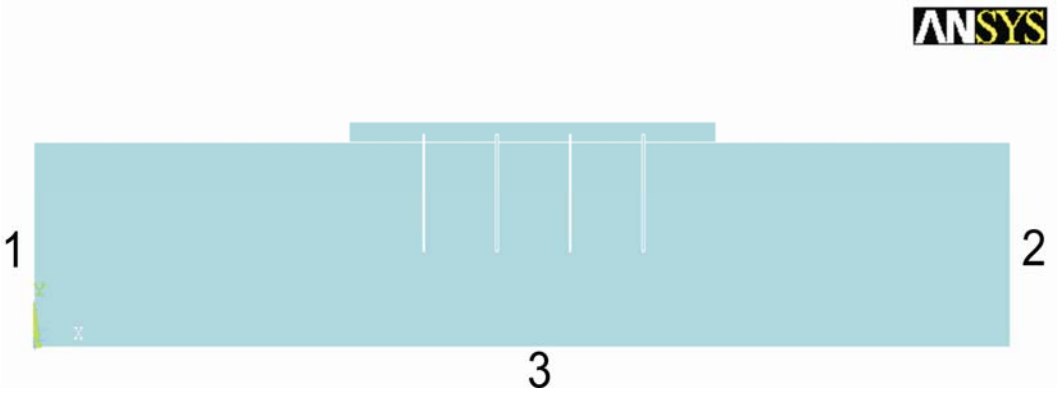

Figure 3.1 *Finite element model developed on ANSYS 11.0.* The model shows an array with 4 electrodes implanted on the cords. Boundaries 1 to 3 are specified in the figure**.**

In the following sections, the influence of various parameters of the array on the mechanical interaction between the multi-electrode array and the cord is studied. To study this interaction, the experimental methodology developed by Cheng et al. is simulated [3]. A 12% elongation on the cord is applied and the deformations along the cord are studied. The applied 12% is the maximum strain measured for a human spinal cord during daily activities [2]. The deformation values are used to calculate the strains across the cord. Assuming that the cord is isotropic, any change in the strains applied across the cord implicates the effect of the array on

the mechanical behaviour of the cord. To measure the strains across the cord, similar to the experimental method, two rows of reference nodes are selected. A row is chosen on the top part of the cord to study the direct impact of the array. The second row is chosen at the bottom of the cord to study the behaviour of the cord that is not in direct contact with the array. For each row, the nodes are placed along the longitudinal length of the electrode, from the extremities of the cord towards the middle part of the array. Figure 3.1 shows the model with the reference points. A set of 4 distances, L1-L4 were selected between the reference points. L1 refers to the area of the cord that is located at the middle of the array and L4 is the distance between the extremities of the cord. Each of the 4 distances were measured before and after applying the 12% strain and the strains were determined accordingly.

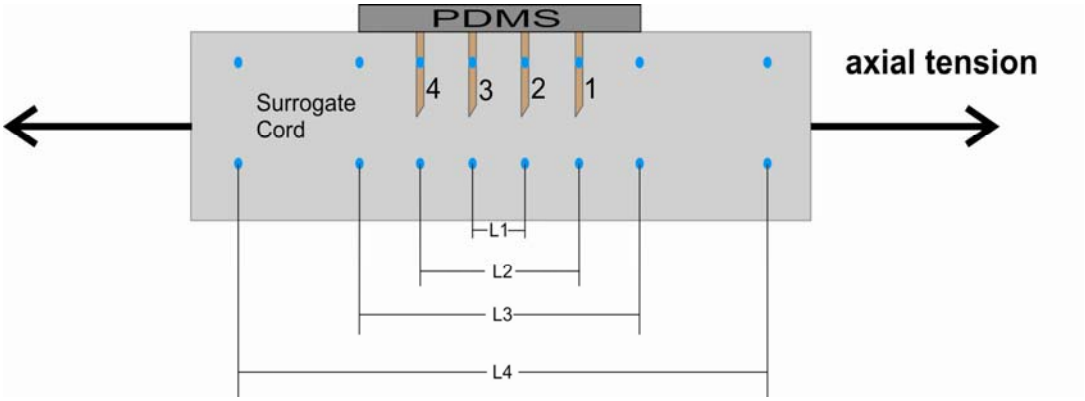

Figure 3.2 *Schematic of the strain test*. The selected distances between the reference dots are shown as L1 to L4.

Boundary 2 (Figure 3.1) was deformed by 12% of the cord initial length (Figure 3.2). The deformation was applied in the x-direction (Figure 3.1). Boundary 1 was fixed in the x and y directions. Boundary 3 was constrained from moving in the y-direction. The electrodes were assumed to be in full contact with the cord. No constraints were applied on the base.

The influence of different geometrical aspects of the array such as the base thickness, electrode diameter and the number of electrodes are examined. The influence of mechanical properties of the different components of the array is also

assessed. In particular, the effect of the change in the modulus of elasticity of the base and the electrodes is studied. The influence of each of the above mentioned parameters is studied by plotting the strains across the cord against the determined distances. The effect of the change of each parameter on the mechanical behaviour of the spinal cord is examined. Finally, the optimal design specifications for a multi-electrode electrode array that would be used to interface with the spinal cord are determined.

3.1 Influence of different geometrical aspects of array

In this section, the effect of changing the geometrical parameters of the different parts of the array on the mechanical interaction between the multi-electrode array and the spinal cord is presented. The studied geometrical aspects are: base thickness, electrode diameter and number of electrodes.

3.1.1. Base thickness

The axial stiffness (equation 3.1) of a structure is directly proportional to the area of the structure and thus the thickness.

$$K=\frac{EA}{L} \ldots\ldots. (3.1)$$

A_C= thickness * width……. (3.2)

From equation 3.1, an increase in the thickness causes an increase in the stiffness. To study the influence of this stiffness change, the finite element model is used to study the mechanical behaviour of the cord when implanted with arrays having different base thicknesses and subjected to the 12% uni-axial strain. The strains along the cord are measured from L1 to L4 as mentioned above. The electrodes diameter was fixed to 80µm and the modulus of elasticity of the base was assumed to be 500kPa. These values were assumed to resemble the values obtained through the experimental work that is presented in chapter 4. While keeping the above mentioned parameters constant, the effect of multiple base thicknesses varying from 0.5mm to 1.75mm in steps of 0.25mm is studied. The

0.75mm thick to 1.75mm thick bases were fabricated experimentally as we will show in chapter 4. The 0.5mm thick bases was also developed; however, it was not repeatable. The measured strains are presented in figure 3.2.

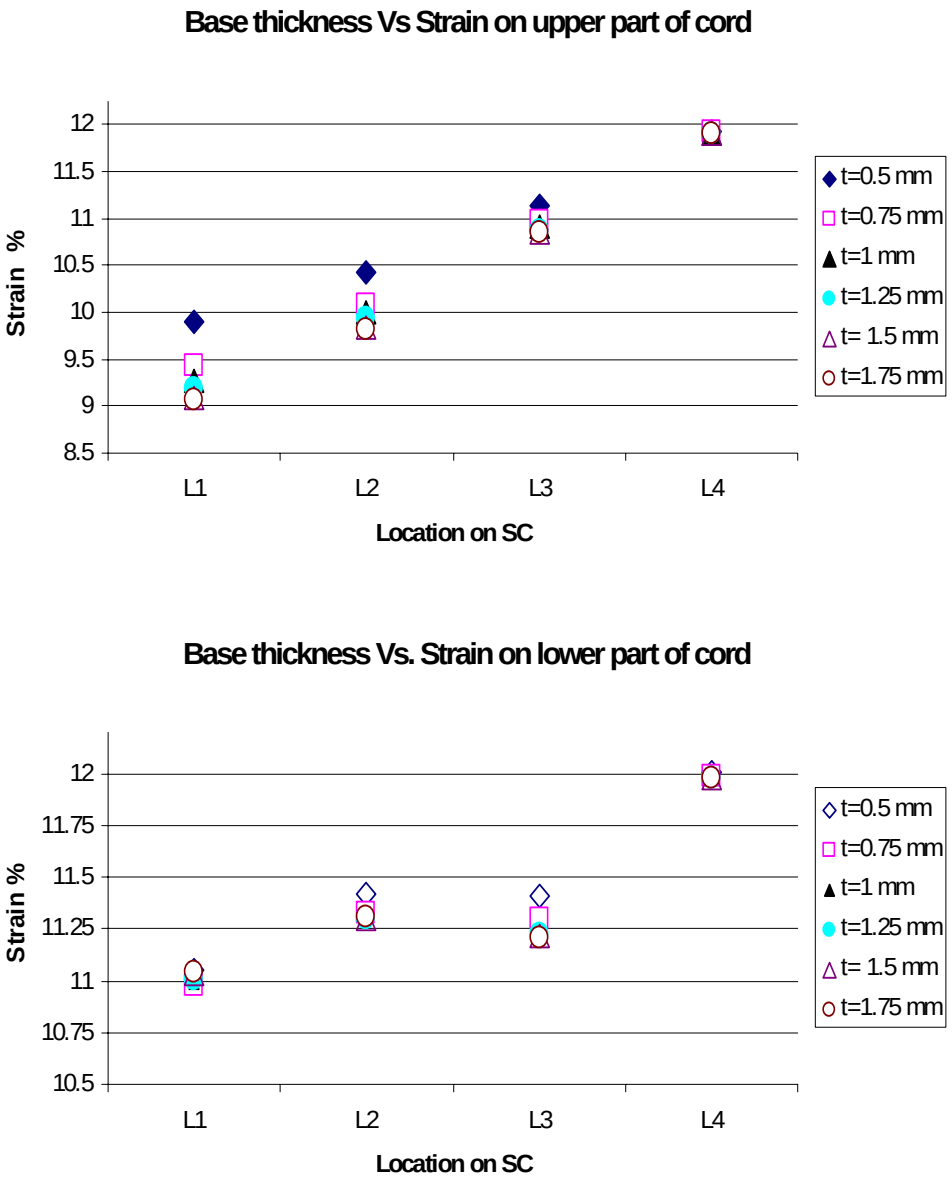

Figure 3.3 Influence of base thickness on the mechanical interaction between multi-electrode array and spinal cord.

The two plots above show that the base thickness has an effect on the mechanical interaction between the multi-electrode array and the spinal cord. When

decreasing the base thickness from 1.75mm to 0.5mm, the measured strains between the reference nodes on the upper part of the cord showed a significant increase. The strain at L1, which is the distance between the two reference nodes chosen at the inner two electrodes, shows 0.9% increase. The strains measured at L2 and L3 also increased (0.7 and 0.3% respectively). L4 which is the strain between the extremities of the cord did not change when varying the thickness and remained at 12% which is the applied strain.

On the other hand, the strains measured between the reference nodes at the bottom of the cord show a less significant change in the mechanical interaction between the two interfacing media due to change in the base thickness. The maximum change in the measured strains is 0.2%.

The results presented in figure 4.2 show that the array thickness has a significant influence on the mechanical properties of the upper part of the spinal cord, which directly interacts with the array. This influence becomes less significant at the bottom part of the cord. This influence is caused by the change in the stiffness of the array, thus the change in the mechanical compliance between the array and the cord. Higher thicknesses cause higher stiffness of the array leading to lower measured strains; i.e. higher motion impedance.

3.1.2. Electrode diameter

The second studied parameter is the electrode diameter. In this section, the effect of the change in the electrode diameter on the mechanical behaviour of the spinal cord, when exposed to a 12% uni-axial strain, is studied. Experimentally, four different microwire electrode diameters were available. Thus, four models were created with four different electrode diameters. The four modeled diameters were 30µm, 50µm, 70µm and 80µm. For these models, the base thickness and modulus of elasticity were fixed at 1mm and 500kPa to resemble the experimental work. Figure 3.4 presents the strains obtained between the reference nodes on the upper and lower parts of the cord.

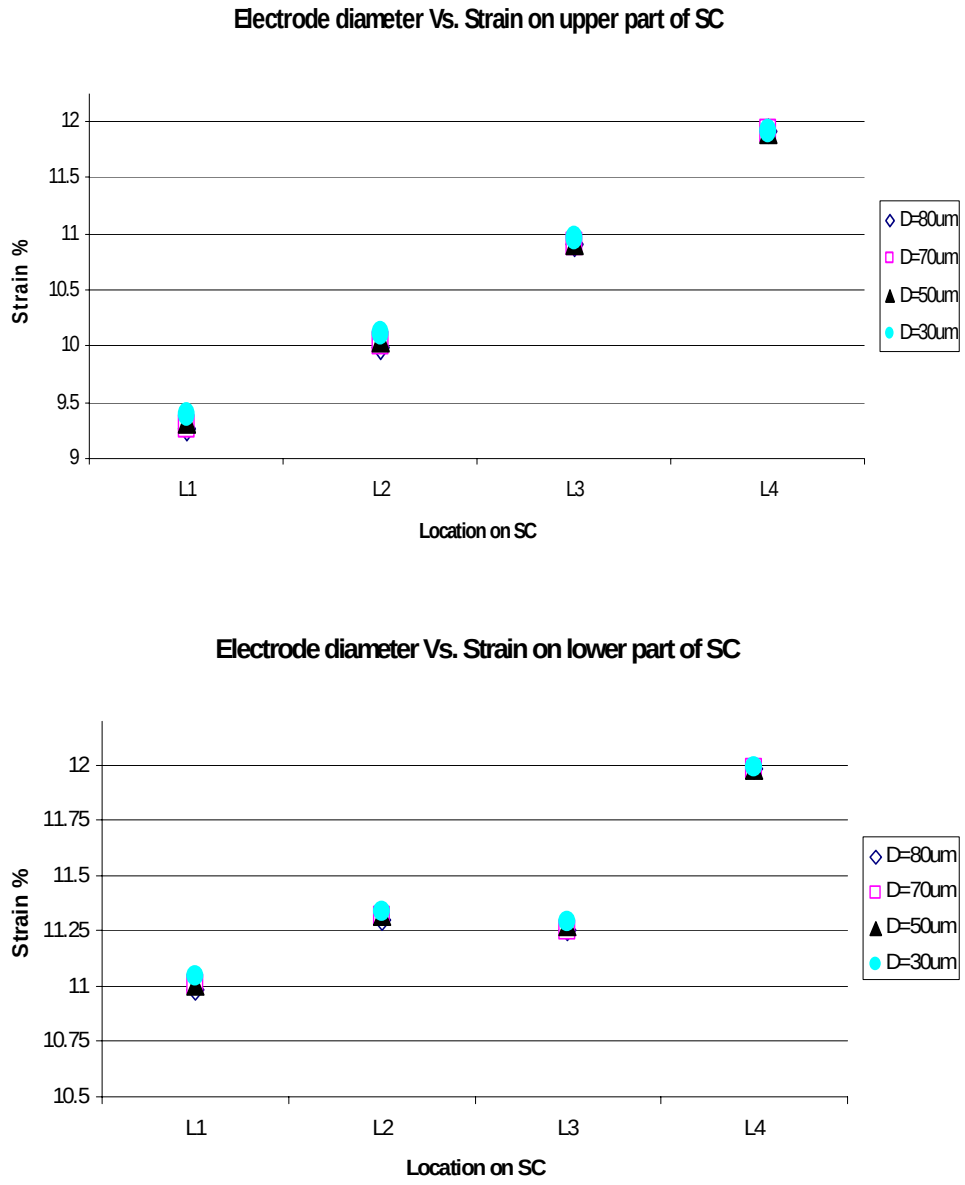

Figure 3.4 Influence of electrode diameter on the mechanical interaction between multi-electrode array and spinal cord.

The strains measured at the upper part and the lower parts of the cord do not show any significant variation when changing the electrode diameter. The largest variation is less than 0.12% for the upper and the lower parts of the spinal cord. This indicates that the implanted electrode diameter does not have a significant influence on the mechanical behaviour of the spinal cord when axially strained. The electrode size and the change at such a small scale, order of micrometers, do

not mechanically affect the tissue of the spinal cord. However, it should be noted the electrodes with smaller diameters have higher potential of buckling, while electrode with higher diameters cause more tissue displacement, thus more pronounced body reaction. Wires up to 85µm in diameter have been reported in the literature.

3.1.3. Number of electrodes

Arrays used for interfacing with the spinal cord are less dense than arrays used to interface with the brain. However, the number of the electrodes may vary according to the application and the case of the patient. Thus, it is critical to study the effect of the number of electrodes in the array on the mechanical interaction between the multi-electrode array and the cord. Three models were created with three different numbers of electrodes. The latter was varied between two and four. The number of electrodes was chosen to study their influence on the interaction and the trend they will cause in the strains measured along the cord. The base thickness and modulus of elasticity were also fixed at 1mm and 500kPa respectively. The electrode spacing was, also fixed at 3mm. The mechanical behaviour of the spinal cord implanted with these arrays is studied using the same uni-axial strain test. Figure 3.5 presents a comparison between the strains that were measured at the top and bottom parts of the cords implanted with arrays consisting of different number of electrodes.

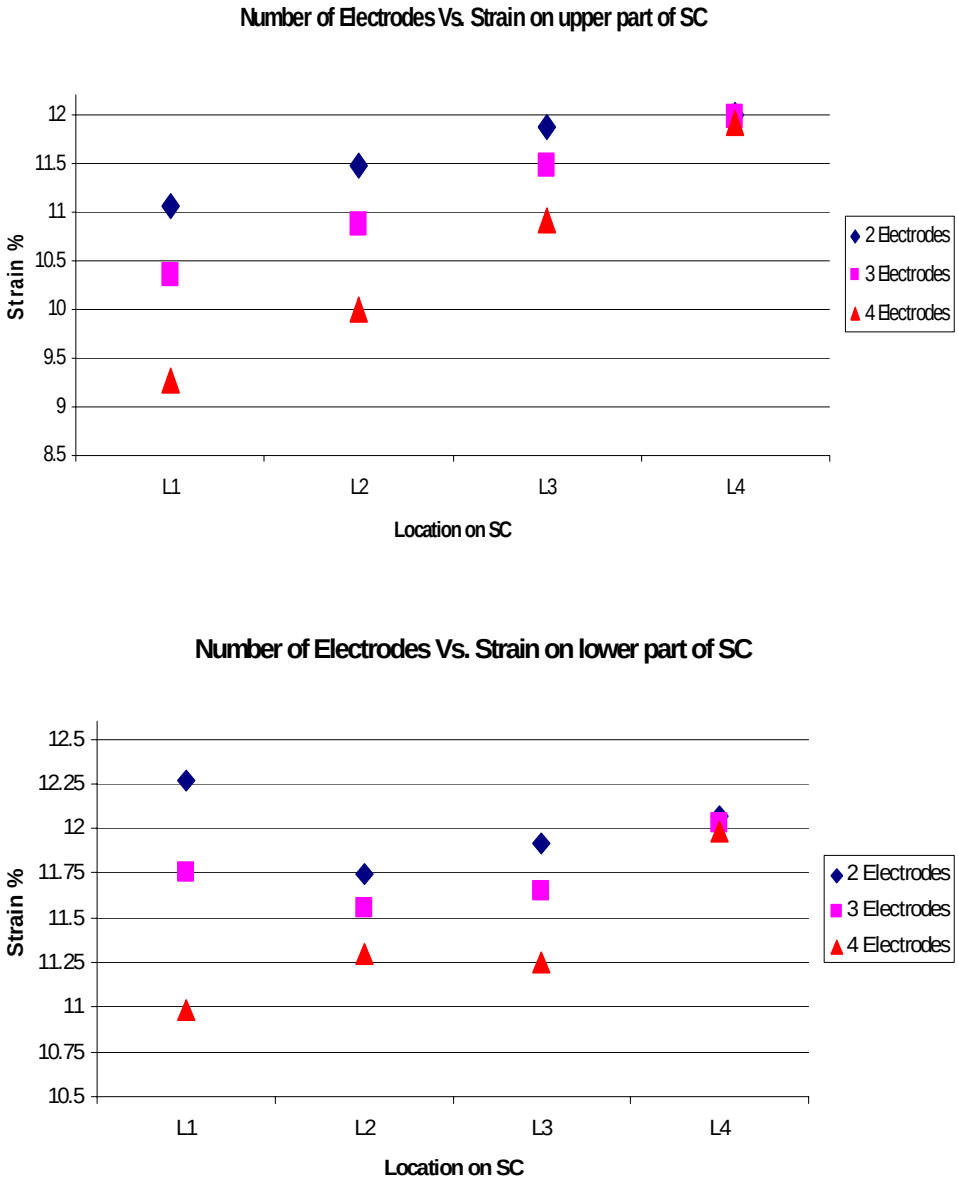

Figure 3.5 Influence of array structure (number of electrodes) on the mechanical interaction between the multi-electrode array and the spinal cord**.**

Figure 3.5 shows that the number of implanted electrodes in the multi-electrode array affects the mechanical behaviour of the spinal cord. The strains measured between the reference nodes on the upper and lower parts of the spinal cord change drastically with the change in the number of electrodes. L1 and L2 which are the distances under the electrodes show the largest variation in strains with respect to the change in the number of electrodes. In the upper part of the spinal

cord, the change in the electrode number from two to four causes a strain drop of 1.8% and 1.5% at L1 and L2 respectively. The strain drop is 1.3% for L1 and 0.5% for L2 in the lower part of the spinal cord.

Thus, the increase in the density of electrodes in the array causes higher deformation impedance to the spinal cord implanted with the array. This can be referred to better anchoring between the array and the cord. Higher density of electrodes gives higher interface surface area between the array and the cord. Thus, higher number of electrodes makes the mismatch in the mechanical properties between the base and the cord more pronounced.

3.2 Influence of material properties of the different components of the array

The previous sections showed that the geometry of the different components of the array play a critical role in the interaction between the multi-electrode array and the spinal cord. In the following two subsections, the influence of the material properties of the different components of the implanted array on the mechanical behaviour of the spinal cord is studied. In particular, the influence of the modulus of elasticity of the base and the electrodes on the interaction between the two interfacing media is examined.

3.2.1. Modulus of elasticity of the base

The axial stiffness of a structure is proportional to the modulus of elasticity as shown in equation 3.1. Thus, the modulus of elasticity of the base of the multi-electrode array is very critical in the interaction with the spinal cord. In this section, the effect of the change in the latter parameter on the interaction between the implanted intra-neural array and the spinal cord is presented. The modulus of elasticity of the array's base is varied from 500 kPa to 2 GPa. The lower bound represents a flexible-based array while the upper bound represents a hypothetical value of a rigid-based array. Figure 3.6 presents the strains calculated across the spinal cord when implanted with arrays having various moduli of elasticity.

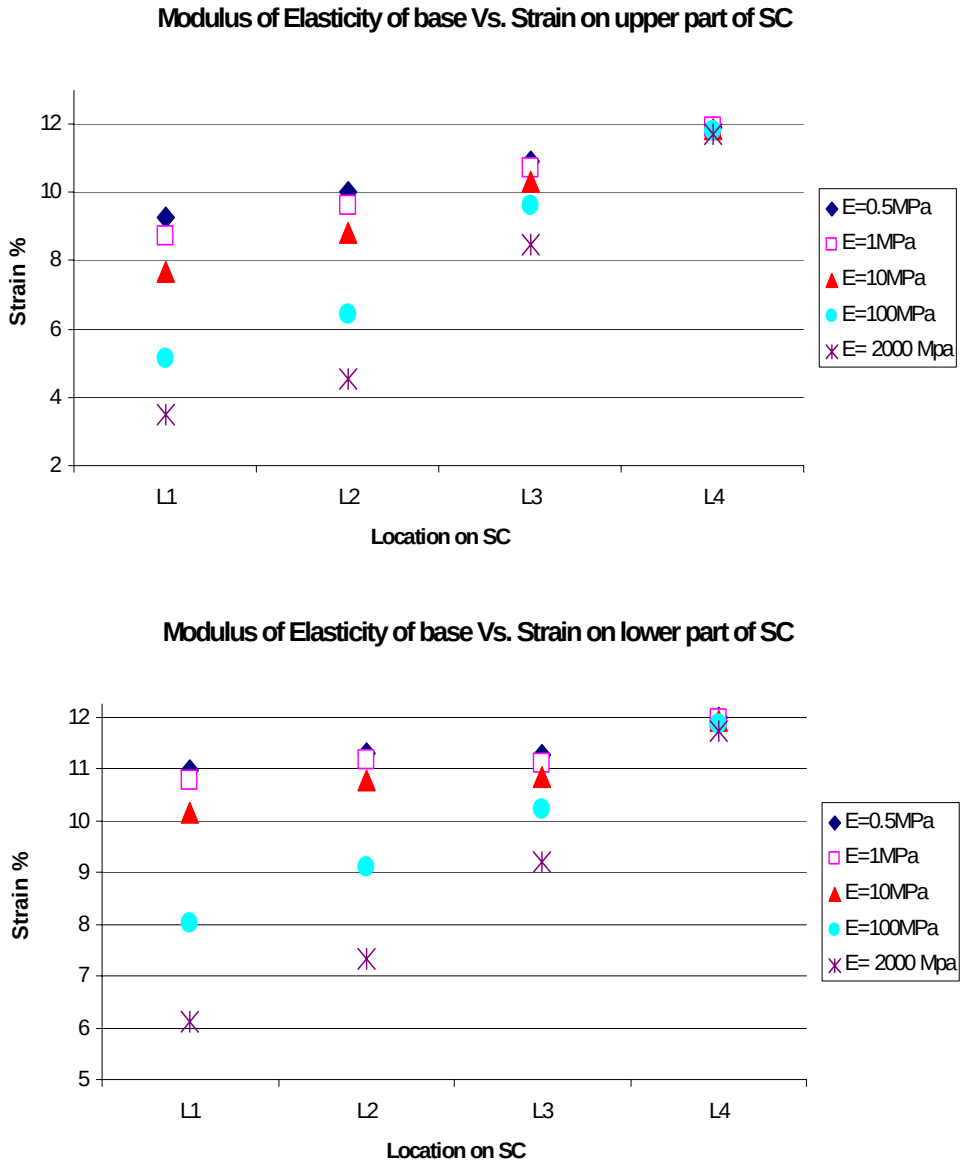

Figure 3.6 Influence of modulus of elasticity of base on the mechanical interaction between the multi-electrode array and the spinal cord.

As expected, the modulus of elasticity of the base has a major influence on the mechanical behaviour of the spinal cord implanted with an intra-neural array. The studied moduli of elasticity range between 500kPa, which represents a flexible-base, to 2GPa, which represents a rigid-base.

The strains measured between the reference nodes at the upper part of the cord show the big influence of the modulus of elasticity of the base. The change in the modulus of elasticity from 500kPa to 2GPa caused a drop of 5.8% in upper L1. This shows that the flexible base allows smaller motion impedance in the cord due to the smaller mismatch in the stiffness of the two media. The drop in the strains at the upper L2 is similar (5.5%) and smaller for the upper L3 (.2.4%) and no change for the upper L4 which represent the extremities of the cord.

On the other hand, the strains measured at the lower part of the spinal cord show a similar change due to the change in modulus of elasticity. The largest strain drop is measured again at the lower L1 to be equivalent to 4.9% when varying the modulus of elasticity from 500kPa to 2GPa. The strain change is similar for the lower L2 (4%), smaller for the lower L3 (2%) and no change for the lower L4.

The change in the modulus of elasticity of the base significantly influences the mechanical behaviour of the cord due to the proportional relationship between the modulus of elasticity and the stiffness of the array. The studied variations in the modulus of elasticity are large; the value of E is increased by 4000 times (from 0.5MPa to 2GPa). Stiffness of the base is proportional to this increase; thus, the mismatch in the mechanical properties between the two interacting media is more pronounced. This leads to higher motion impedance.

3.2.2. Modulus of elasticity of electrodes

Different materials can be used for the electrodes. As shown in the previous chapter, the common materials for our application are either platinum/iridium (Pt/Ir) or stainless steel (S.S) electrodes. These materials are used for various reasons, for example their compatibility with MRI and neural tissue and their electrical properties. To study the effect of the electrodes material properties, the modulus of elasticity of the electrodes is varied in the finite element model. The modulus is varied from 1GPa to 193GPa. The later is the modulus of elasticity of stainless steel which is higher than that of Pt/Ir. In these models, the base

thickness and modulus of elasticity were fixed at 1mm and 500kPa. The electrodes diameter was fixed at 80µm. These values, represent the arrays used experimentally. Figure 3.7 shows the strains measured for each model on the upper and lower parts of the cord.

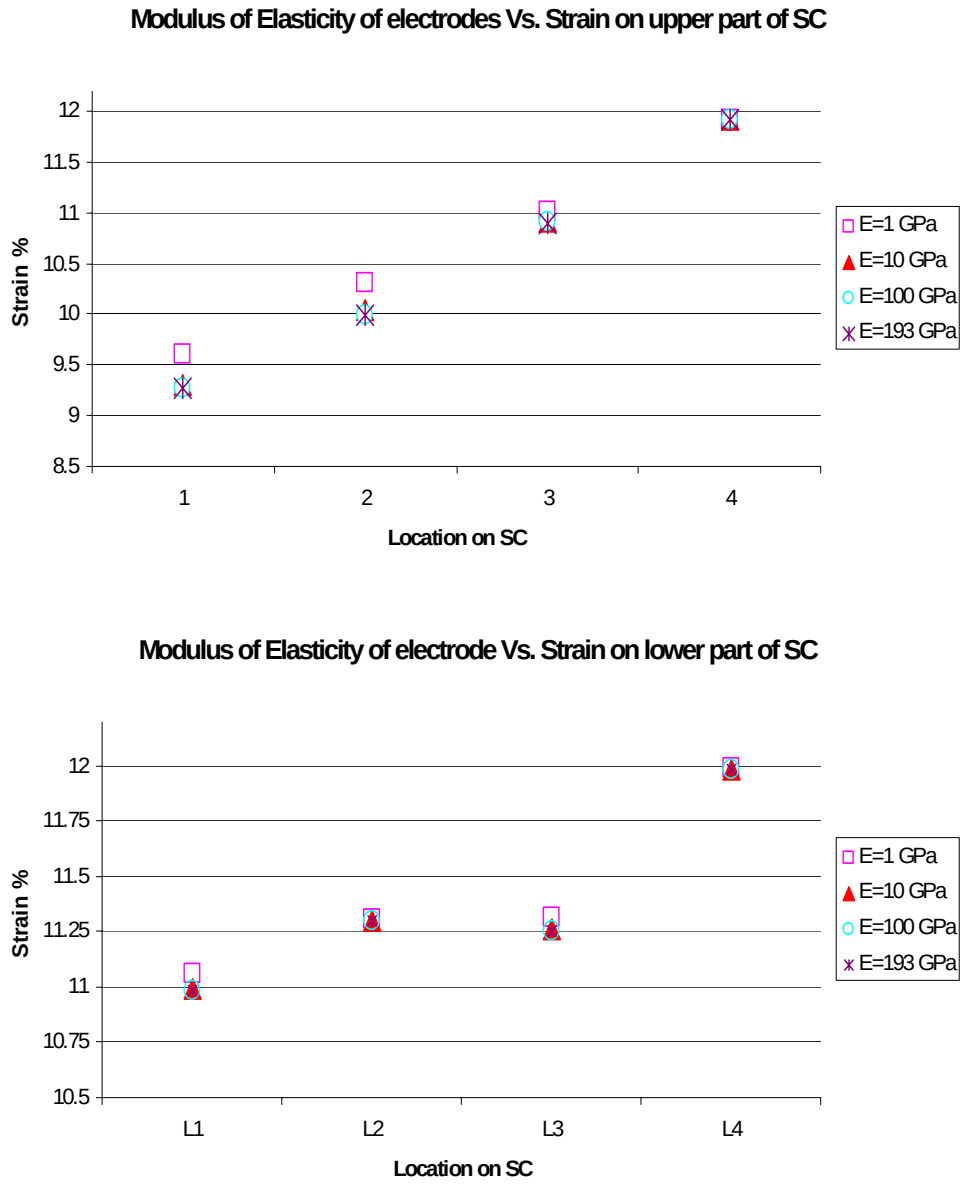

Figure 3.7 Influence of modulus of elasticity of electrodes on the mechanical interaction between the multi-electrode array and the spinal cord.

Figure 3.7 shows that the electrode material has no significant influence on the mechanical behaviour of the spinal cord when implanted with a 3D array. The

largest strain changes are 0.35% and 0.1% measured at L1 in the upper and lower parts of the cord respectively. However, it should be noted that this change is reported for electrodes with a modulus smaller than 10GPa. For moduli larger than 10GPa, the measured strains did not show any change. For our application, we use solid electrodes, thus moduli of elasticity greater than 10GPa is more realistic. The modulus of elasticity of both materials, Pt/Ir and S.S, are bigger than 100GPa. Thus, the electrode material does not have any significant influence on the mechanical behaviour of the spinal cord when implanted with a multi-electrode array and strained. This small significance is due to the small size of the electrodes compared to the size of the spinal cord.

3.3 Compliant Model

In this chapter, a two dimensional finite element model was presented. The model was used to study the influence of the geometrical and material properties of the components of an intra-neural array on the mechanical behaviour of the spinal cord. First, the influence of the geometry of the different components of the array on the mechanical interaction between the array and the spinal cord was studied. It was shown that the thickness of the base and the number of the electrodes have a pronounced influence on the mechanical behaviour of the spinal cord. On the other hand, the electrode diameter does not have any influence on the mechanical behaviour of the cord. However, the biological perspective should be considered. Higher electrode diameters tend to cause larger tissue deformation and thus more pronounced body reaction. Wires up to 85μm have been used in the literature without causing any damage.

Secondly, the influence of the modulus of elasticity of the base and the electrodes was studied. The results showed that the modulus of elasticity of the base has a pronounced influence on the mechanical behaviour of the spinal cord. The deformation of the cord was impeded drastically as the modulus of elasticity of the base increased to the order of Giga-Pascal. On the contrary, the modulus of

elasticity of the implanted electrodes did not affect the mechanical behaviour of the cord.

The above mentioned trends are used to obtain the design specifications of a multi-electrode array that would be mechanically compliant with the spinal cord. To develop such a design, the strains across a cord implanted with free unconstrained 80μm individual microwire electrodes were simulated, i.e. no-base array. The microwire electrodes were assumed to be in full contact with the spinal cord. The obtained trends are utilized to increase the mechanical compliance between the intra-neural array and the spinal cord. Assuming that 4x2 arrays are used, various combinations of base thickness and modulus of elasticity are manipulated and the behaviour of the spinal cord is studied. Figures 3.3 and 3.6 show that a decrease in the values of the latter two factors allows for an increase in the strains measured across the cord; i.e. less motion impedance. Assuming a minimum modulus of elasticity matching that of the SC, we decreased the thickness to simulate strains that are similar to the ones obtained with the individual wires. Figure 3.8 presents the strains measured across the longitudinal length of the cord when implanted with arrays with arrays having different axial stiffness.

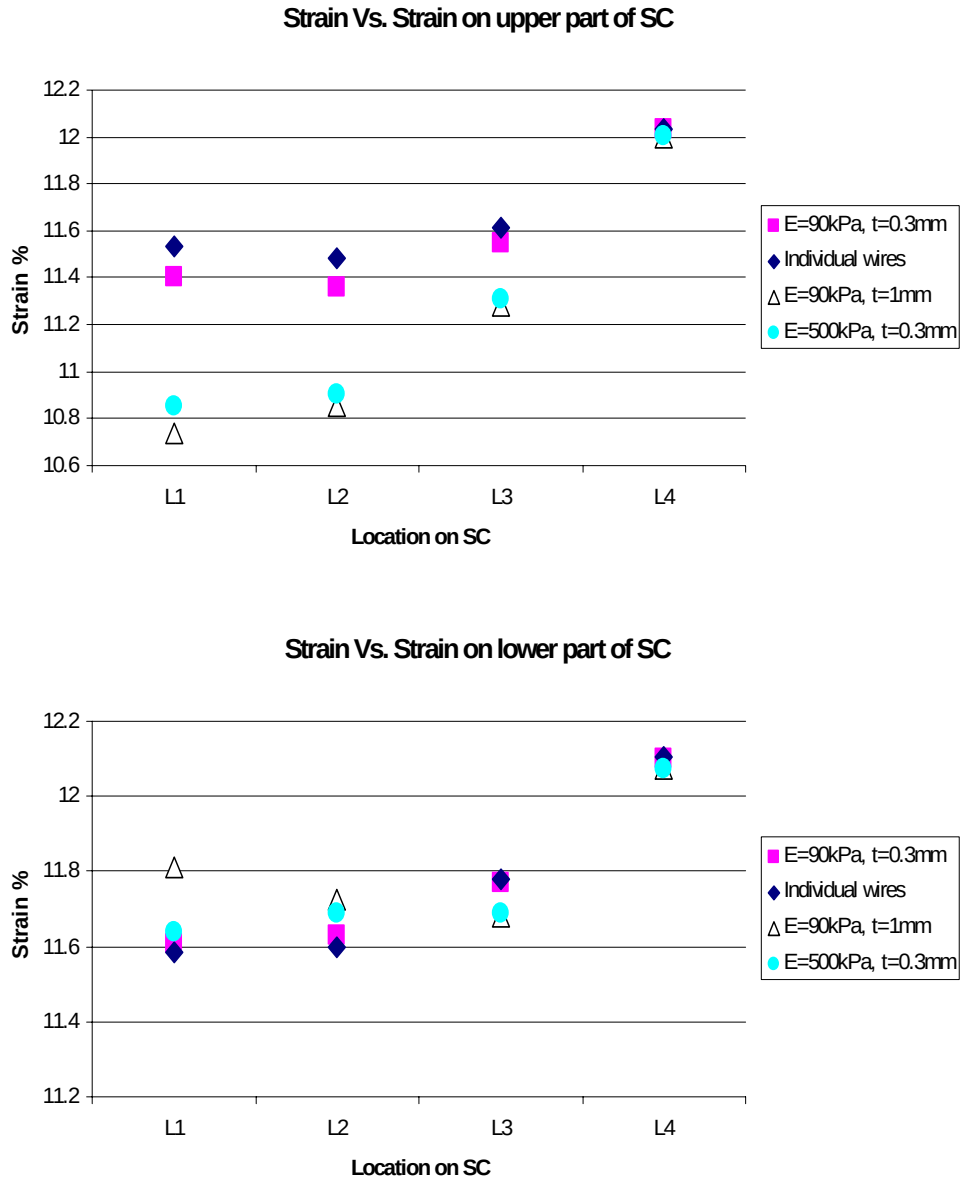

Figure 3.8 Behaviour of the spinal cord when implanted with individual wires and arrays having different combinations of modulus of elasticity and thickness.

The reference cord is the one implanted with individual wires. The goal of this test is to obtain the design specifications of a multi-electrode array that would allow deformations in the cord similar to the ones reported in the reference cord. First, the modulus of elasticity of the base is decreased to 90kPa while keeping the thickness at 1mm. The strains measured for cord are 0.8% less at L1 in the upper part of the cord and 0.2% higher at the bottom cord. Similar results are

observed for an array with a modulus of elasticity of 500kPa and a thickness of 0.3mm. For this array, the strain at L1 in the upper part of the cord is 0.7% less than the ones measured with the individual wires. The strain at L1 in the lower part of the cord is similar to the one measured for the cords implanted with individual wire.

The cords implanted with an array having a modulus of elasticity of 90kPa and a thickness of 0.3mm resembled the cords implanted with individual wires. At the upper part of the cord, the strains measured at L1 and L2 for the cords implanted with the flexible-based arrays are 0.1% smaller than those measured for the cords with the individual wires. At the lower part of the cord, the strains for cords implanted with both kinds of arrays are similar. Thus, the optimal array that would be used to interface with the spinal cord has a base thickness of 0.3mm and a modulus of elasticity of 90kPa. These values indicate a flexible base validating the conclusion of chapter 2

3.4 Bibliography

[1] E. Mazuchowski and L. E. Thibault, "Biomechanical Properties of the Human Spinal Cord and Pia Mater," presented at the Bioengineering Conference, Flodrida, 2003.

[2] S. S. Margulies, D. F. Meaney, L. B. Bilston, L. E. Thibault, N. G. Campeau, and S. J. Riederer, "In Vivo Motion of the Human Cervical Spinal Cord in Extension and Flexion," in *Proceedings of the 1992 International IRCOBI Conference on the Biomechanics of impacts*, VERONA, ITALY, 1992.

[3] .C. Cheng, "Development of Surrogate Spinal Cords for the Evaluation of Electrode Arrays Used in Intraspinal Implants," Thesis, University of Alberta, Edmonton, 2011.

Chapter 4

Array Fabrication and Characterization

4.1. Introduction

Spinal cord injury (SCI) leads to an interruption in the neural signals between the brain and the intact motor neurons below the lesion site, and often causes the loss of function in the lower extremities [1,2]. Intraspinal microstimulation (ISMS) is a neuroprosthetic technique that involves the implantation of micro-sized-electrodes within the spinal cord below the site of injury [3]. Electrical stimulation through these microelectrodes activates the remaining motoneuronal pools and elements of the neural networks involved in locomotion, thus producing coordinated movements of the legs [4,5]. In animal models, this technique has shown substantial promise for restoring standing and walking after SCI [1,3,6–8]

Currently available electrode arrays are capable of recording from or stimulating various regions of the brain. Examples of such arrays include the Utah, Michigan and Huntington Medical Research Institute (HMRI) arrays, all of which consist of arrangements of multiple electrodes that are held together by a rigid base [9–12]. With the exception of the HMRI electrode arrays, a version of which has been implanted in the spinal cord [13], the interaction of the above mentioned arrays with spinal cord tissue as well as their long-term stability in the spinal cord remain unknown. Because the spinal cord undergoes different deformations from the brain during regular daily activities, it introduces mechanical challenges that are dissimilar from those encountered in the brain [14].

An intraspinal electrode array must be mechanically and geometrically compliant with the cord to prevent physical damage. Specifically, because the region for ISMS spans up to 5cm in humans (3cm in cats), the array cannot impede the natural deformation (e.g., elongation, torsion) of the spinal cord during movement. Therefore, we propose that a flexible-based electrode array (FBEA) as opposed to a rigid-based array, may be a suitable alternative for intraspinal microstimulation interfaces. The flexible-base of the array would conform to the surface of the cord and undergo the same deformations as the cord. This in turn

would allow the penetrating electrodes to “float” with the spinal cord tissue as it moves, thus providing enhanced interfacial stability.

The fabrication of an FBEA to interface with the spinal cord requires the development of a customizable and repeatable fabrication protocol to accommodate for variations in curvature and size of the lumbosacral spinal cord between recipients of the device. Moreover, depending on the leg movements to be restored, the target regions for stimulation within the ventral horn could vary [4]. Finally, unlike the brain, the ISMS interface does not require an array with a high density of electrodes [3,8–11].

In this chapter, we describe the development of a FBEA that could be used for ISMS. A fabrication protocol was developed and comparisons between the geometry of the developed prototypes and the target design specifications were made. The effect of base thickness and curing temperatures on the stiffness of the structure was determined, and the best thickness and curing temperature were chosen to achieve maximal compliance with the spinal cord. The tuned designs were implanted into surrogate cords which mimicked the natural spinal cord and possessed many of its mechanical properties [15] The influence of the FBEAs on the mechanical behavior of the cord was assessed. Finally, a validated finite element model of the surrogate spinal cord was used to analyze the stresses that various electrode array types impose on spinal cord tissue. The surrogate cords implanted with FBEAs resembled the behavior of cords implanted with electrodes with no base that did not impede the movement of the cord. Contrary to the latter two arrays, the solid-based arrays impeded the elongation of the surrogate cords. The finite element model also showed that the currently developed FBEA is more mechanically compliant with the spinal cord than the rigid-base arrays; yet, still less compliant than the individual electrodes. On the other hand, the cords implanted with the complaint FBEA resembled the ones implanted with no-base arrays.

4.2. Methods

4.2.1 Design Specifications

An electrode array for intraspinal microstimulation requires geometrical and mechanical properties that are compatible with the spinal cord (Figure 4.1)**.** First, the stiffness of the base should match that of the spinal cord to ensure that the attached electrodes do not impede the natural deformation of the cord. *Mazuckowski et al*. [16] reported the modulus of elasticity of the human spinal cord tissue to be 89 kPa. In the present work, we used this modulus of elasticity as the reference to calculate array stiffness. Second, the curvature of the base should match that of the spinal cord to allow for full contact between both surfaces. This reduces the extent of connective tissue formation between the spinal cord and the base of the array, thus diminishing the chances of array dislodgement [17]. The curvature of the spinal cord can be obtained using magnetic resonance imaging (MRI) [18]. Third, the arrangement of the electrodes within the array should match the target regions within the ventral horn of the lumbosacral enlargement. *Mushahwar et al*. [4] mapped the approximate size and location of different motoneuronal pools that innervate various muscle groups, and similar to earlier work [19–22], found that the different pools have different sizes and medio-lateral, dorso-ventral arrangements within the lumbosacral enlargement. Therefore, to activate different muscles and movement synergies, the microelectrodes within the array should reach the target motoneuronal pools. Finally, because the target locations for producing various synergistic movements are distributed along the rostro-caudal extent of the lumbosacral enlargement, an array with a sparse arrangement (instead of dense distribution) of electrodes along the length of the enlargement would be suitable for interfacing with the spinal cord [3,8].

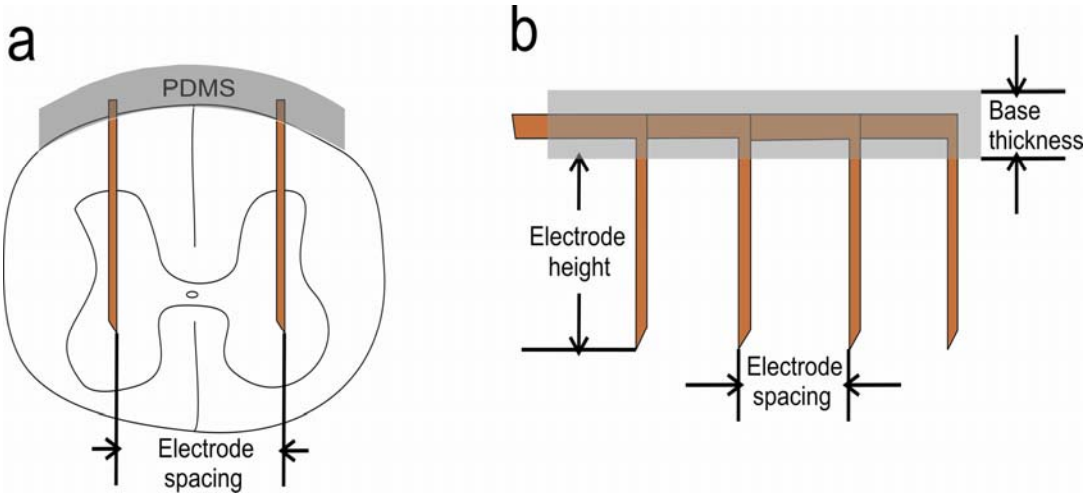

Figure 4.1 *Schematic of the flexible-base electrode array.* a) Cross-sectional view of the spinal cord and flexible-base electrode array. The thickness of the flexible base is uniform and is curved to match the surface geometry of the spinal cord. The electrodes extend vertically relative to the horizontal plane. The transverse spacing is chosen based on the location of the target structures in the ventral horn of the spinal cord. b) Longitudinal view of the flexible-base electrode array. The electrode height and longitudinal electrode spacing are selected based on the desired target locations within the spinal cord.

Taken together, the design of the FBEA should be customizable because the arrays may need to be tailored to each recipient. The material properties of the base should match those of the spinal cord. The fabrication protocol should allow for modifications in the density and spacing between electrodes and curvature of the base. It should also allow for maintaining a uniform base thickness. A summary of the design protocol is provided in Figure 4.2.

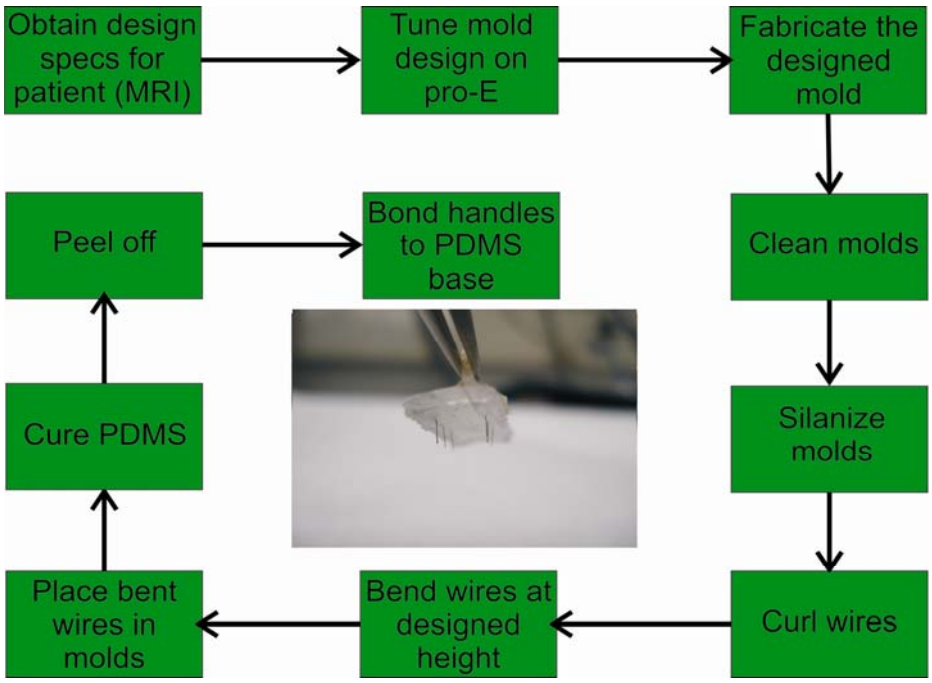

Figure 4.2 *The flexible array fabrication flow chart*. Presented is the protocol developed for the fabrication of the flexible-base-electrode-array.

4.2.2 Base material

Polydimethyl siloxane (PDMS) is a biocompatible silicone elastomer that is commonly used in medical implants and neural interface applications [23–28]. PDMS is optically clear, gas permeable with a tunable modulus of elasticity that is orders of magnitude smaller than that of other polymers, such as polyimide and parylene [28–30].

Two PDMS candidates were obtained: Sylgard 184 (Dow Corning Ltd., Michigan, USA) and MED 6215 (NuSil Technology, Carpinteria, California, USA). Both are two component systems consisting of an elastomer and a cross-linker. The mechanical properties of PDMS can be tuned either by modifying the mixing ratio of the elastomer to cross-linker or by manipulating the curing temperature.

To achieve a modulus of elasticity that matches that of the spinal cord, mixing ratios of 10:1 and 40:1 (elastomer:cross-linker by weight) of the Sylgard 184 were

cured at 100 ^{0}C for 45 minutes. The increase in elastomer to cross-linker mixing ratios caused the material to become sticky and hard to handle; therefore, Sylgard 184 was deemed inappropriate for FBEA applications at this time. An elastomer to cross-linker mixing ratio of 10:1 was used for MED 6215, and cured for 90 minutes at temperatures of 66 ^{0}C, 76 ^{0}C and 86.5 ^{0}C. All samples were prepared and cured in polystyrene containers.

4.2.3 Electrodes

Platinum/Iridium (Pt/Ir) and stainless steel (SS) microwires 30µm in diameter [6–8,31], as well as multi-contact microfabricated cylindrical electrodes 85µm in diameter [32,33] have been used for ISMS applications.

For the present work, initially we order 80µm Pt/Ir electrode from MicroProbes for Life Science (Micro Probe Inc., Gaithersburg, MD, USA); however, most of the electrodes were damaged through shipping due to their small size. Thus, the idea of using these probes was abandoned.

For this work, 30µm and 80µm SS wires were obtained from California Fine Wire (Grover Beach, California, USA). The microwires were bent to the desired height to form a continuous electrode-lead as described in previously published records [6,8]. The effect of wire diameter on the stiffness of the base was assessed using dynamic mechanical analysis (DMA).

4.2.4 Molds

A mold was used for fabricating the FBEA. Three geometrical variables were taken into consideration: the thickness of the base which affects its stiffness, the curvature of the base, and the position/arrangement of extruding electrodes. The mold needed to be easily tunable and modifiable. Moreover, short fabrication times and low cost were desirable features of the mold.

The design of the mold was prepared using 3D CAD software (Pro/Engineer Wildfire 3.0 (Parametric Technology Corporation, Needham, MA, USA). It consisted of two parts: 1) A female component (Figures 4.3a, 4.3b) which controlled the length and curvature of the base and location of electrodes. The length of the base was determined by the closed back side of the mold (Figure 4.3a), and the location of the electrodes was determined by the holes created in the mold (Figure 4.3a). The mold thickness was chosen to be larger than the maximal height of the bent microwires. 2) A male component (Figures 4.3e, 4.3f) controlled the thickness of the base and ensured that its thickness was uniform throughout its length by matching the curvature of the female mold.

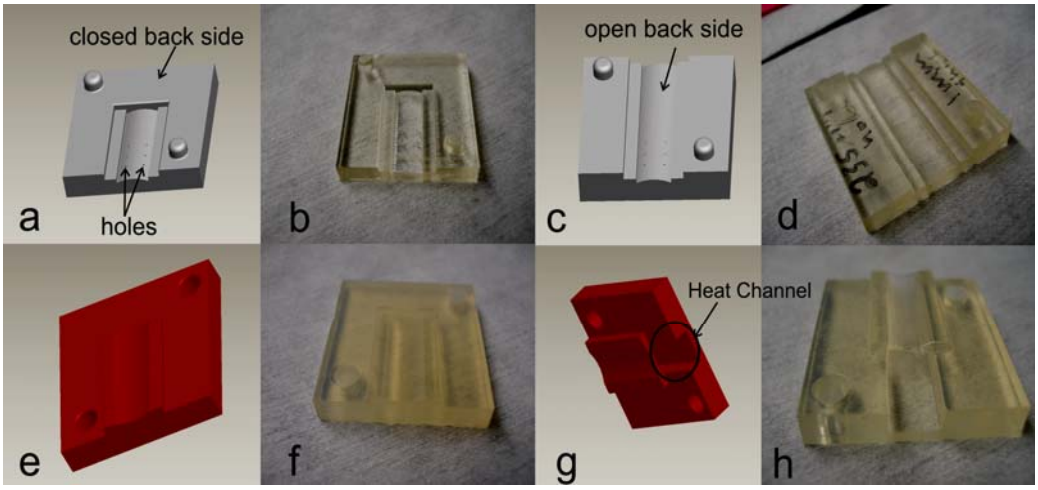

Figure 4.3 *Rapid prototype molds used to fabricate the FBEA.* a, c, e and g represent the CAD design, b, d, f and h represent the rapid prototyped molds. a to d show the female component with holes used to control the arrangement of the electrodes. e to h show the male part used to control the thickness of the base. c, d, g and h present the modified designs.

Rapid prototyping (3D printing) was then used to fabricate the molds. Objet FullCure720 (Objet Ltd, Billerica, MA, USA) was used to print transparent molds with glossy smooth surfaces. The glossy surface was selected to weaken any potential bond between the PDMS and the surface of the molds. The fabricated molds were cleaned first using a water jet. The pressure of the water removed all particles and resins that were attached to the surface of the mold. The molds were then placed in sodium hydroxide solution prepared by mixing 10g of NaOH (Anachemia Canada Inc., Quebec, Canada) in 500ml of distilled water. After 1

hour, the molds were removed, dried and cleaned again by a water jet. The dried molds were then silanized in a vacuum chamber dessicator, with a drop of trichloro(1,1,2,2-perfluorooctyl)silane. The silane layer was used to weaken any potential bond between the polymerized PDMS and the surface of the molds. This allowed for easier peeling of the silicone from the mold.

The initial design of the female and male components of the mold limited heat transfer and polymerization of the PDMS mixture could not take place: the female component was closed from one side (Figure 4.3a) and the male component was too thick (Figure 4.3e). To allow for the polymerization of thin layers of PDMS, the designs of the male and female components were modified to allow for more air exposure and heat transfer, and improve polymerization of the mixture. The female component was opened from both sides (Figures 4.3c, 4.3d) and heat channels were added to the male component (Figures 4.3g, 4.3h) of the mold. The exposed area of silicone mixture to the air was also increased by extending the heat channel through the entire male mold (Figure 4.3g). These modifications allowed for curing PDMS samples down to 0.65mm thick. The latter value is almost two times higher than the desired value (0.3mm) for the compliant array. This indicates that further investigation should be done to minimize this thickness down to 0.3mm.

4.2.5 Temporary stiffening layer

To facilitate the handling of the array and structural preservation during implantation, a temporary stiffening layer was adhered to the top of the flexible base.

Initially, the stiffening layer consisted of gelatin that was deposited on top of the flexible PDMS base. Gelatin is relatively stiff when cured and can be dissolved by water. However, because PDMS is hydrophobic while gelatin is hydrophilic, the two media did not adhere to each other and the approach was abandoned.

Instead, “handles” were designed in pro/E and rapid prototyped. Dr. Anastasia Elias recommended and developed a protocol to bind the RP handles to the silicone base. Polyethylene glycol (PEG) was used to bind the handles to the PDMS bases. The silicone base was polymerized in the rapid prototyped female mold and the top surface was treated by UV ozone for 10 minutes to allow better adherence to the PEG layer. A small drop of PEG was applied and the handle was position in place. PEG was then polymerized for 10 minutes by placing the base and handle approximately 5 cm away from an 8WUV lamp at 365nm. (Figure 4.4).

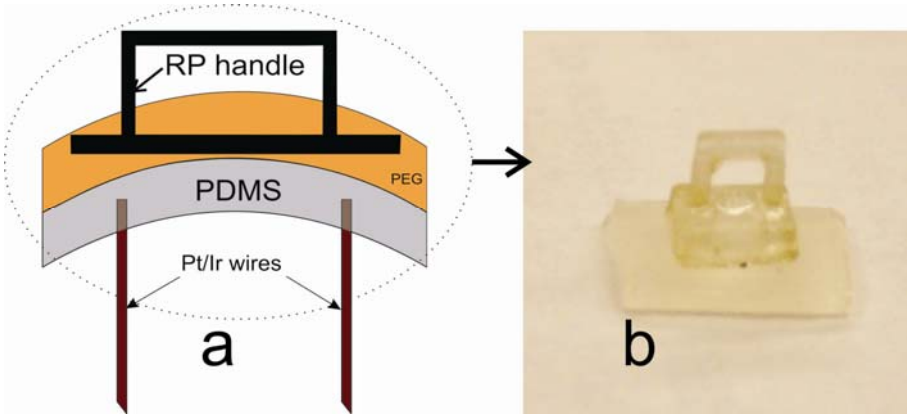

Figure 4.4 *Temporary handle.* The handle was used to temporarily increase the stiffness of the flexible base, improve the ease of handling and preserve the structural integrity of the array during implantation.

4.2.6 Array Characterization

4.2.6.1 Repeatability of fabrication protocol

Three different geometrical features of the fabricated arrays were analyzed to assess the repeatability of the fabrication protocol: base thickness, electrode height and electrode spacing (Figure 4.1). The first feature affects the stiffness of the array and the latter two determine the accuracy of electrode tip placement in the target tissue of the ventral gray matter of the spinal cord.

Flexible bases were fabricated with thicknesses ranging from 0.75 mm to 1.5 mm in steps of 0.25 mm. At least three samples were prepared and tested for each

target thickness. Optical analysis was conducted by taking at least three pictures of each sample using a Sony DSC W40 (Sony Ltd., Toronto, ON, Canada). The thickness was then assessed using Carl Zeiss AxioVision Rel. 4.6 software (Carl Zeiss Canada Ltd, Toronto, ON, Canada). The samples were placed on top of their molds when the pictures were taken; therefore, the mold was used to calibrate the measurements and convert pixels to millimeters. At least three measurements were taken from each picture across the longitudinal and transverse planes. The average measured value for each thickness was then obtained and compared to the target design and the error was calculated.

Electrode height was measured from the bottom surface of the base to the tip of the electrode (Figure 4.1b). Electrode spacing in the transverse (Figure 4.1a) and longitudinal (Figure 4.1b) directions extended from the tip of one electrode to the tip of the neighboring electrode. At least three arrays were fabricated and imaged using Zeiss AxioCam ICc 1 and SteREO Discovery V12 microscope (Carl Zeiss Canada Ltd, Toronto, ON, Canada). Measurements of the electrode height and spacing were obtained using Carl Zeiss AxiVision Rel. 4.6 software. The software was calibrated against a photomask with micro-sized features (accuracy < 1μm) that was fabricated at the University of Alberta nanofabrication facility.

4.2.6.2 Dynamic Mechanical Analysis (DMA)

The axial stiffness of the arrays was used to characterize its mechanical properties. The stiffness was measured using the tension mode of a DMA machine (Perkin Elmer DMA 8000, Waltham, Massachusetts, USA). The array bases were rectangular with dimensions of 13mm (height) x 7mm (width) x variable thicknesses. To remain within the elastic region of PDMS, the strain displacement was limited to 0.01 mm and applied at a frequency of 1 Hz. All measurements were acquired at room temperature (20 to 25 $^{\circ}$C).

The influence of thickness and PDMS curing temperature on the stiffness of the base was assessed in base samples with no extruding electrodes. The influence of

the lead wires on the stiffness of the base was assessed in bases with 8 embedded straight (uncoiled) lead wires connected to extruding electrodes. Three different lead wire diameters (30, 80 and 100µm) were tested. For each test, at least three samples were examined and each sample was tested three times.

4.2.6.3 Lead wire coiling

The lead wires connecting the electrodes to a stimulator in ISMS implants are commonly anchored to a spinous process [3,6]. Because the spinal cord undergoes some deformation during normal movement [14], the relative movement between the spinal cord and the anchoring bone could cause an external force to be applied on the leads. This pulling/pushing force could potentially cause physical damage to the spinal cord tissue.

To allow for a stress relief mechanism, uncoated stainless steel lead wires of 100µm diameter were manually coiled around hypodermic needles (31 gauge) (Figure C.1). Arrays were fabricated in which one coiled lead was either embedded within the flexible base or anchored outside the base. Uni-axial force was then applied to assess the extent of reversible strain that could be safely applied to the array. The base was fixed on one side and force was applied to the other side. Strain was optically measured with reference to a ruler placed under the setup. For both cases (embedded coiled lead or lead anchored outside the base), the force was slowly applied until the first observation of pulling on the extruding electrodes took place. The test was repeated on three samples for each coiled lead location and the resulting strain was then recorded.

4.2.6.4 In vitro testing

To assess the mechanical compatibility of the FBEAs with the spinal cord, arrays with 2 rows of 4 electrodes, base thickness of 1mm and embedded straight lead wires were fabricated. The inter-row separation was 4 mm and inter-electrode spacing was 3mm, resembling the average microwire separations utilized in ISMS implants [3]. The FBEAs were implanted into surrogate spinal cords that

emulated the mechanical properties of the actual human spinal cord [15]. The cords were mounted in a Teflon stand (Figure 4.5) and subjected to 12% uni-axial tensile strain. This represented the maximal strain encountered by the human cord [34]. The results were then compared to those obtained in similar experiments conducted using: a) control, surrogate cords with no implants; b) surrogate cords with implanted electrode arrays in which the electrodes were held by a solid base; and c) surrogate cords with implanted electrode arrays in which the arrays had no base [15].

Figure 4.5 *Teflon stand used for in-vitro testing.* The cords are supported in the middle section by fixed platform. Their extremities are fixated by the two rods which can move axially to elongate the cord.

The same strain analysis technique reported in [15] was used. Briefly, two rows of reference dots were drawn on the upper and lower parts of the surrogate cord (e.g., Figure 4.6). The upper row was used to assess the interaction between the base and the cord, and the lower row was used to determine the mechanical effect of the array on neighboring tissue. At least three pictures were taken of the surrogate cords before and after the application of 12% strain using a Canon EOS 1000D (Canon Inc., Rockville, MD, USA). The distances between the reference dots were measured using Carl Zeiss AxiVision Rel. 4.6 software. The dimensions of the stand were used for calibration and conversion of measurements from pixels to millimeters.

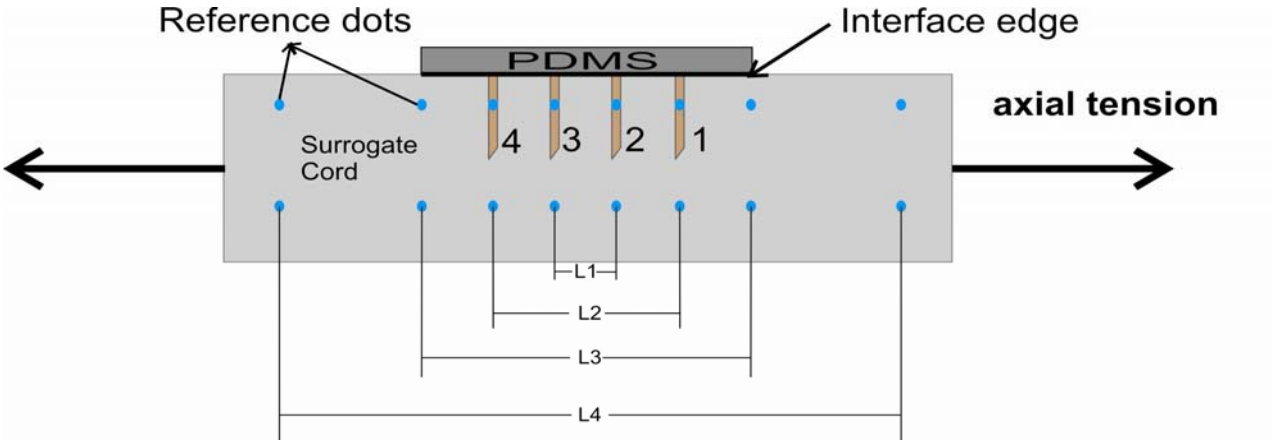

Figure 4.6 *Strain test in bench testing and computer simulations.* The flexible-base electrode array is implanted in a surrogate cord and 12% axial tension is applied to the cord. Two rows of reference dots placed on the surrogate cord (upper and lower) were used to assess the interaction between the array and the cord. L1 to L4 were the distances used to measure the strain in the middle surrogate cord and its extremities.

4.2.7 Finite Element Model

As previously discussed in chapter 3, two dimensional finite element model was constructed using ANSYS 11 (ANSYS Inc, Canonsburg, PA, USA) to simulate the *in vitro* strain test and calculate the stresses experienced by the tissue around the implanted arrays. The dimensions and material properties of the surrogate cord and FBEAs were obtained from experimental measurement. The cord diameter, length and modulus of elasticity were assumed to be 7.5mm, 40mm and 90kPa, respectively. An FBEA with 8 electrodes (2x4), base thickness of 1mm and modulus of elasticity of 500kPa was modeled. The used E was the lowest achieved modulus of elasticity while the thickness was a standard value that we used and was experimentally repeatable. The electrodes were assumed to be in full contact with the cord (i.e., no slippage) and to have a slanted tip [33]. The base was unconstrained and was allowed to move freely with respect to the cord. The cord and the PDMS base were assumed to operate in the elastic range and static analysis was performed.

Boundary 2 (Figure 3.1) was deformed by 12% of the cord initial length (Figure 3.2). The deformation was applied in the x-direction (Figure 3.1). Boundary 1 was

fixed in the x and y directions. Boundary 3 was constrained from moving in the y-direction. Two sets of nodes were selected to simulate the upper and lower reference dots in the *in vitro* experiments. The location of the nodes was chosen to resemble the location of the reference dots in the experimental work. The distance between the nodes was measured before and after the application of the 12% deformation and strains were calculated. The results obtained from the model were validated against the experimental results obtained for the cords implanted with flexible- and solid-based arrays. The solid-based array was simulated by increasing the modulus of elasticity of the model to 2GPa.

The validated model gave us the tool to further understand the mechanical interaction between the different types of arrays and the cords. In the experimental stage, we examined the "global strains" across the cord; i.e. the deformations at different areas of the cords. The validated FEM allowed us to study the local strains; i.e. the strains in the vicinity of the electrodes. By studying the strains along the electrode-cord interface layer, we can get a better understanding of the influence of the electrodes of different types of arrays on the neighbouring tissues. Knowing that the strains are proportional to the stresses and to magnify the difference between the arrays we decided to use the stresses induced by these electrodes on the tissue. To decrease the effect of singularities at the tip of the electrodes, we measured the stress at 10μm from the interface layer. This value was chosen so that the obtained stresses are within the set of elements interfacing the electrodes and the SC tissue. Thus, the validated model was used to study the effective (Von Misses) stresses applied by the electrodes on the spinal cord tissue. The model assumes isotropic material with no hydrostatic pressures. Thus, Von Misses stresses which represent all stress components were selected. Any subsequent use of the term stresses refers to the effective von misses stresses. The stress values in the cord along the longitudinal axis of the electrodes were plotted at 10μm from the electrodes-cord interface. This small distance of the interface line was chosen to decrease the effect of potential discontinuities at the tips of the electrodes. Simulations of implanted cords with 12% uni-axial tension

applied were then performed and the stresses induced by the electrodes of flexible-based, solid-based and no-base arrays were examined. The stresses are plotted from the cord-array interface edge up to 1mm below the electrode tip. The strain plots are found in appendix B. Finally, we studied the stresses induced by the developed flexible-base array on the spinal cord when it is under 5.7º bending [35,36], as shown in Figure 4.7. Due to the symmetry of model geometry, stresses caused by the 2 outer (1 and 4) electrodes (Figure 4.6) were assumed to be similar; the latter also applied to the 2 inner (2 and 3) electrodes. Therefore, the stresses due to 1 outer and 1 inner electrode are presented.

Finally, it should be noted that these stresses are being studied as a mean of comparison between the different types of arrays. These stresses are not being studied to evaluate the failure in the tissue of the cord.

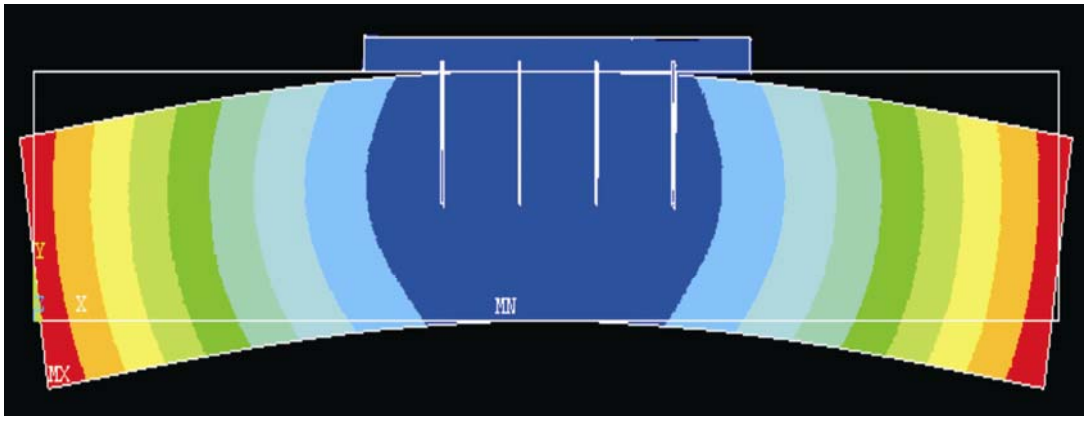

Figure 4.7 *Spinal cord under flexion.* The cord is subjected to a 5º flexion where both extremities are deformed in the negative y-direction and a small segment at the bottom cord is held fixed.

4.2.8 Statistical Analysis

The software package, SPSS 16.0 (SPSS Inc., Chicago, IL, USA), was used for statistical analysis. One-way analysis of variance (ANOVA) and Tukey Honest Significant Difference (HSD) post hoc tests were used to determine the effect of base thickness, PDMS curing temperature and lead wire diameter and structure on the stiffness of base. All data are presented as means ± standard deviation. P-values less than 0.05 represented statistically significant differences.

4.3. Results

The FBEA consisted of three main parts: the base, the electrodes and the lead wires. For ISMS applications, the base of the array needs to have the same curvature and stiffness of that of the spinal cord. Moreover, customizable electrode spacing and adequate stress-relieve in the lead wires are needed.

4.3.1 Fabrication repeatability

4.3.1.1 Base thickness

Arrays with different base thicknesses were prepared and compared to target design thicknesses (0.75mm – 1.50mm). The largest error was 4.60% for the 1.00mm thick bases, where the thickness of the prepared samples ranged from 1.03mm to 1.06mm. The smallest error was for the 1.50mm thick bases (range: 1.39mm to 1.56mm). Table 1 summarizes the mean, standard deviation and percent error of the thickness of prepared samples relative to the target design thickness.

Table 4.1 *Characterization of base thickness.*

Target thickness [mm]	Mean measured thickness [mm]	Standard deviation	Error [%]
0.75	0.77	0.028	2.30
1.00	1.05	0.017	4.60
1.25	1.21	0.024	2.83
1.50	1.48	0.089	1.37

4.3.1.2 Electrode height

Five FBEAs consisting of microwire electrodes (80µm diameter) extruding to a target height of 2.00mm were prepared. The resulting electrode heights ranged from 1.95mm to 2.03mm. The average measured height (1.99mm) had an error of 0.43% relative to the target height.

4.3.1.3 Electrode spacing

Five 2x3 electrode arrays with inter-row and inter-electrode spacing of 4.00 and 3.00 mm, respectively, were prepared. The resulting inter-row spacing was 3.97 ± 0.087mm (error of 0.87%) and inter-electrode spacing 3.02 ± 0.086mm (error of 0.58%).

4.3.2 Mechanical properties of the base

The effect of base thickness, PDMS polymerization temperature and lead wire geometry on the stiffness of the base was assessed using the DMA.

4.3.2.1 Base thickness

The effect of thickness on the stiffness of the base was examined for 4 different thicknesses ranging from 0.75 to 1.50mm (Figure 4.8). All the samples were prepared at 66ºC. As expected, the increase in thickness caused an increase in the stiffness of the base. The stiffness values for the different base thicknesses were significantly different from each other ($p < 0.001$).

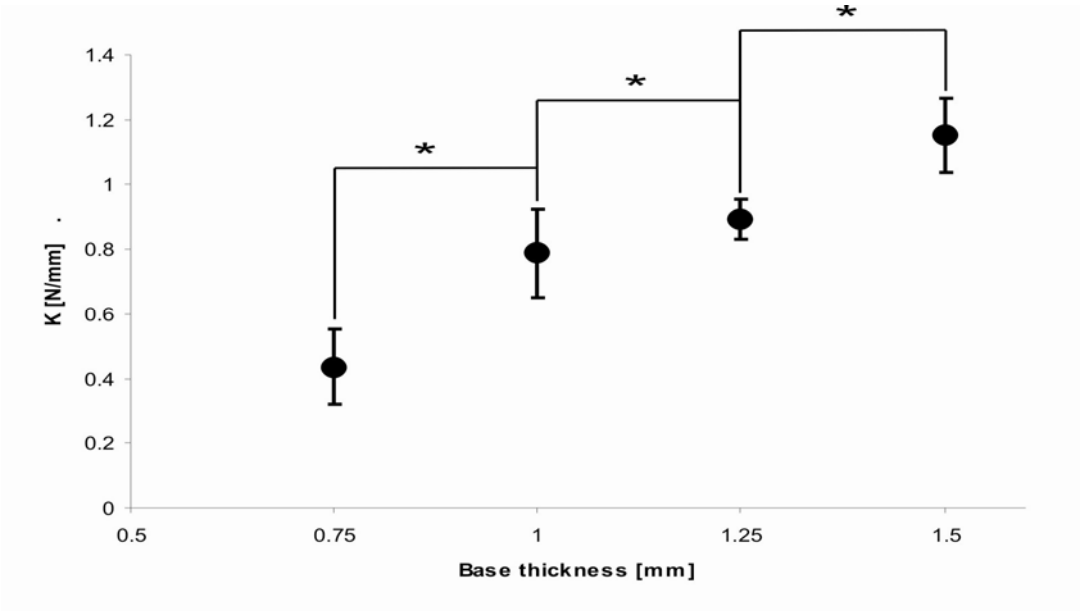

Figure 4. 8 *Effect of base thickness on stiffness of the flexible-base*. Each data point represents the average of at least 5 samples with a minimum of 70 readings for each sample. The error bars represent standard deviation. * represents significant difference ($p<0.05$) obtained from ANOVA and Tukey post hoc analysis.

4.3.2.2 PDMS polymerization temperature

Twelve PDMS samples (1mm thick) without lead wires were polymerized at three different temperatures (66, 76 and 86.5^{0}C). The effect of the PDMS curing temperature is shown in Figure 4.9. The increase in polymerizing temperature caused an increase in stiffness, which was due to an increase in the modulus of elasticity of the material. The lowest stiffness (0.813N/mm) was achieved at a curing temperature of 66^{0}C. The stiffness values measured at different polymerizing temperatures were significantly different from each other ($p < 0.001$). The lowest modulus of elasticity that was achieved was ~500kPa which is still higher than the desired modulus of elasticity (90kPa). Thus more investigation should be done to lower this parameter to the desired value.

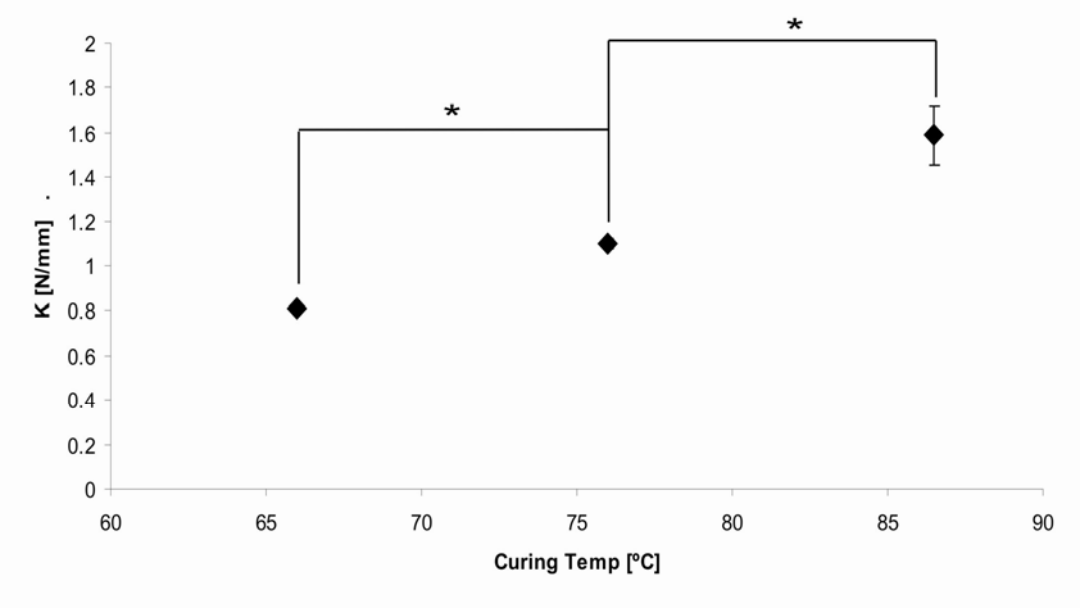

Figure 4.9 *Effect of the PDMS curing temperature on stiffness of flexible-base.* Shown are the mean stiffness ± standard deviation of PDMS flexible bases cured at three different temperatures. Standard deviation bars are smaller than symbol size. * represents significant difference ($p<0.05$) obtained from ANOVA and Tukey post hoc analysis.

4.3.2.3 Lead wire diameter

The effect of the diameter of base-embedded, straight (i.e., uncoiled) lead wires (100µm, 80µm and 30µm) on the stiffness of the base was assessed (Figure 4.10). For each lead wire diameter, two control PDMS samples without wires were prepared at the same temperature for comparison. The presence of the lead wires

within the base did not have any significant effect on the stiffness of the base. For the 100µm, 80µm and 30µm wires, the stiffness of bases embedded with the lead wires were not significantly different from those of the control of each ($p>0.05$).. Due to slight differences in the curing temperature (caused by the used oven), the stiffnesses of the control samples were slightly different from each other. This limited us to compare the stiffness of the bases with embedded lead wires to their perspective control samples with no lead wires.

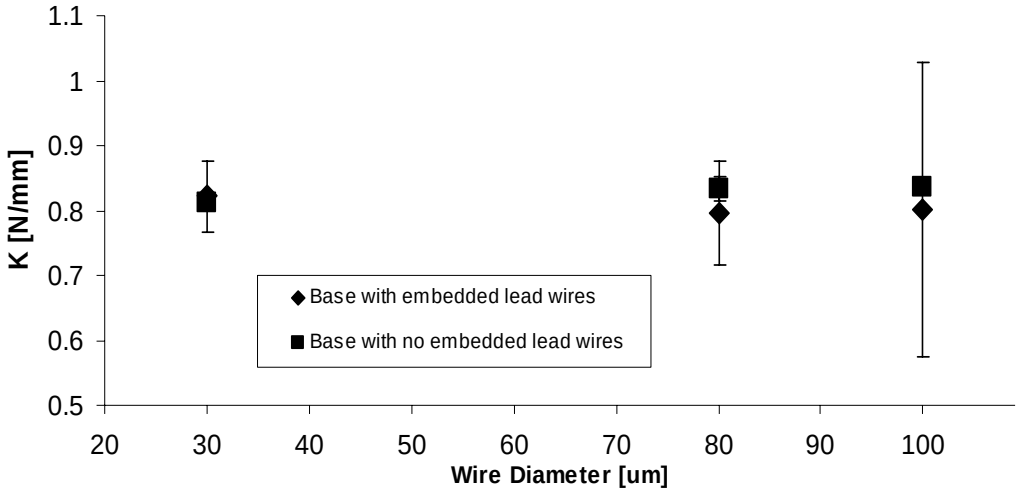

Figure 4.10 *Effect of lead wire diameter on stiffness of the flexible-base*. Shown are the mean stiffness ± standard deviation of PDMS flexible bases cured with straight lead wires with three different diameters. The measured stiffness for each diameter is compared to the stiffness of a control sample with no wires.

4.3.2.4 Lead wire coiling

To identify the best location of the coiled lead wires, two types of FBEAs were prepared. One type had a coiled lead wire embedded inside the base and the second had the wire outside the base. A uni-axial force was applied to one side of the arrays while fixing the other side, and strain values were measured after at least one coil reached full extension. The test was conducted on three samples for each coiled lead wire location. Both arrays withstood tensile deformations higher than the 12% strain experienced by the human spinal cord. The array with the coiled lead wires embedded within the base failed after applying 21.6% strain,

while the array with the coiled lead wires outside the base failed at 25% strain (Figure 4.11).

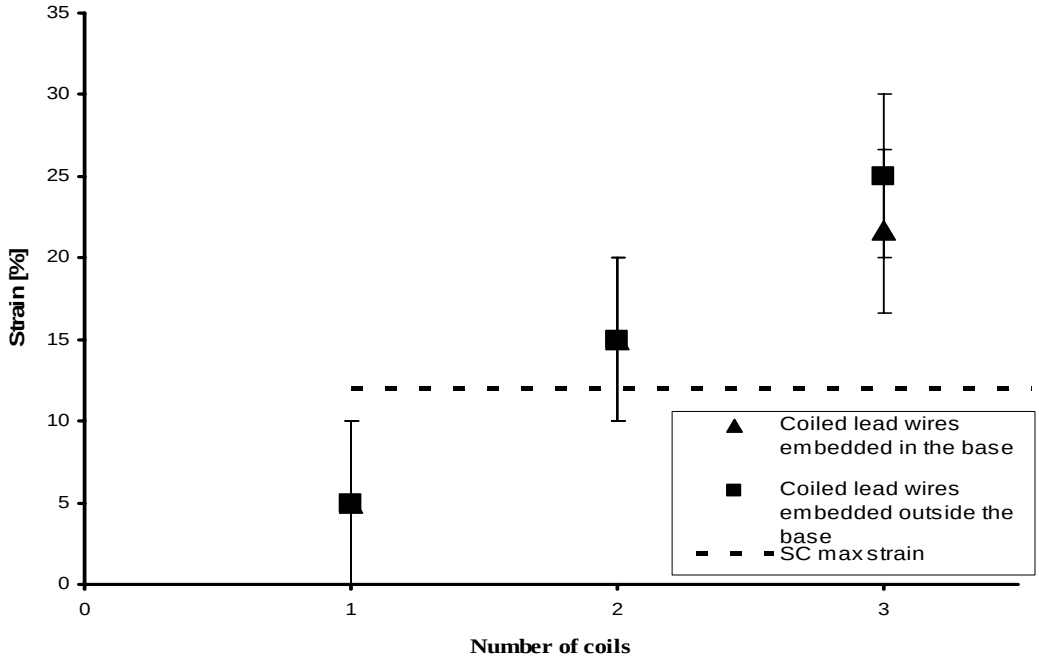

Figure 4.11 *Effect of lead wire coiling on strain.* A test of whether the coiled part of the lead wire should be embedded within or placed outside the base.

4.3.3. In vitro testing

Design parameters that provided the best mechanical compatibility of the FBEAs with the human spinal cord were chosen to prepare arrays that would then be tested for their interaction with surrogate spinal cords [15]. The base was polymerized at 66 ^{0}C with thickness of 1.00mm. The curing temperature was chosen because it allowed for the minimal modulus of elasticity which was 500kPa and the 1.00mm thickness was chosen due to the repeatability of the fabrication at such thicknesses. The electrodes consisted of 2 rows of 80µm wires separated by 4 mm. Each row contained 4 electrodes separated by 3 mm. The number of electrodes was chosen to resemble the same number used in the solid-based and no-base arrays that were tested by Cheng et al. The surrogate cord with the implanted array was subjected to 12% axial strain and the distances between reference marks on the cord (Figure 4.6) were optically measured before and after the application of strain. The results were compared to those obtained by Cheng et

al. [15] for surrogate cords with no implants (control); surrogate cords with implanted electrode arrays in which the electrodes were held by a solid base; and surrogate cords with implanted electrode arrays in which the arrays had no base. The rigid-based and no-base arrays had the same electrode layout as the FBEAs in this study.

Surrogate cords implanted with FBEAs showed deformations that were very similar to those implanted with no-base arrays (Figure 4.12). The strains measured between the reference points in the surrogate cord implanted with the FBEAs ranged between 9 ±1% to 12±1% which were very similar to the strain values obtained for the no-base array (9 ±1% to 13±1%) and control samples with no implanted wires (10 ±1% to 12±1%). No statistically significant differences between the strains measured in control surrogate cords and cords implanted with FBEAs and individual wires were found. ($p > 0.1$ for all comparisons of strain values between reference points).

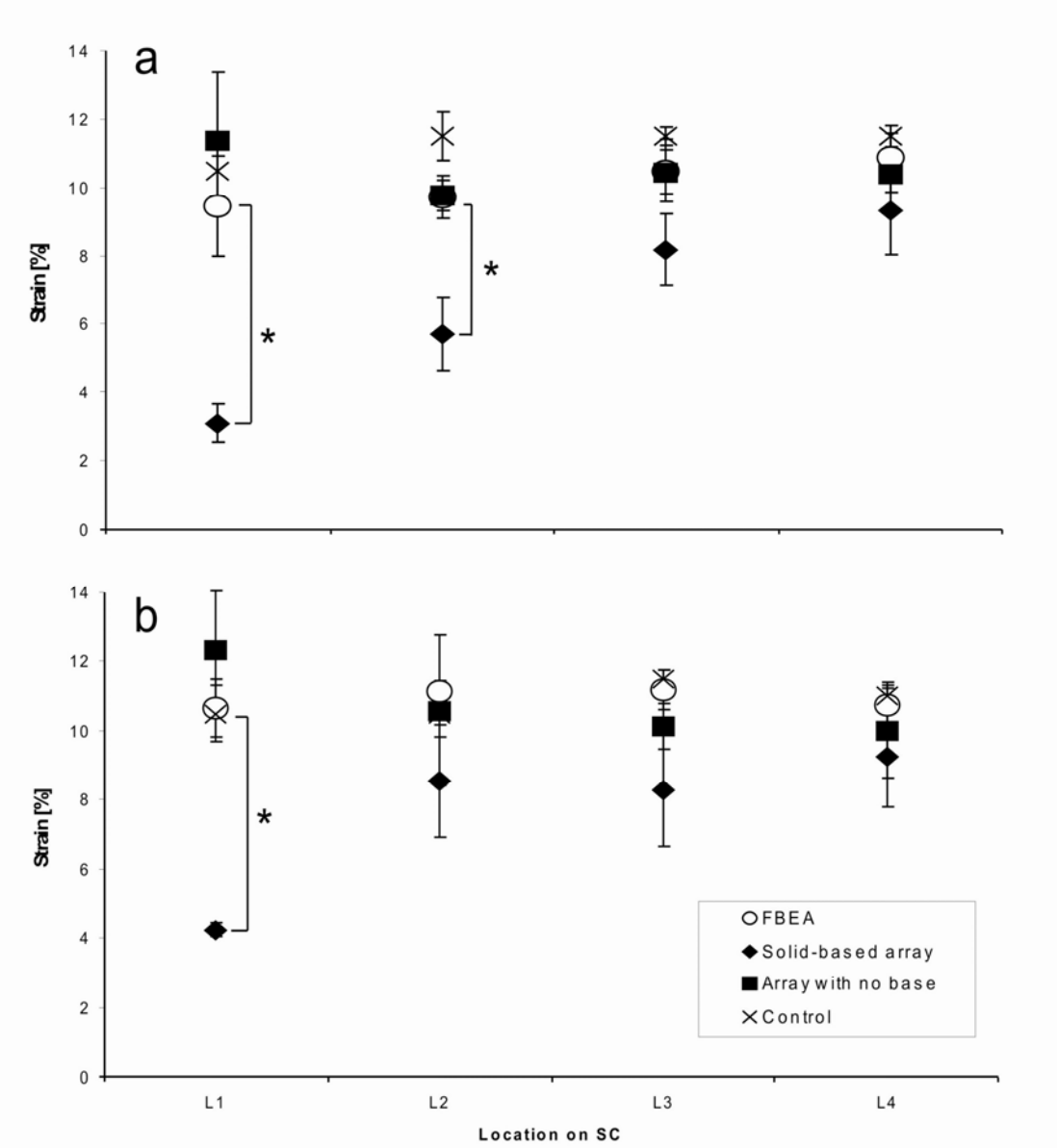

Figure 4.12 *In-vitro testing*. Assessment of the interaction between the no-base, solid-base and flexible-base arrays implanted within surrogate cords when applying 12% axial tension to the cord. a and b represent the strains measured between the upper set of dots and lower set of dots, respectively. The control sample shows the measured strains for a surrogate cord with no implanted array. The data for the solid-base, no-base and control are reproduced from [1]. The p-values obtained from ANOVA and Tukey post hoc analysis are shown. * shows significant difference ($p<0.05$).

The strains measured in cords implanted with FBEAs were significantly different from those measured in cords implanted with rigid-based arrays. The strain values associated with the upper row L1 and L2 reference points in implants with rigid-base arrays were significantly smaller ($p=0.02$ and 0.008, respectively) than in

those with FBEAs (Figure 4.12)**.** For the lower row, the L1reference point strain was significantly smaller in the rigid-based array than in the FBEA. This indicates that the rigid base impedes the natural deformation of the cord while the FBEA does not.

4.3.4. Finite element model

4.3.4.1. Model validation

The calculated strains in the numerical model of the cords implanted with FBEAs and solid-based arrays were plotted against the experimental measurements obtained from the physical model (Figure 4.13). The FEM had the following parameters: Base thickness= 1.00mm, $E_{solid\text{-}base}$=2GPa, E_{FBEA}=500kPa, Cord height = 7.5mm, Electrode height=4mm. For the cords implanted with the FBEAs, the strains calculated between L1 and L3 in the numerical model were within the standard deviations of their perspective strains in the physical model (within 0.5% error). Similar results were observed for the solid-based arrays except for the strain measured at L1 between the lower set of reference points. The difference between the two models at this location was approximately 2%. On the other hand, the strains calculated at L4, between the upper and lower sets of reference points, in the numerical model of the FBEA and the solid-based arrays had an approximate error between 1.5 and 2% from the perspective strains in the physical model.

The validated numerical model was used to calculate the stresses induced by the electrodes of various types of arrays on the surrounding spinal cord tissue.

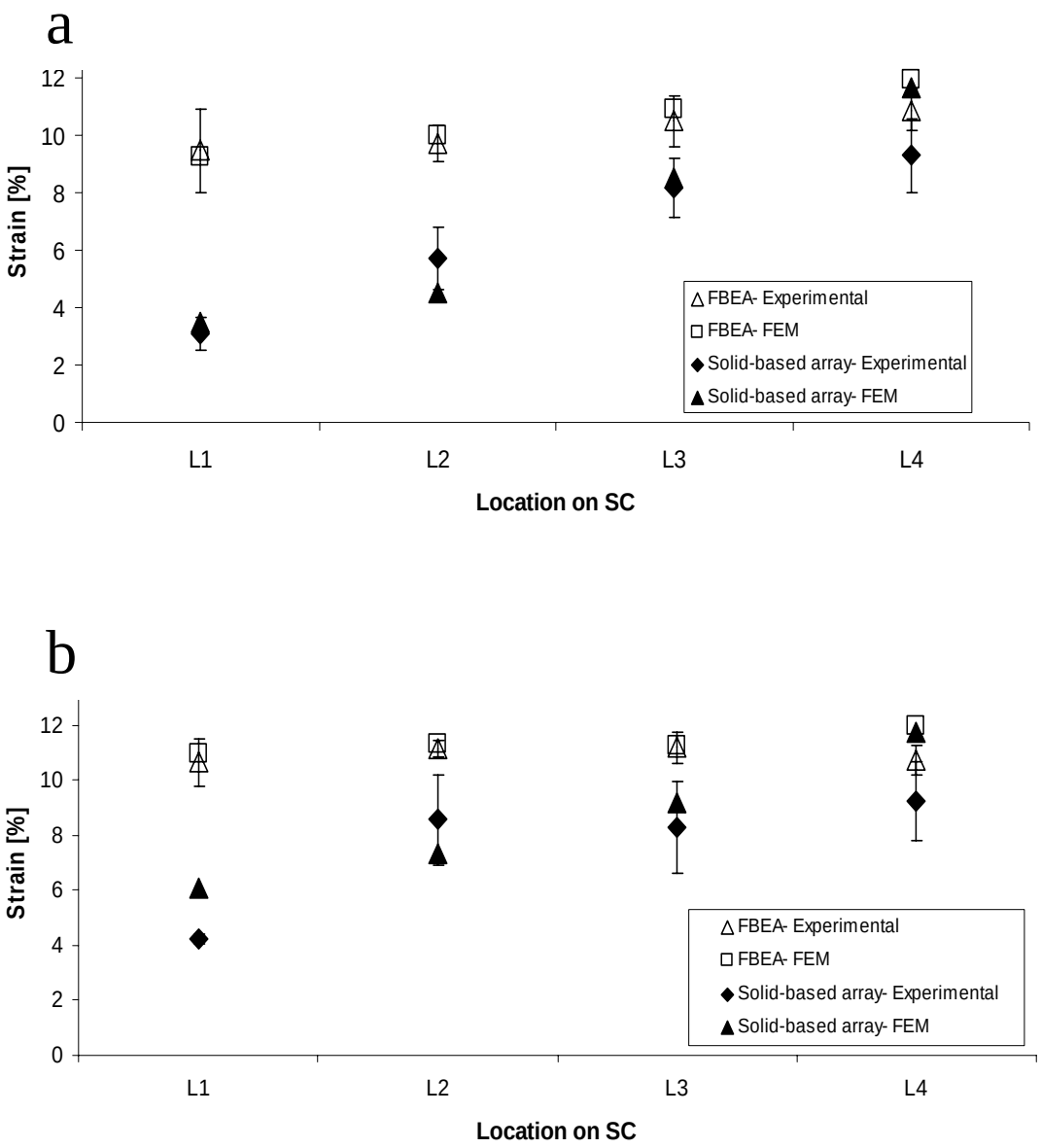

Figure 4.13 *Strain test in finite element model*. Presented is a comparison between the strains measured experimentally and strains obtained from the numerical model for flexible-base and solid-base arrays. a and b represent the strains measured between the upper set of dots and lower set of dots, respectively. Standard deviation bar for L1 in the experimental solid-base array is smaller than symbol size.

4.3.4.2. Stresses induced by the arrays when cords are elongated

Cords implanted with no-base arrays were modeled by allowing electrodes to move freely with the cord. This simulation was based on the assumption that no external forces are being transferred to the individual electrodes (ideal case). The

stresses induced by electrodes of the no-base, developed flexible-based, rigid-based and compliant flexible-based arrays on spinal cord tissue are shown in Figure 4.14. The stress induced by electrodes in all array types was highest at the interfacing edge of the cord (Figure 4.6**)**, decreased exponentially along the length of the electrode and increased again around the tip (at 4mm). The magnitude of the stresses induced by the electrodes differed between the three different arrays. The stress magnitudes on the surrounding tissue induced by the outer and inner electrodes in the arrays with no base and the compliant FBEA were nearly identical (Figures 4.14a, b, g and h); however, substantial differences between the stresses induced by the outer and inner electrodes were seen in the developed flexible- and rigid-based arrays (Figures 4.14c, d and e, f, respectively). The outer electrodes in the arrays with no base induced a stress of 41.41 kPa and 21.05kPa at the top and tip, respectively (Figure 4.14a**)**; while the inner electrodes induced 39.72kPa and 24.27kPa at the top and tip respectively (Figure 4.14b). Similarly, outer electrodes in the compliant FBEA induced a stress of 42.95kPa and 20.67kPa at the top and tip respectively (Figure 4.14g); while the inner electrodes induced 38.65kPa and 24.1kPa (Figure 4.14h). In the developed FBEA, the outer electrodes induced a stress of 64.14kPa at the top and 21.03kPa at the tip (Figure 4.14c) while the inner electrodes induced 29.60kPa and 25.39kPA at the top and tip respectively (Figure 4.14d). Therefore, the outer electrodes induced 34.54kPa more stress and 4.36kPa less stress than the inner electrodes at the top and tip, respectively. In comparison, the outer electrodes in the rigid-based array induced 66.93kPa and 26.47kPa at the top and tip (Figure 4.14e) respectively, and the inner electrodes similarly induced 9.4kPa and 17.82kPa (Figure 4.14f). The ratio of induced stresses by the outer and inner electrodes in the rigid-based array was 7.12 and 1.49 at the top and tip, respectively. The stress ratios are shown in figure 4.15

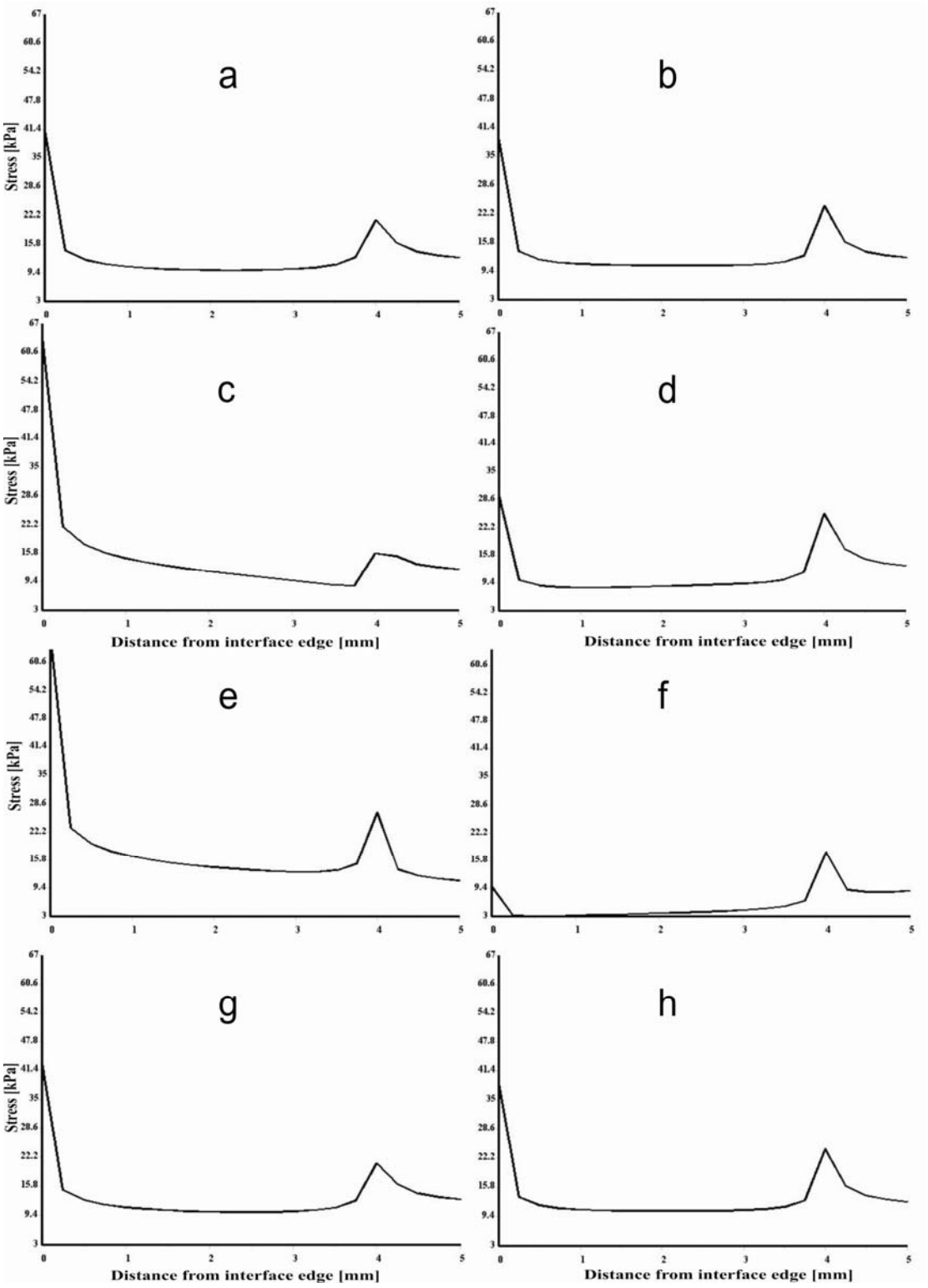

Figure 4.14 *Stresses induced by electrodes on elongated cord*. a, c, e, g show the stresses induced by the outer electrodes of arrays (1 or 4) on the cord tissue. b, d, f, h represent the stresses induced by the inner two electrodes of arrays (2 or 3) on the cord tissue. a and b present the stresses calculated with the individual electrodes. c and d show the stresses induced by the electrodes of the flexible base. e and f illustrate the stresses induced by the

electrodes of the rigid-based array. g and h show the stresses induced by the electrodes of the compliant flexible-based array.

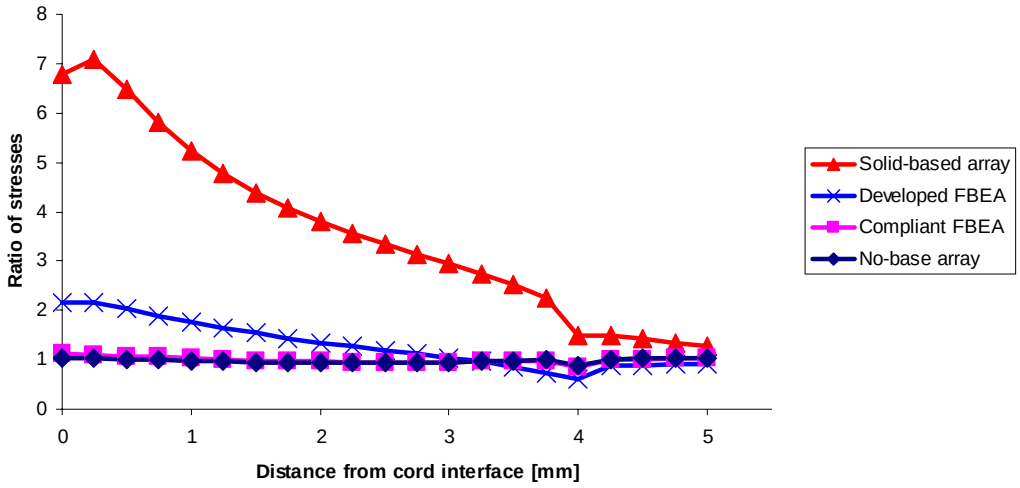

Figure 4.15 Stress ratio of the stress induced by outer electrodes to those induced by inner electrodes.

4.3.4.3. Stresses induced by the arrays when cords are under bending

Figure 4.16 shows that the stresses induced by the electrodes on the flexed cord have similar trends to the ones generated by elongating the cord; however, the magnitude of the stresses is less significant. Figures 4.16a, 4.16b, 4.16g and 4.16h show that the individual electrodes and the electrodes of the compliant FBEA induce the same stresses. Small differences are reported between stresses induced by the inner and the outer electrodes. For the individual electrodes, the ratios of change in the stresses induced at the top and tip of the outer electrodes to the ones induced by the inner electrodes are 0.95 and 0.29 respectively. For the compliant FBEA the ratios of the stress induced by the outer electrodes to the ones induced by the inner electrodes at the top and tip are 1.02 and 0.26 respectively

On the other hand, the outer electrodes of the developed flexible- and rigid-based arrays induce maximal stresses at the cord interface edge (Figure 4.16c and 4.16e) of 15.6kPa and 19.43kPa respectively. The stresses at the tips are 3.95kPa and 5.94kPa respectively. The inner electrodes of the developed FBEA induce maximal stresses of 5.83kPa at the cord interface surface and 3.84kPa at the tip (Figure 4.16d). These stresses are 2.7 times smaller and equal to those induced by

the outer electrodes respectively. The inner electrodes of the rigid-based array induce a stress of 0.184kPa at the interface edge and 5.94kPa at the tip (Figure 4.16f). Those stresses are 105.6 times smaller and equal to those induced by the outer electrodes respectively.

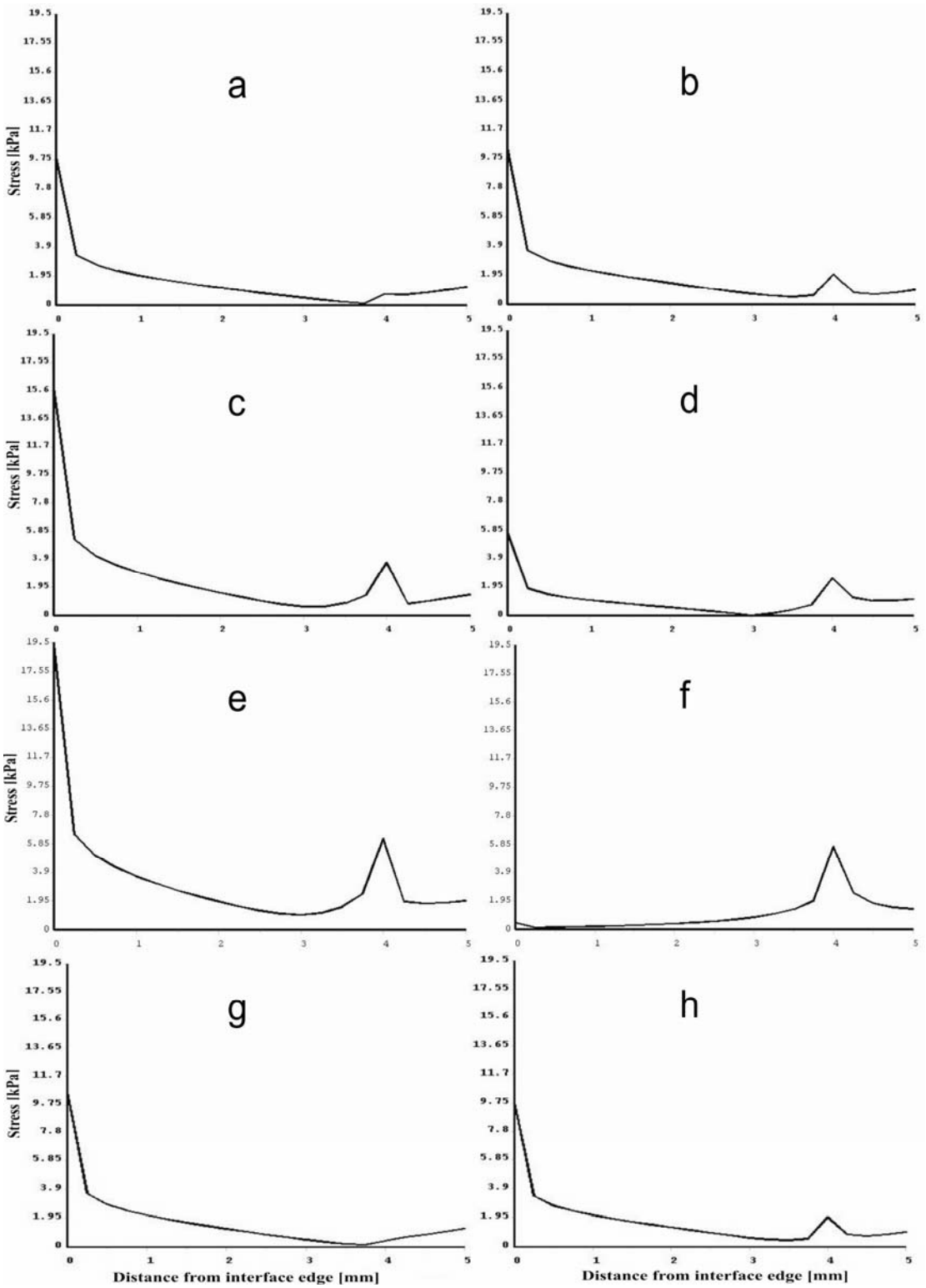

Figure 4.16 *Stresses induced by electrodes on flexed cord*. a, c, e show the stresses induced by the outer electrodes (electrodes 1 or 4) of arrays on the cord tissue. b, d, f, represent the stresses induced by the inner two electrodes (electrodes 2 or 3) of arrays on the cord tissue. a and b present the stresses calculated with the individual electrodes. c

and d show the stresses induced by the electrodes of the compliant flexible base. e and f illustrate the stresses induced by the electrodes of the developed flexible-base array.

4.4. Discussion

4.4.1. Overview

The goal of the present work was to develop a customizable, rapid fabrication process for a multi-electrode array for ISMS applications. Most of the currently available arrays are rigid and have been developed to interface with the brain [9–12,17]. Due to the small size of the arrays relative to the brain, the imposed mechanical and geometrical constraints on the interfacing rigid arrays are not very significant. The spinal cord on the other hand, consists of a much smaller tissue volume. Therefore, it undergoes relatively more pronounced deformations during natural movements and requires that arrays implanted within it possess compatible mechanical properties. In this study, we fabricated several FBEAs and characterized the developed prototypes. The geometrical aspects of the arrays were characterized to test the repeatability of the fabrication process. The DMA was used to measure the effect of the different parameters of the array on the stiffness of the device. The design was modified accordingly to produce the maximal mechanical compliance between the array and the human spinal cord. The prototypes were then implanted in surrogate cords and subjected to uni-axial strain tests that mimicked the highest strain undertaken by the human spinal cord. The results of the test were then compared to results from similar experiments in which control, unimplanted surrogate cords and cords with implanted no-base and rigid-based electrode arrays were used.

4.4.2. Development of a repeatable, feasible and quick fabrication protocol

A major focus of our work was to design a repeatable and feasible fabrication protocol that would be used to assemble the different components of the flexible-base array. Most of the currently available arrays are developed with well established microfabrication techniques; Hoogerwerf and Wise [11] micro-assembled planar silicon shanks to develop the Michigan Array, Richard Normann's lab [9] used photolithography techniques to fabricate the silicon based

Utah Electrode array. The use of microfabrication techniques allow for high flexibility, precision and repeatability. However, such techniques usually have high costs and long turn around time (order of days).

It was shown that the FBEA developed protocol is repeatable; the measured errors on the inter-row spacing, inter-electrode spacing and electrode height were 30µm, 20µm and 10 µm respectively. Mushahwar et al. [1,4] reported minimal activation pool dimensions of 0.7mm in width for the Tibialis Anterior and 1.2mm in height for the Quadriceps. The largest error reported for the base thickness was less than 5% when compared to the target thickness. The thickness is proportional to the stiffness and its error reflects the error on the stiffness (<5%). The reported errors can be due to the way we are closing the molds and due to the tolerances of the rapid prototype machine. Also, the highest error was reported with the 1mm thick mold and it was almost twice the errors reported for other thicknesses. It is believed that this error is more significant at this thickness because these molds were used the most experimentally. This suggests that the RP molds are not designed to be reused in our application for more than one array. We believe that the temperature cycles that the molds go through while curing the PDMS can affect their tolerances; thus increase the error on the thickness of the base. Finally, the total turn around time for this protocol is less than 24 hours.

It should be noted that with the currently used molds and fabrication process, the minimum thickness and modulus of elasticity we achieved was 0.65mm and 500kPa. These values are still higher than the desired thickness and E of the compliant base which are 0.3mm and 90kPa respectively. This shows that further investigation should be done to lower the thickness and modulus of elasticity of the base to achieve the desired values.

4.4.3. Mechanical compatibility between the implanted array and the cord

In vitro testing suggested that the mechanical compliance between the surrogate spinal cord and the implanted arrays has a significant influence on the mechanical

behavior of the cord [15]. The latter study showed that solid-based arrays impede the motion of the cords when elongated. Rousche et al. [37] proposed flexible-based intracortical arrays which consisted of polyimide base and electrodes. The polyimide layers had a modulus of elasticity of 2.97GPa which is 33.37 folds bigger than that of the spinal cord. Thus, it was important to develop a new type of compliant arrays with stiffness that matches that of the spinal cord.

While no similar arrays were developed before, it was important to asses the influence of each component on the stiffness of the structure. It was shown that the base thickness and polymerization temperature of PDMS are directly proportional to stiffness of the structure. The lead wires had no effect on the stiffness of the base.

4.4.4. Cords implanted with flexible-base arrays resembled the ones implanted with no base

The spinal cord undergoes three types of deformations during daily activities; elongation, torsion and flexion. These three deformation were quantified by several groups [34,38]. Margulies et al. [34] used motion-tracking MRI to report a maximal strain of 12% during regular daily activities. *Cheng et al.*[15] presented a methodology to assess the influence of implanted arrays on the mechanical behavior of the spinal cords. The methodology studied the behavior of cords elongated by 12% when implanted with solid-based and no-base arrays. It was shown that the solid-based arrays are mechanically incompatible with the cord; i.e. the solid-base arrays impeded the motion of the cord, while individual wires did not cause any significant change in the mechanical behavior of the cord. The motion impedance caused by the solid-base arrays is believed to cause physical damage to cord if chronically implanted. Based on these results, the influence of the FBEA on the surrogate spinal cord was assessed by replicating the same test with the same equipment. The results were compared to those found for cords implanted with solid-base and no-base arrays. They were also compared to control unimplanted surrogate cords.

As shown in Figure 4.12, cords implanted with the flexible-based arrays showed strains that resembled those measured for the cords implanted with individual electrodes and the control cords with no implanted arrays. The strains measured between the upper reference marks for the FBEA were the same as the ones measured for the cords with individual wires and almost three times bigger than those reported for the cords implanted with solid-base arrays. This result is supported by the fact that larger strains were also reported between the bottom reference points of the cords implanted with FBEAs over those implanted with solid-based arrays. This suggests that the mechanically compatible FBEA deforms at the same rate with the cord unlike the solid-base array. The similarity in the obtained strains between the cords implanted with the flexible-base arrays and the ones implanted with individual wires suggests that the FBEA, if chronically implanted, should show the similar histological results reported by Bamford et al. [31] for individual wires. The latter showed that chronically individual wires are tolerated by the spinal cord. However, further analysis about the mechanical behavior between the flexible-base arrays and the cords is needed before validating such an assumption.

4.4.5. Finite element validation and stress analysis

The finite element model is a very important tool to give a further understanding of the mechanical interaction between the electrodes of different types of arrays and the spinal cord. The experimental results showed that the elongated cords implanted with FBEAs statistically resembled the ones implanted with individual wires. However, the experimental setup had various sources of errors that were reported by Cheng et al [15]. Examples of these errors are the fixation of the cord to the mold, the subjective nature of the strain measurement, optical error associate with the used optics, etc. Thus, the finite element model can give us a better indication of the difference between cords implanted with the different kinds of arrays. It can also indicate whether the flexible-base and solid-base arrays will cause any potential damage to the cords. This can be done by

comparing the stresses imposed by the electrodes of the latter two arrays on the cord to those induced by the individual electrodes.

The next step was to validate the developed model. The results presented in Figure 4.13 show similar strains measured for L1-L3 between the physical and the finite element models. The error shown for L4 can be referred to the imperfect clamping between the surrogate cord and the Teflon stand. While we had full control over the boundary conditions of the finite element model, the physical model was fixated to the base by two Teflon bolts (Figure 4.5). The pressure applied by the bolts on the cord is thought to effect the deformation at the extremities of the cord, thus the measured strains at L4. On the other hand, the strain difference measured at the lower L1 between the finite element model and the solid-base array is thought to be an experimental error. In the experimental setup the deformation between the reference points are measured optically. L1 is the distance between the inner two reference points, thus it is the smallest measured distance and small errors in the deformation measurements causes more pronounced errors. Thus, the overall resemblance in the strains between the physical and the finite element model validates the latter model.

The stresses are maximal at the layer interfacing between the base and the cord (distance from edge = 0 in Figure 4.14) due to the mismatch in the stiffness between the base, the electrode and the spinal cord. The increase in the stress at the tip is due to mismatch in the material properties between the electrode and the spinal cord, in addition to the discontinuities (singularities) caused by the sharp edge of the tip [39].

The inner and outer individual electrodes induced similar stresses across the cord (Figures 4.14a, b). This is due to the similarity of deformations across the cords implanted with no-base array; i.e. the electrodes move freely with respect to each other due to the absence of any base. The same stresses are reported for the compliant FBEAs validating their mechanical compliance with the spinal cord.

On the other hand, the outer electrodes showed significantly higher stresses than the inner electrodes for the flexible- and rigid-based arrays, with the latter showing a bigger jump in stresses between the electrodes. This indicates that the strains measured at the inner electrodes of both arrays are smaller than those measured at the outer electrodes. Thus, the inner electrodes deform to a smaller extent than the outer electrodes. This is validated by the fact that experimentally measured strains at L2 are higher than the ones observed for L1

When comparing Figures 4.14a, c and e, it is obvious that outer electrodes of stiffer bases caused the higher stresses. The higher stresses at the outer electrodes are due to the higher strains observed in the tissues that are micrometers away from these electrodes. This can be related to higher tension in the tissue interfacing with the outer two electrodes of the array. Higher strains/stresses at this location of the tissue are believed to indicate more potential damage on the tissue. On the other hand, Figures 4.14b, d and f show that the inner electrodes of stiffer bases induced smaller stresses/strains in the tissue. This is due to the fact that the inner electrodes of stiffer bases deform less than those of flexible-based. The lower strains in here mean less deformation in the tissue and thus higher potential of physical damage. In other words, the lack of mechanical compliance between an array and the cord caused the outer electrodes of the array to shield the strain from the inner electrodes. This shielding is caused by the mismatch between the mechanical properties of the two interfacing media. Higher mismatch causes higher shielding; i.e. bigger difference in the stresses measured along the outer electrodes and the ones measured along the inner electrodes. This discontinuity in the profile of the stresses along the SC is believed to cause damage to its tissue. In the case of 12% elongation, it is evident that developed FBEAs showed more compliance (i.e. less shielding) with the cord than the rigid-based arrays. This is shown by the fact that the stress ratio between the outer and inner electrodes for the FBEA is much smaller than that of the rigid-based arrays (Figure 4.15). This validates the mechanical improvements obtained in the experimental work and validates the need of a FBEA for such applications.

While similar analysis applies for the cords under flexion, it should be noted that the stresses obtained for the bending are smaller than the ones obtained for the cord elongation by at least 3.5 times (rigid-based array). Thus, for such small degrees of bending, the 12% cord elongation is more critical and has the potential to cause more damage. However, it should be noted that in the case of bending shown in figure 4.7 the outer electrodes shield the strains from the inner electrodes, thus not allowing the upper part of the cord to undergo tension. The ratio of stresses between the outer electrodes and the inner electrodes also shows that the developed FBEA shows better compliance with the cord than the rigid-based array, while the compliant FBEA shows full compliance with the cord.

Contrary to the experimental results, the simulated stress ratios show that the developed FBEA is not fully compliant with the spinal cord (Figure 4.15). Unlike the cords implanted with individual electrodes, the ones implanted with the developed FBEA showed a change in the stresses induced by the outer and inner electrodes indicating a mismatch between the mechanical properties of the developed FBEAs and the cords. However, Figure 4.15 shows the significant improvement that the developed FBEA have shown when compared to the solid-based arrays. Also, Figures 4.15 show that the electrodes of the compliant FBEA (E=90kPa and thickness=0.3mm) induce stress ratios that are similar to the ones obtained with the individual wires for the elongated and bent cords.

The discrepancy between the in-vitro strain test and the finite element model is believed to be due to experimental error in the measurement technique of the strains in the in-vitro tests. For example, the cords are assumed to be isotropic; thus, the application of the 12% elongation should have caused uniform 12% strains across the cord (L1-L4). However, Cheng et al. reported smaller strains for the control samples [15]. Also the cords implanted with individual microelectrode wires showed big variations in the strains. For example, the strains measured between the upper L1 reference points varied almost 4%. This suggests that the

experimental methodology of constraining the cords and measuring the strains is potentially not be very accurate. It is believed that finite element model is more precise and describes the actual physical interaction between the arrays and the cords.

While no attempts have been done to measure the yield strength of spinal cord tissue, it is suggested that the stresses induced by the no-base arrays are tolerated by the spinal cord. Thus, the stresses imposed by the outer electrodes of the currently developed FBEA and the rigid-based array are believed to cause higher compression on the tissue or potentially tearing. On the contrary, the low strains induced by the inner electrodes of the solid-based arrays and FBEAs (much lower for the former) show that the outer electrodes are shielding deformation of the tissue due to the mismatch in the mechanical properties of the two types of arrays with the spinal cord. Yet, it was proven that the already developed FBEAs are more mechanical compliant with the spinal cord than the rigid-based arrays. It was also shown that the compliant FBEAs resemble the same mechanical behavior as the electrodes implanted with no base.

4.4.6. Other neural systems

Currently developed electrode arrays are designed and fabricated to interface with a specific neural target. For example, the Utah, Michigan and HMRI arrays are designed to interface with the brain [9–12]. For instance, the HMRI was able to record from and simulate the subthalamic nucleus of cats. It was also implanted for a short time (less than 150 days) into feline spinal cord for 85 days to regain control of the bladder and bowel [13]. Cheng et al. [15] showed that these arrays drastically impeded the motion of the surrogate cord as it deforms. The motion impediment is caused by the mechanical properties mismatch between the solid-based arrays and the spinal cord.

The current work presents the first study to assemble microwire electrodes into a flexible-based array. It is also the first to assess the influence of these arrays on

the mechanical behavior of surrogate spinal cords. A customizable, feasible and repeatable fabrication process for such arrays was presented. The flexibility of the design allows variations in the curvature and geometry of the base. The density and location of the electrodes can also be customized. The thickness of the base and the polymerization temperatures are used to control the mechanical properties of the structure. The experimental and FEM results (Figure 4.12) showed that such arrays can be mechanically compliant with the target neural system and behave similar to individual wires.

The high flexibility of the developed design makes it a good candidate to interface with other neural systems, such as the brain. The arrays can be modified to match the curvature of the targeted system to ensure full contact between both surfaces. The mechanical properties of the array can also be tuned to match the target stiffness resulting in maximal mechanical compliance between the two interfacing media. The fabrication protocol also allows for the use of different kinds and densities of electrodes depending on the targeted neural tissue.

4.5. Conclusion

In the present work, we presented a fabrication protocol for a flexible-based electrode array. The repeatability of the fabrication protocol was studied. Then, the influence of the different components of the array on its mechanical properties was analyzed. Prototypes were fabricated according to the fabrication and protocol. The prototypes were then implanted into a surrogate cord that resembles the mechanical properties and behavior of human spinal cord and a 12% strain, which is the maximum strain reported for a human spinal cord, was applied to the cords. The influence of the FBEAs on the mechanical behavior of the cords was compared to those caused by solid-based, no-base arrays and to control cords with no implanted arrays.

The geometrical characterization of the developed prototypes proved that the fabrication protocol is repeatable. The maximum measured errors were less than

5% for the base thickness and 1% for the electrode height and spacing. Once the protocol repeatability was validated, the influence of the different components of the array on its stiffness was assessed. The polymerization temperature of the PDMS base showed to have an influence on the stiffness. Higher polymerization temperatures gave higher structure stiffness. The lowest polymerization temperature was 66 ^{0}C. The modulus of elasticity at this temperature was ~500kPa which is 5.56 times higher than that of the desired E of the compliant array which is 90kPa. The thickness of the base also had a proportional relationship with the stiffness. The lowest thickness we achieved was 0.65mm which is 2.17 times higher than that of the desired compliant FBEA (0.3mm). Developed flexible-based arrays were implanted into surrogate cords that mimic the human spinal cord. The application of the 12% elongation on the cords showed that the FBEAs, similar to the individual wires, did not influence the mechanical behavior of the surrogate cord. The cords with implanted FBEAs showed strains that are more than 200% bigger than those implanted with solid-based arrays. This improvement was validated by the FEM which showed that the developed FBEA cause less stress shielding than the solid-based arrays. However, the finite element model showed that the stiffness of the developed FBEA should be further reduced to decrease the stress ratios between the outer and inner electrodes and to emulate those obtained for no-base arrays. A base thickness and modulus of elasticity of 0.3mm and 90kPa respectively proved to be mechanically compliant with the cords; with these parameters the array, similar to individual wires, showed no signs of stress shielding and electrodes moved freely with respect to each other. The model also validated the assumption that stiffer bases have higher potential of causing physical damage to the cord due to the higher shielding of stresses by the outer electrodes. Finally, we concluded that enhanced FBEAs are excellent candidates to interface with the spinal cord and potentially other neural systems.

4.6 Bibliography:

[1] V. K. Mushahwar and K. W. Horch, "Proposed specifications for a lumbar spinal cord electrode array for control of lower extremities in paraplegia," *IEEE Transactions on Rehabilitation Engineering: A Publication of the IEEE Engineering in Medicine and Biology Society*, vol. 5, no. 3, pp. 237-243, Sep. 1997.

[2] J. Hunter and P. Ashby, "Secondary changes in segmental neurons below a spinal cord lesion in man," *Archives of Physical Medicine and Rehabilitation*, vol. 65, no. 11, pp. 702-705, Nov. 1984.

[3] V. K. Mushahwar, P. L. Jacobs, R. A. Normann, R. J. Triolo, and N. Kleitman, "New functional electrical stimulation approaches to standing and walking," *Journal of Neural Engineering*, vol. 4, no. 3, p. S181-S197, Sep. 2007.

[4] V. K. Mushahwar and K. W. Horch, "Selective activation of muscle groups in the feline hindlimb through electrical microstimulation of the ventral lumbo-sacral spinal cord," *IEEE Transactions on Rehabilitation Engineering: A Publication of the IEEE Engineering in Medicine and Biology Society*, vol. 8, no. 1, pp. 11-21, Mar. 2000.

[5] V. K. Mushahwar, D. M. Gillard, M. J. . Gauthier, and A. Prochazka, "Intraspinal micro stimulation generates locomotor-like and feedback-controlled movements," *IEEE Transactions on Neural Systems and Rehabilitation Engineering*, vol. 10, no. 1, pp. 68-81, Mar. 2002.

[6] R. Saigal, C. Renzi, and V. K. Mushahwar, "Intraspinal Microstimulation Generates Functional Movements After Spinal-Cord Injury," *IEEE Transactions on Neural Systems and Rehabilitation Engineering*, vol. 12, no. 4, pp. 430-440, Dec. 2004.

[7] B. Lau, L. Guevremont, and V. K. Mushahwar, "Strategies for generating prolonged functional standing using intramuscular stimulation or intraspinal microstimulation," *IEEE Transactions on Neural Systems and Rehabilitation Engineering: A Publication of the IEEE Engineering in Medicine and Biology Society*, vol. 15, no. 2, pp. 273-285, Jun. 2007.

[8] V. K. Mushahwar, D. F. Collins, and A. Prochazka, "Spinal Cord Microstimulation Generates Functional Limb Movements in Chronically Implanted Cats," *Experimental Neurology*, vol. 163, no. 2, pp. 422-429, Jun. 2000.

[9] P. K. Campbell, K. E. Jones, R. J. Huber, K. W. Horch, and R. A. Normann, "A silicon-based, three-dimensional neural interface: manufacturing processes for an intracortical electrode array," *Biomedical Engineering, IEEE Transactions on*, vol. 38, no. 8, pp. 758-768, 1991.

[10] E. M. Maynard, C. T. Nordhausen, and R. A. Normann, “The Utah Intracortical Electrode Array: A recording structure for potential brain-computer interfaces,” *Electroencephalography and Clinical Neurophysiology*, vol. 102, no. 3, pp. 228-239, Mar. 1997.

[11] A. C. Hoogerwerf and K. D. Wise, “A three-dimensional microelectrode array for chronic neural recording,” *IEEE Transactions on Bio-Medical Engineering*, vol. 41, no. 12, pp. 1136-1146, Dec. 1994.

[12] D. McCreery, A. Lossinsky, V. Pikov, and X. Liu, “Microelectrode array for chronic deep-brain microstimulation and recording,” *IEEE Transactions on Bio-Medical Engineering*, vol. 53, no. 4, pp. 726-737, Apr. 2006.

[13] D. McCreery, V. Pikov, A. Lossinsky, L. Bullara, and W. Agnew, “Arrays for chronic functional microstimulation of the lumbosacral spinal cord,” *IEEE Transactions on Neural Systems and Rehabilitation Engineering: A Publication of the IEEE Engineering in Medicine and Biology Society*, vol. 12, no. 2, pp. 195-207, Jun. 2004.

[14] D. E. Harrison, R. Cailliet, D. D. Harrison, S. J. Troyanovich, and S. O. Harrison, “A review of biomechanics of the central nervous system--Part II: Spinal cord strains from postural loads,” *Journal of Manipulative and Physiological Therapeutics*, vol. 22, no. 5, pp. 322-332, Jun. 1999.

[15] C. Cheng, “Development of Surrogate Spinal Cords for the Evaluation of Electrode Arrays Used in Intraspinal Implants,” Thesis, University of Alberta, Edmonton, 2011.

[16] E. L. Mazuchowski and L. E. Thibault, “Biomechanical Properties of the Human Spinal Cord and Pia Mater,” presented at the Summer Bioengineering Conference, Sonesta Beach Resort in Key Biscayne, Florida, 2003, pp. 1205,1206.

[17] P. J. Rousche and R. A. Normann, “Chronic recording capability of the Utah Intracortical Electrode Array in cat sensory cortex,” *Journal of Neuroscience Methods*, vol. 82, no. 1, pp. 1-15, Jul. 1998.

[18] J. A. Bamford and V. K. Mushahwar, “Intraspinal microstimulation for the recovery of function following spinal cord injury,” *Progress in Brain Research*, vol. 194, pp. 227-239, 2011.

[19] V. G. Vanderhorst and G. Holstege, “Organization of lumbosacral motoneuronal cell groups innervating hindlimb, pelvic floor, and axial muscles in the cat,” *The Journal of Comparative Neurology*, vol. 382, no. 1, pp. 46-76, May 1997.

[20] G. J. Romanes, “The motor cell columns of the lumbo-sacral spinal cord of the cat,” *The Journal of Comparative Neurology*, vol. 94, no. 2, pp. 313-363, Apr. 1951.

[21] R. E. Burke, P. L. Strick, K. Kanda, C. C. Kim, and B. Walmsley, “Anatomy of medial gastrocnemius and soleus motor nuclei in cat spinal cord,” *Journal of Neurophysiology*, vol. 40, no. 3, pp. 667 -680, May 1977.

[22] J. M. Van Buren and K. Frank, “Correlation between the morphology and potential field of a spinal motor nucleus in the cat,” *Electroencephalography and Clinical Neurophysiology*, vol. 19, no. 2, pp. 112-126, Aug. 1965.

[23] K. W. Meacham, R. J. Giuly, L. Guo, S. Hochman, and S. P. DeWeerth, “A lithographically-patterned, elastic multi-electrode array for surface stimulation of the spinal cord,” *Biomedical Microdevices*, vol. 10, no. 2, pp. 259-269, Oct. 2007.

[24] J. Kitzmiller, D. Beversdorf, and D. Hansford, “Fabrication and testing of microelectrodes for small-field cortical surface recordings,” *Biomedical Microdevices*, vol. 8, no. 1, pp. 81-85, Mar. 2006.

[25] Z. Yu, O. Graudejus, C. Tsay, S. P. Lacour, S. Wagner, and B. Morrison, “Monitoring hippocampus electrical activity in vitro on an elastically deformable microelectrode array,” *Journal of Neurotrauma*, vol. 26, no. 7, pp. 1135-1145, Jul. 2009.

[26] S. H. Kim, J.-H. Moon, J. H. Kim, S. M. Jeong, and S.-H. Lee, “Flexible, stretchable and implantable PDMS encapsulated cable for implantable medical device,” *Biomedical Engineering Letters*, vol. 1, pp. 199-203, Sep. 2011.

[27] D. D. Zhou and E. Greenbaum, “Implant Packaging and Biocompatibility of Materials,” in *Implantable Neural Prostheses 1: Devices and Applications*, Springer, 2009, p. 21.

[28] S. L. Peterson, A. McDonald, P. L. Gourley, and D. Y. Sasaki, “Poly(dimethylsiloxane) thin films as biocompatible coatings for microfluidic devices: Cell culture and flow studies with glial cells,” *Journal of Biomedical Materials Research Part A*, vol. 72, no. 1, pp. 10-18, Jan. 2005.

[29] K. W. Meacham and S. Hochman, “Selective stimulation of the spinal cord surface using a stretchable microelectrode array,” *Frontiers in Neuroengineering*, vol. 4, p. 5, 2011.

[30] M. C. Bélanger and Y. Marois, “Hemocompatibility, biocompatibility, inflammatory and in vivo studies of primary reference materials low-density

polyethylene and polydimethylsiloxane: a review," *Journal of Biomedical Materials Research*, vol. 58, no. 5, pp. 467-477, 2001.

[31] J. A. Bamford, K. G. Todd, and V. K. Mushahwar, "The effects of intraspinal microstimulation on spinal cord tissue in the rat," *Biomaterials*, vol. 31, no. 21, pp. 5552-5563, Jul. 2010.

[32] S. Snow, K. W. Horch, and V. K. Mushahwar, "Intraspinal Microstimulation using Cylindrical Multielectrodes," *IEEE Transactions on Biomedical Engineering*, vol. 53, pp. 311-319, Feb. 2006.

[33] S. Snow, S. C. Jacobsen, D. L. Wells, and K. W. Horch, "Microfabricated cylindrical multielectrodes for neural stimulation," *IEEE Transactions on Biomedical Engineering*, vol. 53, no. 2, pp. 320-326, Feb. 2006.

[34] S. S. Margulies, D. F. Meaney, L. B. Bilston, L. E. Thibault, N. G. Campeau, and S. J. Riederer, "In Vivo Motion of the Human Cervical Spinal Cord in Extension and Flexion," in *Proceedings of the 1992 International IRCOBI Conference on the Biomechanics of impacts*, VERONA, ITALY, 1992.

[35] T. Ishii et al., "Kinematics of the cervical spine in lateral bending: in vivo three-dimensional analysis," *Spine*, vol. 31, no. 2, pp. 155-160, Jan. 2006.

[36] J. M. Macpherson and Y. Ye, "The cat vertebral column: stance configuration and range of motion," *Experimental Brain Research. Experimentelle Hirnforschung. Expérimentation Cérébrale*, vol. 119, no. 3, pp. 324-332, Apr. 1998.

[37] P. J. Rousche, D. S. Pellinen, D. P. Pivin, J. C. Williams, R. J. Vetter, and D. R. kirke, "Flexible polyimide-based intracortical electrode arrays with bioactive capability," *Biomedical Engineering, IEEE Transactions on*, vol. 48, no. 3, pp. 361-371, 2001.

[38] Q. Yuan, L. Dougherty, and S. S. Margulies, "In vivo human cervical spinal cord deformation and displacement in flexion," *Spine*, vol. 23, no. 15, pp. 1677-1683, Aug. 1998.

[39] J. Subbaroyan, D. C. Martin, and D. R. Kipke, "A finite-element model of the mechanical effects of implantable microelectrodes in the cerebral cortex," *Journal of Neural Engineering*, vol. 2, pp. 103-113, Dec. 2005.

Chapter 5

Conclusion/ Future Directions

This chapter presents a summary of the work presented in the previous three chapters and introduces the recommendations for the future work. The conclusion section summarizes the work that was done to fabricate a passive flexible-based electrode array. It lists the motivation behind the work and the outline followed to fabricate, characterize and bench test the array. Then, the stresses caused by the electrodes of three different types of arrays on an elongated and bent spinal cord are presented. Finally, the next steps that are required to enhance the design of the array so it can be chronically implanted are recommended based on the work done.

5.1 Conclusion

The number of patients suffering from spinal cord injury (SCI) is increasing drastically. In Canada, for example, it is expected to have more than 120,000 patients suffering from SCI within the next two decades [1]. The symptoms of such injuries can vary widely depending on the location of the injury. Injuries in the lumbar and sacral regions of the spinal cord can lead to loss of control and function in the lower parts of the body including legs, hips, bowel and bladder. In addition to the emotional and psychological effects on the patient, such injuries have tremendous costs. For example, it is estimated that the annual cost of such injuries in Canada alone is approximately 3.6 billion Canadian dollars [2].

Intraspinal microstimulation (ISMS) is a promising technique that is being developed to help patients in restoring function and control of the lower extremities. This technique is based on implanting very small, hair-like, electrodes into the lumboscral regions of the spinal cord. These electrodes are used to stimulate the functional regions of the spinal cord to emulate signals issued by the brain. However, the electrodes are implanted individually which can be very tedious for the surgeon and potentially dangerous to the patient as minor mistakes from the surgeon can lead to another SCI. Thus, the goal of this work was to develop a preliminary process that sets the ground and allows for further development in the fabrication of arrays the would be used for ISMS.

To develop such an array, it was critical to study the currently available technology to derive the required design criteria of an array that would be used for the ISMS application. A thorough study was done on the arrays that were developed to interface with the neural system. The arrays were divided into two categories based on their structure and invasiveness; Epi-neural arrays (2D, non-invasive) or intra-neural arrays (3D, invasive). Under each category, arrays were divided into two subcategories based on the target neural system; arrays interfacing with the peripheral nervous system or the central nervous system. In each subcategory, the arrays were ordered chronologically according to the time they were developed. The cons and pros of each array were studied and compared to its target and to the nature of the interface. From this study, it was concluded that a 3D multi-electrode array is needed for the ISMS application. The array has to have a flexible biocompatible base that has compliant mechanical properties with the spinal cord. For such an application, the array is patient specific. Thus, the base thickness and electrode layout is variable and case specific. Also, full contact between the base of the array and the spinal cord can be achieved through a matching curvature between the two interfacing media. This curvature is also patient specific. In addition, the lead wires should ameliorate the external forces transferred to the electrodes as these forces can cause physical damage to the interfacing tissue. Thus, the fabrication protocol should be customizable and allow for full control over the layout of the electrodes, the base thickness and the base curvature. Also, a methodology is needed to relief any forces applied on the lead wires. Finally, it is desirable to have a short turn-around time and a low cost to fabricate such an array.

Polydimethysiloxane (PDMS) was chosen as the base material. PDMS is a silicone based elastomer. It is used in implantable medical devices, biocompatible, gas permeable and transparent [3, 4]. It has tunable mechanical properties with a modulus of elasticity orders of magnitude lower than other materials used for interfacing applications [5]. The electrodes were selected to be

either Platinum/Iridium (Pt/Ir) or stainless steel (SS) due to their biocompatibility, MRI compatibility and controllable impedance.

A 2 dimensional finite element model was developed on ANSYS to determine the design specifications (base thickness and modulus of elasticity) for the compliant flexible-based array. The model was used to study the influence of the geometrical and material properties of the base and the electrodes on the interaction between the array and the cord. It was shown that the thickness and modulus of elasticity of the base have a pronounced influence on the interaction between the two media. The decrease in the value of any of the two parameters lowered the stiffness of the array and caused a better compliance. On the other hand, the electrode diameter and modulus of elasticity did not influence the interaction between the two media. The obtained trends were used to determine the specifications of the compliant flexible-based array. To obtain an array-cord interaction similar to the one observed with no-base arrays, it is desired to have a base thickness of 0.3mm with a modulus of elasticity of 90kPa.

Rapid prototyping was chosen to create the molds of the arrays. This technique is fully controllable, inexpensive and has a short turn-around time. The design of the molds was done on Pro/Engineering software. The molds consisted of a female mold which controls the base curvature and the layout of the electrodes. The latter mold has holes where electrodes are manually placed before casting the PDMS. The designs are fabricated in the mechanical engineering fabrication shops. Usually they are delivered in less than a day and cost almost 25$/mold. The male mold is used to control the thickness of the base. However, these types of molds and the used PDMS limited the minimum achievable base thickness and modulus of elasticity to 0.65mm and 500kPa. These limitations were caused by the pure heat conductivity of PDMS and type of PDMS used.

Microwire electrodes that are currently being used for ISMS by Mushahwar et al.[6–8], were used in the fabrication of the array. The lead wires were coiled into

a coil shape to relief any external forces applied on them. A strain test showed that coiled lead wires can relief strains that are higher than the maximum ones attained by human spinal cord.

A protocol was defined to assemble the flexible-based arrays. The location of the electrodes is tuned in the pro/E design to meet the specifications obtained from the MRI images of the patients. The mold design is fabricated at the Mechanical Engineering Machine Shop. The fabricated molds are cleaned and a placed in a vacuum chamber to grow a small layer of silane on their surfaces. The lead wires are coiled and the electrodes are bent to the desired height. The electrodes and lead wires are placed manually in the female mold. PDMS (MED 6215) is mixed at a ratio of 10:1 by mass and degassed then poured on top of the female mold. The mold is closed and the PDMS is cured under a temperature of 66^0C for 90 min. The molds are taken out and opened. The flexible-based array is peeled off manually from the female mold using tweezers. Finally, rapid prototype handles are adhered to the top of the base using a layer of Polyethylene glycol (PEG).

Various prototypes were developed to characterize the array and study the repeatability of the fabrication process. To examine the repeatability of the fabrication process three geometrical parameters were assessed. The base thickness, electrode height and electrode spacing were optically measured and compared to the targeted values. The optical measurements showed that the cured bases had a maximum error less than 5% when compared to the target thickness. The electrode height error was less than 0.5% and the measured electrode spacing in the longitudinal and transverse planes had an error less than 1% the targeted values. These measured errors show that the fabrication process is repeatable.

Validating the repeatability of the fabrication process allowed us to move to the bench testing phase. In this phase, the influence of three parameters on the mechanical properties of the array was tested. The three parameters were: PDMS curing temperature, base thickness and lead wire structure. The axial stiffness was

measured using the dynamic mechanical analysis (DMA). The obtained measurements showed that the base thickness and curing temperature have a proportional relationship with the stiffness of the structure. The lowest average achieved curing temperature for MED 6215 was 66^0C and gave a modulus of elasticity of 500kPa. The lead wires caused did not effect the stiffness of the structure.

Flexible-based arrays were fabricated according to the fabrication protocol and were implanted in surrogate cords that mimic the mechanical behaviour and properties of human spinal cord. A protocol developed by Cheng et al. was used to study the influence of the flexible-based arrays on the mechanical behaviour of the surrogate cords. A 12% uni-axial strain was applied to cords implanted with the arrays and the strains across the cords were measured. The 12% strain was used because it resembles the maximum axial strain measured for human spinal cord during normal daily activities [9]. The results obtained from the strain test were compared to the results obtained for the same test using rigid-based, no-base (individual electrodes) and control cords with no implanted arrays. The latter tests were performed and reported by Cheng et al. [10]. The strain test showed that the cords implanted with flexible-based arrays statistically resembled a similar behaviour to those implanted with the individual electrode wires. The test also showed the flexible-based arrays allowed significant strain improvement (almost triple) in the cords over the rigid-base arrays.

The experimental results obtained from the strain test were used to validate the finite element model that was developed to simulate the strain test. The results obtained from the finite element model were within the standard deviations of the experimental results. These results validated the model and allowed using it to further understand the interaction between the different types of arrays and the spinal cord.

To have a further understanding of the mechanical interaction between the array and the spinal cord, the stresses induced by the electrodes of different types of arrays were examined. The stresses were plotted for the no-base (individual wires), developed flexible-based, rigid-based and compliant flexible-based arrays. By studying the ratio of stresses induced by the outer electrodes to those induced by the inner electrodes, it was shown that the experimentally developed flexible-base arrays are more mechanically compliant with the cord than the rigid-based arrays; yet, less compliant than the no-base arrays. On the other hand, the compliant flexible-based array showed similar mechanical compliance with the spinal cord to that shown for the no-base arrays where electrodes moved independently from each other.

This stress analysis showed us that the mismatch in the mechanical properties between the arrays and the cords causes the outer electrodes of such arrays to shield stress from the inner electrodes causing a discontinuity in the stress/strain profile over the longitudinal axis of the cord. Such shielding is believed to cause damage to the tissue of the SC. On the other hand, the individual electrodes and the compliant FBEA showed no signs of shielding which indicates that the latter two arrays are tolerated by the SC tissue.

Finally, the model was used to study the interaction between the different types of arrays and the spinal cord when it undergoes bending. Cords implanted with the developed flexible-based, compliant flexible-based, rigid-based and no-base arrays were exposed to bending and the stresses induced by the electrodes on the cord were examined. It was shown that under bending, the maximum reported stresses were more almost 3 times smaller than those reported for the elongated cords. Similar to the elongation case, the developed flexible-based arrays showed improvement over the rigid-based arrays. Also, the compliant flexible-based arrays induced the same stresses as the ones induced by individual wires. Both tests, showed that the mismatch in the mechanical properties between the array and the cord causes the outer electrodes of the array to shield the stresses and

strains from the inner electrodes. Higher shielding is believed to indicate higher physical damage on the cord.

The compliant flexible-based arrays proved to emulate the mechanical effects of the individual microwires when implanted in a spinal cord. The flexibility of the reported fabrication protocol and array design allows these arrays to be used with other neural systems, such as the brain. The mechanical properties and the geometry of the different components of the array can be easily modified to interface with any neural system for various applications.

5.2 Future Work

The ultimate goal of developing a flexible-based array is to chronically implant such an array in the spinal cord of patients. The current work is the first step in developing such a device. In this manuscript, a fabrication protocol for passive flexible-based electrode arrays was presented. This preliminary work focused on developing a primary prototype that would be used in vitro bench testing to validate the theory. A feasible fabrication methodology was presented and its repeatability was validated. The fabricated prototypes showed big improvement on the currently available rigid-based arrays. Then, the preliminary developed 2D finite element model was validated by the experimental work. The validated model was used to obtain the optimal design of an intra-neural array to be used for ISMS application.

To improve on the design and prepare the array for the next step which would be animal testing the following two parallel paths are recommended: The first one is theoretical and the second one is experimental.

I suggest improving the 2D model by creating a 3D model that would resemble the actual spinal cord. The 3D model would allow a further understanding of the behaviour of the cord implanted with the array under twisting. It can be also used to create a dynamic model that would resemble the actual behaviour of the spinal

cord. Such a model, can give a good understanding of the interaction between the array and the spinal cord during daily activities. Also, as 3D model would allow the understanding of out of plane stresses. The model can be further improved by simulating the actual properties of the spinal cord.

In parallel to the previous step, it is recommended to improve the presented methodologies to lower the thickness and the modulus of elasticity of the base. The targeted thickness and modulus of elasticity are 0.3mm and 90kPa respectively. Since the low heat conductivity limits the capabilities of the RP molds, a potential solution for this problem is to change the material used for the molds. The best material would be a heat conductive material. Using such a good heat conductor has the potential of allowing for smaller thicknesses and curing temperatures. The latter will lead to smaller moduli of elasticity. Another potential solution is to try to find another biocompatible PDMS that would allow for lower moduli of elasticity.

Once the targeted thickness and moduli of elasticity are achieved, it is recommended to develop a methodology to experimentally test the behaviour of the spinal cord under bending and twisting when implanted with flexible-based array.

Once the experimental and theoretical data are obtained, I recommend moving into in-vitro testing. Implant the flexible-based arrays into the spinal cord of animal subjects for a short term and maintain imaging the implanted array. Then, perform histology tests on the spinal cords of the subjects.

In the array fabrication protocol we presented, the electrodes were bent and placed in the female molds manually. To have a higher throughput, it is recommended to develop an automized methodology for the electrode bending and placement. It is, also, suggested to design and fabricate the electrodes. The currently used electrodes have one active site at the tip. An improved electrode

design would have multiple active sites through out its height. Such a concept would be achieved through developing a new electrode design that will be fabricated at the University of Alberta Nanofab.

5.3 Bibliography

[1] A. Farry and D. Baxter, "The Incidence and Prevalence of Spinal Cord Injury in Canada Overview and estimated based on current evidence," Rick Hensen Institute, Project publication, Dec. 2010.

[2] "First of its kind research shows that as many as 86,000 Canadians are living with spinal cord injury | CPA Ontario." [Online]. Available: http://www.cpaont.org/news/all-regions/first-its-kind-research-shows-many-86000-canadians-living-spinal-cord-injury. [Accessed: 28-Oct-2011].

[3] D. D. Zhou and E. Greenbaum, "Implant Packaging and Biocompatibility of Materials," in *Implantable Neural Prostheses 1: Devices and Applications*, Springer, 2009, p. 21.

[4] S. H. Kim, J.-H. Moon, J. H. Kim, S. M. Jeong, and S.-H. Lee, "Flexible, stretchable and implantable PDMS encapsulated cable for implantable medical device," *Biomedical Engineering Letters*, vol. 1, pp. 199-203, Sep. 2011.

[5] R. K.-J. Huang, "Flexible neural implant," Thesis, California Institute of Technology, California, 2011.

[6] V. K. Mushahwar and K. W. Horch, "Selective activation of muscle groups in the feline hindlimb through electrical microstimulation of the ventral lumbo-sacral spinal cord," *IEEE Transactions on Rehabilitation Engineering: A Publication of the IEEE Engineering in Medicine and Biology Society*, vol. 8, no. 1, pp. 11-21, Mar. 2000.

[7] V. K. Mushahwar, D. F. Collins, and A. Prochazka, "Spinal Cord Microstimulation Generates Functional Limb Movements in Chronically Implanted Cats," *Experimental Neurology*, vol. 163, no. 2, pp. 422-429, Jun. 2000.

[8] V. K. Mushahwar and K. W. Horch, "Proposed specifications for a lumbar spinal cord electrode array for control of lower extremities in paraplegia," *IEEE Transactions on Rehabilitation Engineering: A Publication of the IEEE Engineering in Medicine and Biology Society*, vol. 5, no. 3, pp. 237-243, Sep. 1997.

[9] S. S. Margulies, D. F. Meaney, L. B. Bilston, L. E. Thibault, N. G. Campeau, and S. J. Riederer, "In Vivo Motion of the Human Cervical Spinal Cord in

Extension and Flexion," in *Proceedings of the 1992 International IRCOBI Conference on the Biomechanics of impacts*, VERONA, ITALY, 1992.

[10] C. Cheng, "Development of Surrogate Spinal Cords for the Evaluation of Electrode Arrays Used in Intraspinal Implants," Thesis, University of Alberta, Edmonton, 2011.

Appendices

Appendix A

Protocols

1. Mold Fabrication and cleaning

The following steps identify the fabrication and clean protocol of the rapid prototype molds:

1. Design the male and female mold on Pro/E
2. Save the file as ".stl"
3. Send the ".stl" file to the UofA MECE shop to (tuula.hilvo@ualberta.ca)
4. In the e mail, specify that the molds have to be glossy and transparent.
5. Once you receive an e mail that the molds are ready, pick them up from the MECE fabrication shop in the first flour of the MECE building.
6. Manually remove the resin from the molds.
7. Use the water jet in the MECE shop to rinse the molds.
8. Wear Nitrile gloves in the subsequent steps.
9. In the fume hood, pour 490mL distilled water into a glass beaker.
10. Add 10g of NaOH.
11. Stir with stick until NAOH completely dissolves in water
12. Place molds in the beaker on at a time. Make sure that the part of the mold that will be contacting the PDMS is exposed to the solution
13. Leave molds in the solution for 1 hour.
14. Remove the molds on at a time. Immediately after removal, thoroughly wash the molds with distilled water.
15. Immediately dry off the molds with a wiping cloth.
16. Place cleaned molds in a beaker.

2. PDMS preparation, casting and peeling

The following steps identify the protocol used to prepare, cast and polymerize the PDMS in the rapid prototypes molds.

1. Set up a microbalance in the fume hood.
2. Place a Teflon boat or a plastic beaker on the balance and zero the balance
3. Pour MED 6215 elastomer base to the desired amount. Record the measured mass.
4. Zero the microbalance.
5. Add the required elastomer curing agent (to mix at a ratio of 10:1, divide the value obtained at step 3 by 10)
6. Stir mixture with a stainless steel spatula for 2 to 3 minutes to thoroughly mix the 2 agents.
7. Degas the mixture in desiccator at room temperature for 15-20 minutes.
8. Repeat step 7 until the mixture is clear of air bubbles.
9. Place one drop of trichloro(1,1,2,2- perfluorooctyl)silane into the a designated silane vial.
10. Place the vial in the middle of the desiccator.
11. Place molds in the desiccator with molding side open to chamber environment.
12. Close the desiccator and open the vacuum valve.
13. Leave substrates under vacuum for at least 90 minutes.
14. Close the vacuum valve and open the air valve and take the molds out.
15. Pour a very small amount of distilled water in a glass petri dish.
16. Manually place the bent wires into the female molds.
17. Place the female molds in the petri dish with molding face up.
18. Cast the PDMS on top of the curved area.
19. Close the female mold with the male mold.
20. Place the molds in the oven (it should be steady at the desired temperature) for enough time to fully polymerize the PDMS.
21. Turn the oven off and take the molds out.

22. Let the molds cool down for at least 1 hour.

23. Open the male mold and manually (using tweezers) peel of the array.

Comments:

- Always wear nitrile gloves. Do not use Latex gloves as they inhibit the curing of PDMS.
- Do not leave the rapid prototypes in NaOH for more than 2 hours.

Appendix B

Strain plots

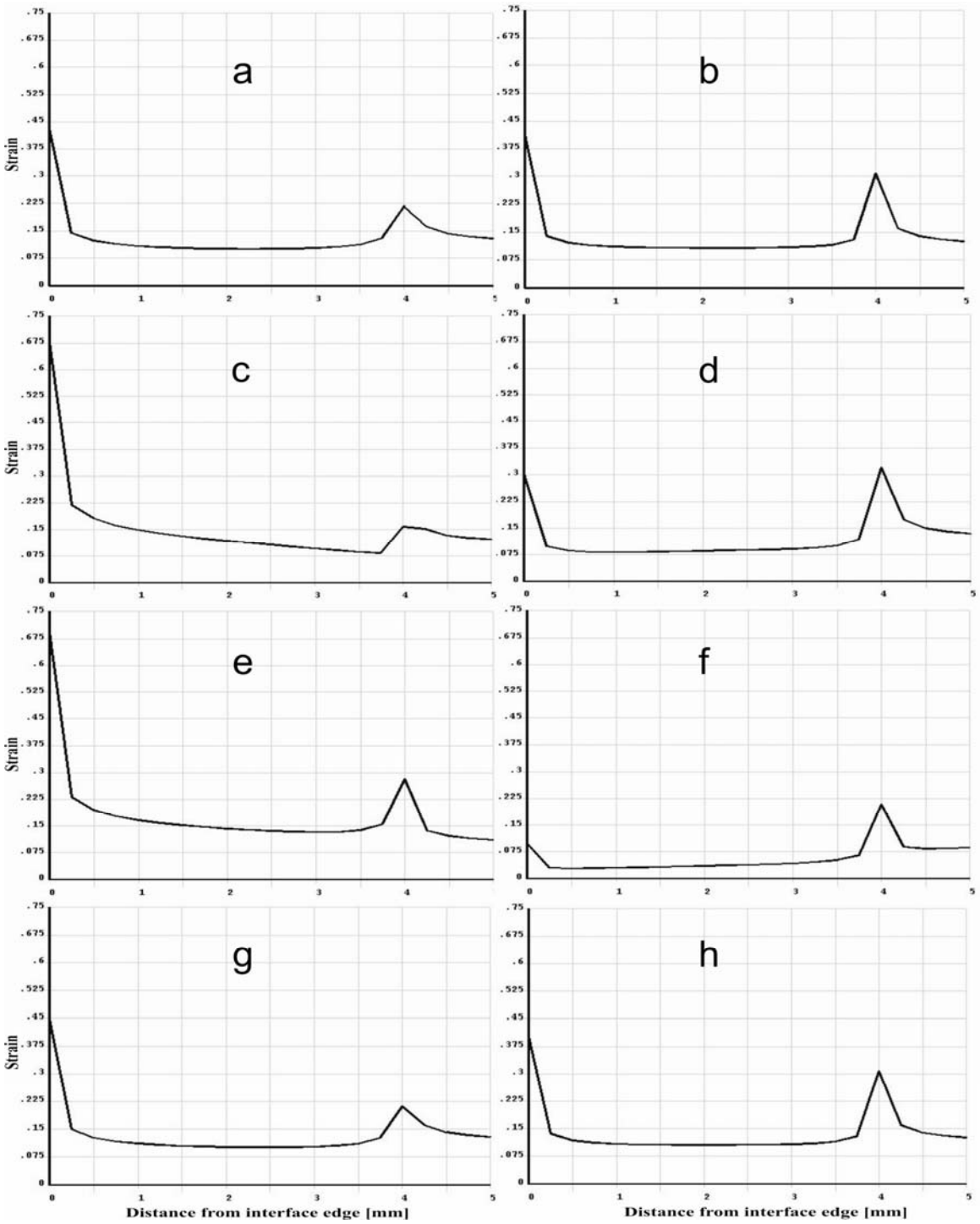

Figure B.1 Local *strains in the vicinity of electrodes* in an elongated cord. a, c, e, g show the strain near the outer electrodes (1 or 4). b, d, f, h represent the strains near the inner two electrodes (2 or 3) a and b show the strains calculated with the individual electrodes. c and d show the strains near the electrodes of the developed FBEA. e and f illustrate the strains measured near the electrodes of the rigid-based array. g and h show the strains formed near electrodes of the compliant FBEA.

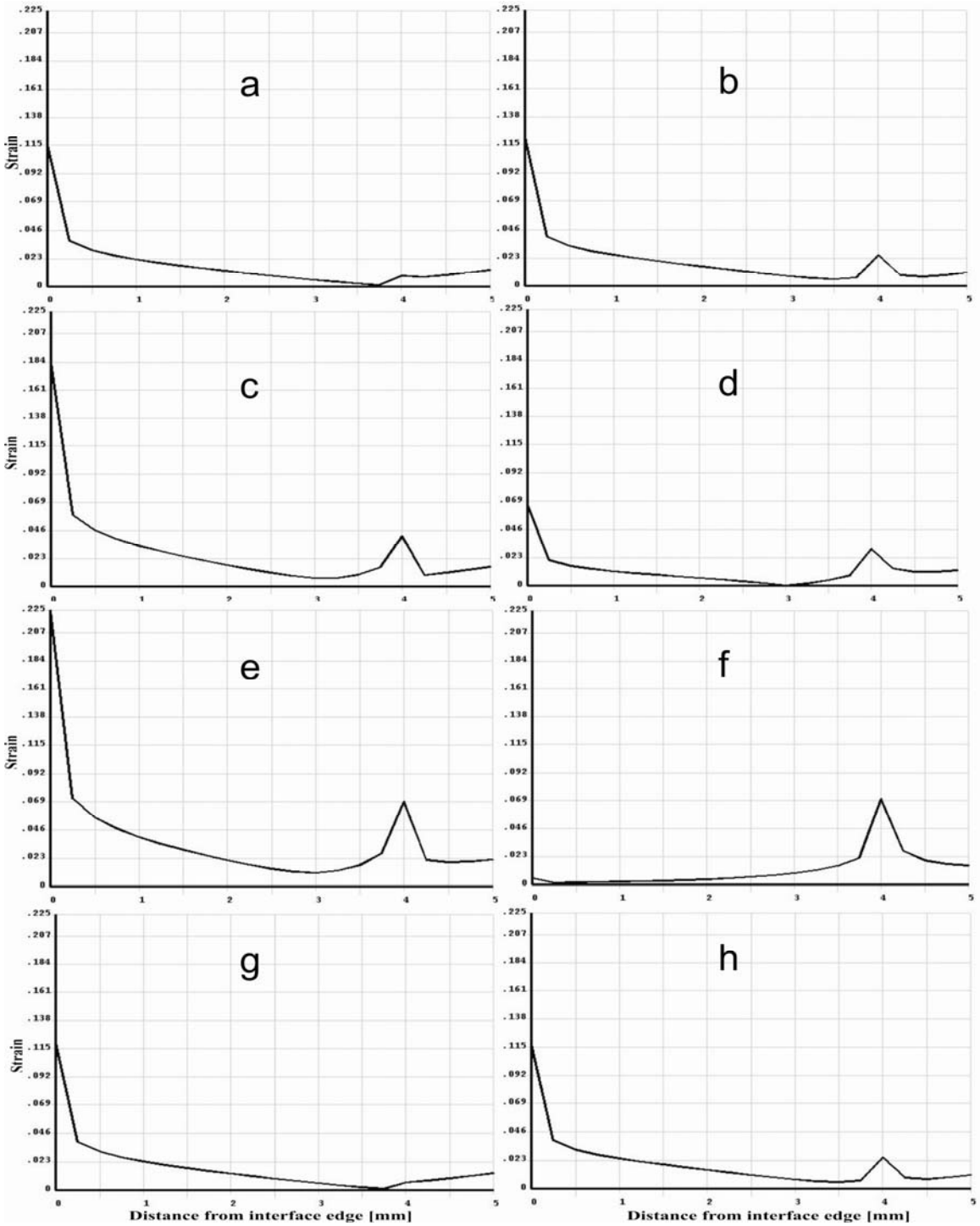

Figure B.2 Local *strains in the vicinity of electrodes* in the bent cord. a, c, e, g show the strain near the outer electrodes (1 or 4). b, d, f, h represent the strains near the inner two electrodes (2 or 3) a and b show the strains calculated with the individual electrodes. c and d show the strains near the electrodes of the developed FBEA. e and f illustrate the strains measured near the electrodes of the rigid-based array. g and h show the strains formed near electrodes of the compliant FBEA.

Figures B.1 and B.2 show the same trends presented in figures4.14 and 4.15, respectively. The same analysis and discussion presented in sections 4.3.4.2, 4.3.4.3 and 4.4.5 applies to each of the above the two figures.